

*Midwest State's Regional Pooled Fund Research Program
Fiscal Years 1996-1997 (Year 7) and 1997-1998 (Year 8)
Research Project Number SPR-3(017)*

PHASE II DEVELOPMENT OF A BULLNOSE GUARDRAIL SYSTEM FOR MEDIAN APPLICATIONS

Submitted by

Bob W. Bielenberg, B.S.M.E., E.I.T.
Graduate Research Assistant

John D. Reid, Ph.D.
Assistant Professor

Ronald K. Faller, Ph.D., P.E.
Research Assistant Professor

John R. Rohde, Ph.D., P.E.
Associate Professor

Dean L. Sicking, Ph.D., P.E.
Associate Professor and MwRSF Director

Eric A. Keller, B.S.M.E., E.I.T.
Computer Design Technician II

James C. Holloway, M.S.C.E., E.I.T.
Research Associate Engineer

MIDWEST ROADSIDE SAFETY FACILITY

University of Nebraska-Lincoln
1901 "Y" Street, Building "C"
Lincoln, Nebraska 68588-0601
(402) 472-6864

Submitted to

MIDWEST STATE'S REGIONAL POOLED FUND PROGRAM

Nebraska Department of Roads
1500 Nebraska Highway 2
Lincoln, Nebraska 68502

MwRSF Research Report No. TRP-03-78-98

December 18, 1998

1. Report No. SPR-3(017)		2.		3. Recipient's Accession No.	
4. Title and Subtitle Phase II Development of a Bullnose Guardrail System for Median Applications				5. Report Date December 18, 1998	
				6.	
7. Author(s) Bielenberg, B.W., Reid, J.D., Faller, R.K., Rohde, J.R., Sicking, D.L., Keller, E.A., and Holloway, J.C.				8. Performing Organization Report No. TRP-03-78-98	
9. Performing Organization Name and Address Midwest Roadside Safety Facility (MwRSF) University of Nebraska-Lincoln 1901 Y St., Bldg. C Lincoln, NE 68588-0601				10. Project/Task/Work Unit No.	
				11. Contract © or Grant (G) No. SPR-3(017)	
12. Sponsoring Organization Name and Address Midwest States Regional Pooled Fund Program Nebraska Department of Roads 1500 Nebraska Highway 2 Lincoln, Nebraska 68502				13. Type of Report and Period Covered Final Report 1997-1998	
				14. Sponsoring Agency Code	
15. Supplementary Notes Prepared in cooperation with U.S. Department of Transportation, Federal Highway Administration					
16. Abstract (Limit: 200 words) The research study consisted of Phase II of the development and full-scale vehicle crash testing of a bullnose barrier concept for the treatment of median hazards. The bullnose guardrail consisted of a 12-gauge thrie beam rail supported by twenty-two wood posts, eleven posts on each side of the system. Horizontal slots were cut in the valleys of selected thrie beam sections to aid in vehicle capture as well as to reduce the buckling and bending capacities of the rail. Two full-scale crash tests were performed, both using a 2000-kg pickup truck. The first crash test, impacting at a speed of 100.2 km/h and an angle of 0 degrees, was unsuccessful following the rupture of the thrie beam and subsequent uncontrolled penetration of the vehicle behind the barrier. Computer simulation of the failed test was performed using LS-DYNA. Analysis of the simulation and full-scale test results led to the addition of two steel cables placed behind the top and middle humps of the thrie beam nose section to aid in truck containment without stiffening the barrier. Computer simulation of the modified design demonstrated successful containment of the pickup truck. The second test, impacting at a speed of 103.5 km/h and an angle of 0 degrees was determined to be successful according to the safety standards set forth by the Test Level 3 (TL-3) evaluation criteria described in the NCHRP Report No. 350, <i>Recommended Procedures for the Safety Performance Evaluation of Highway Features</i> . The next phase of the bullnose barrier system design will be to complete the remaining crash tests needed for compliance with the NCHRP Report No. 350 safety standards for median barriers.					
17. Document Analysis/Descriptors Highway Safety, Guardrail Longitudinal Barrier, Bullnose Barrier, Median Protection				18. Availability Statement No restrictions. Document available from: National Technical Information Services, Springfield, Virginia 22161	
19. Security Class (this report) Unclassified		20. Security Class (this page) Unclassified		21. No. of Pages 119	
				22. Price	

DISCLAIMER STATEMENT

The contents of this report reflect the views of the authors who are responsible for the facts and the accuracy of the data presented herein. The contents do not necessarily reflect the official views or policies of the state highway departments participating in the Midwest State's Regional Pooled Fund Program or the Federal Highway Administration. This report does not constitute a standard, specification, or regulation.

ACKNOWLEDGMENTS

The authors wish to acknowledge the following organizations that made this project possible:

(1) the Midwest States Regional Pooled Fund Program funded by the Iowa Department of Transportation, Kansas Department of Transportation, Minnesota Department of Transportation, Missouri Department of Transportation, Nebraska Department of Roads, Ohio Department of Transportation, South Dakota Department of Transportation, and Wisconsin Department of Transportation for sponsoring this project; (2) MwRSF personnel for constructing the barriers and conducting the crash tests; (4) Center for Infrastructure Research, Engineering Research Center, for matching support; (5) the Federal Highway Administration for matching support; (6) Daniel Mushett of Buffalo Specialty Products - Timber Division for donating timber posts and blockouts; and (7) Martin Snow and Jim Fowers of Universal Industrial Sales for donating the slotted sections of thrie beam rail.

A special thanks is also given to the following individuals who made a contribution to the completion of this research project.

Midwest Roadside Safety Facility

Kenneth L. Krenk, Field Operations Manager
Mike Hanua, Laboratory Mechanic I
Undergraduate and Graduate Assistants

Missouri Department of Transportation

Vince Imhoff, P.E., Senior Research and Development Engineer

Nebraska Department of Roads

Leona Kolbet, Research Coordinator
Ken Sieckmeyer, Transportation Planning Manager

Kansas Department of Transportation

Ron Seitz, P.E., Road Design Squad Leader

Iowa Department of Transportation

David Little, P.E., Design Methods Engineer

Minnesota Department of Transportation

Ron Cassellius, Research Program Coordinator
Glenn Korfhage, P.E., Design Standards Engineer

Ohio Department of Transportation

Larry Shannon, P.E., Standards and Geometrics Engineer
Monique Evans, P.E., Design Standards Engineer

South Dakota Department of Transportation

David Huft, P.E., Research Engineer

Wisconsin Department of Transportation

Rory Rhinesmith, P.E., Chief Roadway Development Engineer
Fred Wisner, Standards Development Engineer

Federal Highway Administration

Milo Cress, P.E., Nebraska Division Office
Frank Doland, P.E., Research Engineer
Martin Hargrave, P.E., Research Engineer

Dunlap Photography

James Dunlap, President and Owner

Universal Industrial Sales

Martin Snow, President
Jim Fowers

TABLE OF CONTENTS

	Page
TECHNICAL DOCUMENTATION PAGE	i
DISCLAIMER STATEMENT	ii
ACKNOWLEDGMENTS	iii
TABLE OF CONTENTS	v
List of Figures	vii
List of Tables	ix
1 INTRODUCTION	1
2 BARRIER DESIGN	5
2.1 Phase II Barrier Design	5
2.2 Nose Section Design	6
2.3 Barrier Design Details	6
3 PERFORMANCE EVALUATION CRITERIA	16
3.1 Test Requirements	16
3.2 Evaluation Criteria	18
4 TEST CONDITIONS	20
4.1 Test Facility	20
4.2 Vehicle Tow and Guidance System	20
4.3 Test Vehicles	20
4.4 Data Acquisition Systems	25
4.4.1 Accelerometers	25
4.4.2 Rate Transducers	26
4.4.3 High Speed Photography	26
4.4.4 Pressure Tape Switches	30
4.4.5 Strain Gauges	30
5 CRASH TEST MBN-3	34
5.1 Test MBN-3	34
5.2 Test Description	34
5.3 Vehicle Damage	35
5.4 Barrier Damage	35
5.5 Occupant Risk Values	36

5.6 Discussion	36
5.7 Barrier Instrumentation Results	38
6 COMPUTER SIMULATION	51
6.1 Simulation Objective	51
6.2 Finite Element Model	51
6.2.1 Bullnose Model	51
6.2.2 Truck Model	52
6.3 Material Failure	53
6.4 Rotating Tires	55
6.5 MBN-3 Bullnose Simulation	56
7 BARRIER MODIFICATIONS (DESIGN FOR MBN-4)	61
8 SIMULATION OF MODIFIED DESIGN FOR MBN-4	67
9 CRASH TEST MBN-4	69
9.1 Test MBN-4	69
9.2 Test Description	69
9.3 Vehicle Damage	70
9.4 Barrier Damage	70
9.5 Occupant Risk Values	71
9.6 Discussion	71
10 SUMMARY AND CONCLUSIONS	83
11 RECOMMENDATIONS	86
12 REFERENCES	87
13 APPENDICES	90
APPENDIX A - ACCELEROMETER DATA ANALYSIS	90
APPENDIX B - STRAIN GAUGE DATA	103

LIST OF FIGURES

	Page
1. Phase I Bullnose Barrier Design Concept	3
2. Bullnose Barrier Design Layout	7
3. Modified Groundline Strut	8
4. Layout of Bullnose Rails No. 1 and 2	10
5. Rail Section No. 1 Detail	11
6. Rail Section No. 2 Detail	12
7. Rail Section No. 3 Detail	13
8. Bullnose Barrier Design	14
9. Bullnose Barrier Design	15
10. Proposed Full Scale Crash Tests for Bullnose Barrier Evaluation	17
11. Vehicle Dimensions, Test MBN-3	21
12. Vehicle Dimensions, Test MBN-4	22
13. Vehicle Target Locations, Test MBN-3	23
14. Vehicle Target Locations, Test MBN-4	24
15. Location of High-Speed Cameras, Test MBN-3	28
16. Location of High-Speed Cameras, Test MBN-4	29
17. Strain Gauges for Full Scale Test MBN-3	33
18. Impact Location, Test MBN-3	39
19. Summary and Sequential Photos, Test MBN-3	40
20. Additional Sequential Photos, Test MBN-3	41
21. Full-Scale Crash Test MBN-3	42
22. Full-Scale Crash Test MBN-3	43
23. Vehicle Trajectory, Test MBN-3	44
24. Vehicle Damage, Test MBN-3	45
25. Barrier Damage, Test MBN-3	46
26. Barrier Damage, Test MBN-3	47
27. Barrier Damage, Test MBN-3	48
28. Bumper Impact Height, Test MBN-1 and MBN-3	49
29. Physical Testing of Slot Tabs	54
30. Lower Rail Catches on Tire	56
31. Rotating Tire	57
32. MBN-3 Simulation - Truck Tears Through Guardrail	59
33. Velocity Comparison for MBN-3	60
34. Bullnose Barrier Design, Test MBN-4	63
35. Bullnose Design for Test MBN-4	64
36. Bullnose Design for Test MBN-4	65
37. Cable Detail and Cable Plate, Test MBN-4	66
38. Simulation Results, Test MBN-4	68
39. Impact Location, Test MBN-4	73

40. Summary and Sequential Photographs, Test MBN-4	74
41. Additional Sequential Photographs, Test MBN-4	75
42. Full-Scale Crash, Test MBN-4	76
43. Full-Scale Crash, Test MBN-4	77
44. Vehicle Trajectory, Test MBN-4	78
45. Vehicle Damage, Test MBN-4	79
46. Barrier Damage, Test MBN-4	80
47. Barrier Damage, Test MBN-4	81
48. Barrier Damage, Test MBN-4	82
A-1. Graph of Longitudinal Deceleration, Test MBN-3	91
A-2. Graph of Longitudinal Occupant Impact Velocity, Test MBN-3	92
A-3. Graph of Longitudinal Occupant Displacement, Test MBN-3	93
A-4. Graph of Lateral Deceleration, Test MBN-3	94
A-5. Graph of Lateral Occupant Impact Velocity, Test MBN-3	95
A-6. Graph of Lateral Occupant Displacement, Test MBN-3	96
A-7. Graph of Longitudinal Deceleration, Test MBN-4	97
A-8. Graph of Longitudinal Occupant Impact Velocity, Test MBN-4	98
A-9. Graph of Longitudinal Occupant Displacement, Test MBN-4	99
A-10. Graph of Lateral Deceleration, Test MBN-4	100
A-11. Graph of Lateral Occupant Impact Velocity, Test MBN-4	101
A-12. Graph of Lateral Occupant Displacement, Test MBN-4	102
B-1. Strain Gauge No. 1 Data, Strain Data, Test MBN-3	104
B-2. Strain Gauge No. 1 Data, Stress Data, Test MBN-3	105
B-3. Strain Gauge No. 2 Data, Strain Data, Test MBN-3	106
B-4. Strain Gauge No. 2 Data, Stress Data, Test MBN-3	107
B-5. Strain Gauge No. 3 Data, Strain Data, Test MBN-3	108
B-6. Strain Gauge No. 3 Data, Stress Data, Test MBN-3	109
B-7. Strain Gauge No. 4 Data, Strain Data, Test MBN-3	110
B-8. Strain Gauge No. 4 Data, Stress Data, Test MBN-3	111
B-9. Strain Gauge No. 5 Data, Strain Data, Test MBN-3	112
B-10. Strain Gauge No. 5 Data, Stress Data, Test MBN-3	113
B-11. Strain Gauge No. 6 Data, Strain Data, Test MBN-3	114
B-12. Strain Gauge No. 6 Data, Stress Data, Test MBN-3	115
B-13. Strain Gauge No. 7 Data, Strain Data, Test MBN-3	116
B-14. Strain Gauge No. 7 Data, Stress Data, Test MBN-3	117
B-15. Strain Gauge No. 8 Data, Strain Data, Test MBN-3	118
B-16. Strain Gauge No. 8 Data, Stress Data, Test MBN-3	119

LIST OF TABLES

	Page
Table 1. Summary of Safety Performance Evaluation for MBN-1 and MBN-2	4
Table 2. NCHRP Report 350 Evaluation Criteria for 2000P Pickup Truck Crash Test 3-31 and 820C Small Car Crash Test 3-30	19
Table 3. Strain Gauge Locations, Test MBN-3	32
Table 4. Strain Gauge Data, Test MBN-3	50
Table 5. Summary of Safety Performance Evaluation	85

1 INTRODUCTION

The use of the divided highway separated by a median area has been a valuable safety feature in modern roadway design. The median allows a safe recovery area for errant vehicles to come to rest without impeding upon oncoming traffic. It is possible, however, that the median is not always a safe zone for vehicle recovery. Many roadway structures are built in the median such as bridge supports, drainage structures, and large sign supports. These structures present hazards to vehicles in the median.

The three main treatments that have been used in the protection against median hazards are crash cushions, open guardrails, and closed guardrail envelopes. Bridge piers are often treated by surrounding them with rigid barriers and placing crash cushions on each end. This alternative is very short and therefore reduces the number of run-off-road accidents to a minimum. Unfortunately, this type of treatment is very costly and therefore is hard to justify for most median situations. Another popular treatment involves using open guardrail envelopes. This design incorporates long runs of guardrail upstream from the hazards. Although this alternative is less expensive than crash cushion designs, the long runs of guardrail generate many guardrail related accidents, and when used in narrow medians, the backside of the guardrails can become a major hazard. Enclosed guardrail envelopes, commonly called bullnose systems, involve wrapping the guardrail completely around the hazards. These designs are smaller and therefore generate fewer guardrail accidents. Further, bullnose designs are generally the least costly alternatives. Unfortunately, bullnose guardrail designs have never met current safety standards. This report describes an effort to develop a new bullnose guardrail design that will meet modern safety standards.

The objective of this research project was to continue development and evaluation of a bullnose guardrail system that meets the Test Level 3 (TL-3) safety performance criteria provided in National Cooperative Highway Research Program (NCHRP) Report No. 350, *Recommended Procedures for the Safety Performance Evaluation of Highway Features* (1). Phase I of the design process, which is covered in a previous report (2), included two full-scale crash tests which provided information for redesign and computer simulation of the bullnose barrier system. The bullnose barrier developed as a result of the Phase I development is shown in Figure 1. The initial design concept was subjected to two full-scale crash tests, tests MBN-1 and MBN-2. Test MBN-1 was a head-on impact involving a 2000-kg pickup truck, while test MBN-2 was a one-quarter offset, head-on impact using an 820-kg small car. The results of those tests are shown in Table 1. Although only one of the two tests was successful, these tests demonstrated that the bullnose barrier concept had potential but required further development to meet the impact safety standards.

Phase II of the bullnose barrier system design consisted of the continued development and testing of the bullnose barrier to meet the NCHRP Report No. 350 requirements for test 3-31, a head-on impact of a 2000-kg pickup truck. Two full-scale tests were performed for a head-on impact with the bullnose at a target speed and angle of 100 km/h and 0 degrees, respectively. The test results were analyzed, documented, and evaluated. Conclusions and recommendations were then made with regards to the safety performance of the bullnose barrier terminal. Computer simulation of the testing using LS-DYNA was successfully used to analyze and predict the performance of the bullnose design. The following sections of this report document the development, computer simulation modeling, testing, and evaluation of the bullnose barrier terminal concept.

Table 1. Summary of Safety Performance Evaluation for Tests MBN-1 and MBN-2 (Phase I)

Evaluation Factors	Evaluation Criteria	Test MBN-1	Test MBN-2						
Structural Adequacy	C. Acceptable test article performance may be by redirection, controlled penetration, or controlled stopping of the vehicle.	U	S						
Occupant Risk	D. Detached elements, fragments or other debris from the test article should not penetrate or show potential for penetrating the occupant compartment, or present an undue hazard to other traffic, pedestrians, or personnel in a work zone. Deformations of, or intrusions into, the occupant compartment that could cause serious injuries should not be permitted.	S	S						
	F. The vehicle should remain upright during and after collision although moderate roll, pitching, and yawing are acceptable.	S	S						
	H. Occupant impact velocities should satisfy the following: Occupant Impact Velocity Limits (m/s) <table><tr><td><u>Component</u></td><td>Preferred</td><td>Maximum</td></tr><tr><td>Longitudinal and Lateral</td><td>9</td><td>12</td></tr></table>	<u>Component</u>	Preferred	Maximum	Longitudinal and Lateral	9	12	S	S
<u>Component</u>	Preferred	Maximum							
Longitudinal and Lateral	9	12							
	I. Occupant ride down accelerations should satisfy the following: Occupant Ride down Acceleration Limits (G's) <table><tr><td><u>Component</u></td><td>Preferred</td><td>Maximum</td></tr><tr><td>Longitudinal and Lateral</td><td>15</td><td>20</td></tr></table>	<u>Component</u>	Preferred	Maximum	Longitudinal and Lateral	15	20	S	S
<u>Component</u>	Preferred	Maximum							
Longitudinal and Lateral	15	20							
Vehicle Trajectory	K. After collision it is preferable that the vehicle's trajectory not intrude into adjacent traffic lanes.	S	S						
	N. Vehicle trajectory behind the test article is acceptable.	U	S						

S - (Satisfactory)

U - (Unsatisfactory)

2 BARRIER DESIGN

2.1 Phase II Barrier Design

The design layout for test MBN-3 was only altered slightly from the final design developed in Phase I. The first change was to switch from the 150-mm wide by 200-mm deep by 554-mm long thrie blockouts used in the original design to shorter 150-mm wide by 200-mm deep by 360-mm long blockouts on all posts except post no. 1. The second change in the design was the use of foundation tubes in the embedment of post no. 3 on each side of the barrier. Finally, post no. 5 was changed to a Cable Release Terminal (CRT) (3) post instead of a standard wooden post. This led to accelerated post fracture and the decreased potential for high loads being imparted to the thrie beam rail. High rail stresses were reduced in conjunction with a more gradual dissipation of the vehicle's kinetic energy. A more detailed discussion of the entire bullnose barrier is presented below.

2.2 Nose Section Design

After reviewing the Pooled Fund member states' bullnose standards, a 4,500-mm design was selected for use in the current study. The shape of the nose section was chosen after analysis of prior bullnose (4-7) and short radius guardrail designs (8-13). The nose section was formed using one 1,580-mm radius curved section of guardrail with one 10,400-mm radius curved section attached to each end of the nose section. The overall shape was chosen using simple curves to simplify the design and fabrication of the rail. The curve radii were sized based on ease of fabrication as well as to maintain the design width of the system.

The front-end section of the bullnose barrier was designed without a post at the centerline of the nose, since the end post tends to rotate back after impact, thus creating a potential for vaulting of the vehicle to vault over the rail. It was determined that a nose section without the centerline post

would have sufficient structural strength to maintain the shape of the rail while not causing the vaulting hazard.

2.3 Barrier Design Details

The complete layout of the bullnose barrier system used for the test MBN-3 is shown in Figure 2. A one-half barrier system was designed for testing purposes to limit costs and time of construction. The bullnose barrier was 4,500-mm wide by 20,144-mm long. The system was constructed with twenty-two wood posts with eleven posts positioned on each side of the system. The first two posts on each side of the system were 140-mm wide by 190.5-mm deep Breakaway Cable Terminal (BCT) (3) posts set in Sequential Kinking Terminal (SKT) (14) foundation tubes with soil plates and groundline channel strut. Post no. 1 on each side of the barrier used no blackout while post no. 2 on each side used a 150-mm wide by 200-mm deep by 360-mm long thrie blackout. Post no. 3 on each side of the system was a BCT post set in a SKT foundation tube without a bearing plate. Post nos. 4 and 5 on each side of the barrier were CRT posts. The next four posts along both sides of the bullnose barrier were standard 150-mm wide by 200-mm deep by 1,980-mm long wood posts spaced 1,905-mm apart, as shown in Figure 2. Each of these posts uses a 150-mm wide by 200-mm deep by 360-mm long thrie blackout to space the rail away from the post. The top mounting height of the rail was 804 mm, as measured from the ground surface. Post nos. 3 through 9 had a soil embedment depth of 1,153 mm. The last two posts on each side of the bullnose barrier were 140-mm wide by 190.5-mm deep BCT posts set in foundation tubes without soil plates but with a groundline channel strut.

A modified ground strut, shown in Figure 3, between post nos. 1 and 2 on each side of the system, was designed to compensate for the curve of the nose section. The ground strut was altered by angling the upstream yoke of the strut 12.2 degrees.

Bull-Nose 350 Test Layout MBN-3 Test

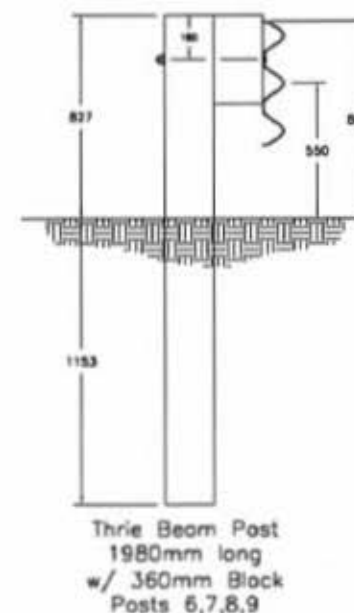
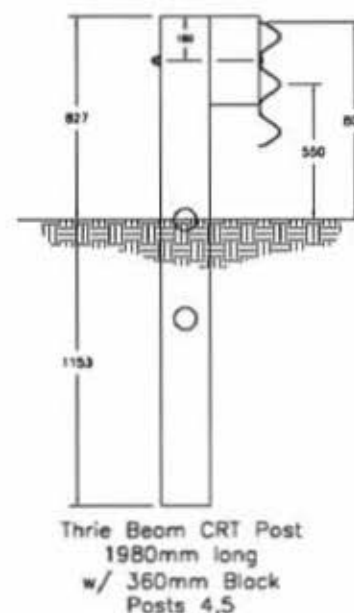
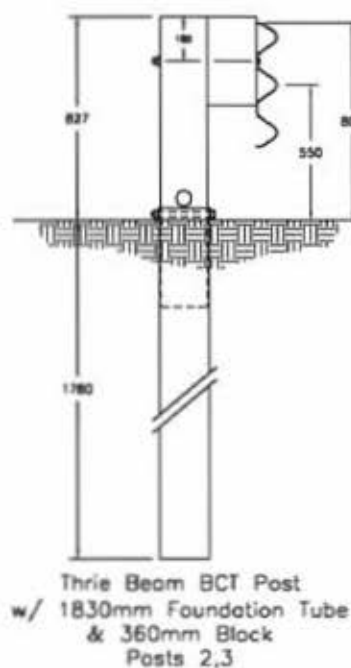
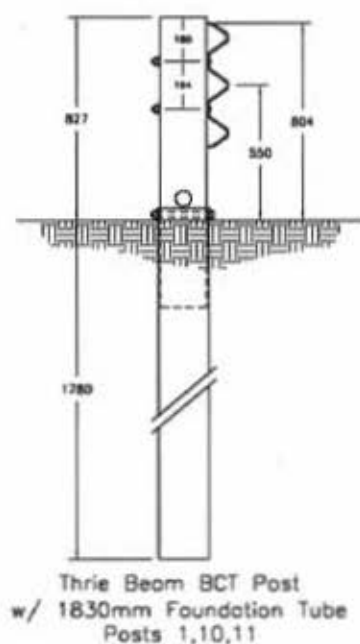
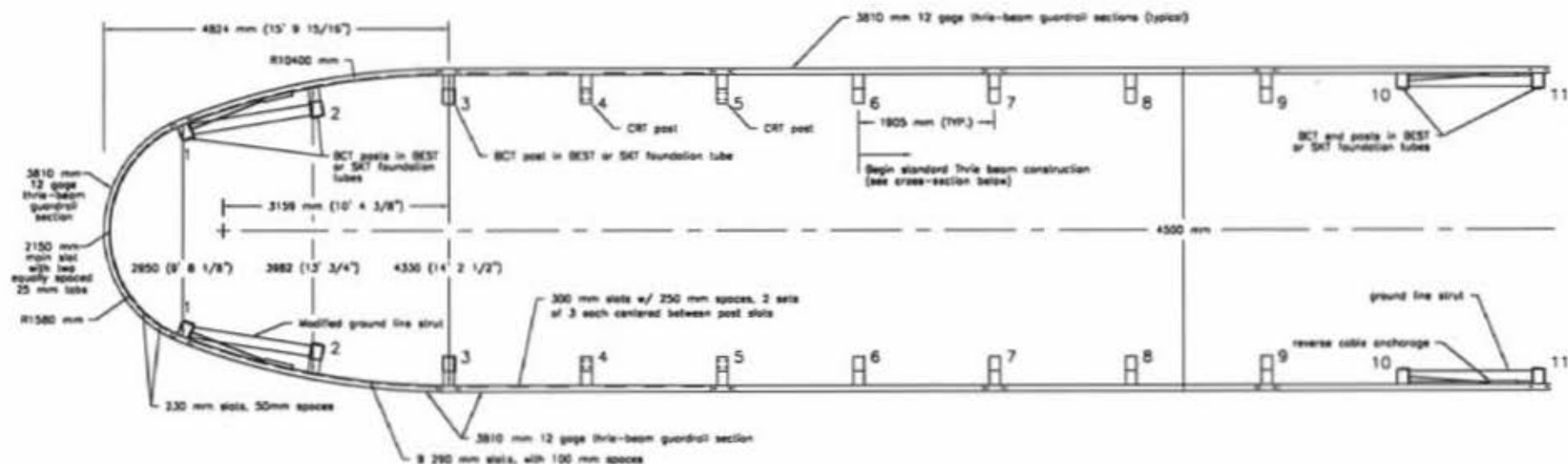
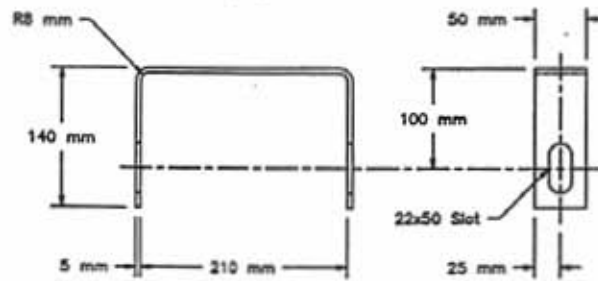
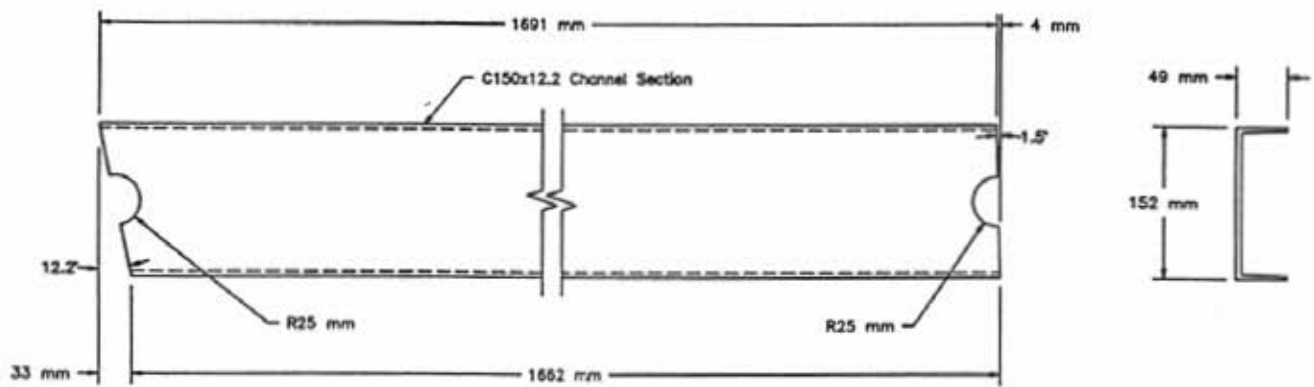


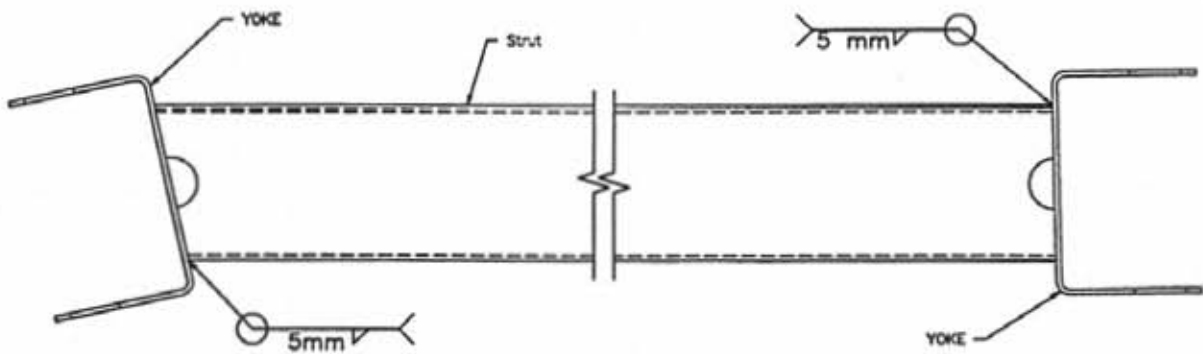
Figure 2. Bullnose Barrier Design Layout



Yoke



Strut



Assembly

NOTE: Strut as shown for one side of the system,
for other side the mirror image is required.

Figure 3. Modified Groundline Strut

A cable anchor system was used between post nos. 1 and 2 on each side of the system to develop the tensile strength of the thrie beam guardrail downstream of the post no. 2. A reverse cable anchor system was used between post nos. 11 and 12 to replicate the rail strength of an actual installation. This setup was used for testing purposes only in order to simulate the effects of a complete bullnose barrier system with both halves connected.

All guardrail used in the bullnose barrier consisted of 12-gauge steel thrie beam. Eleven 3,810-mm long sections of thrie beam were spliced together with a standard lap splice on each interior end. The first three rail sections were cut with slots in the valleys. The nose section of the rail consisted of a 3,810-mm long section bent into a 1,580-mm radius, as shown in Figure 4. The nose section bends were prefabricated with these radii. The nose section was cut with slots in the valleys to aid in vehicle capture, as shown in Figure 5. There were six main 700-mm slots centered about the midspan of the rail, three in each valley. Each of the main slots is divided by two equally spaced 25-mm tabs and separated by a 25-mm gap on each end. Eight additional smaller 230-mm long slots, four on each end of the rail section, were also cut with a 50-mm gap between them. All slots were 25-mm wide. The second rail section on each side was bent to form a 10,400-mm radius curve, as shown in Figure 4. These sections were cut with a different pattern of slots, as shown in Figure 6. There were nine 290-mm long slots in each valley. A 100-mm gap separated each slot. The slot pattern for the third rail section on each side consisted of two sets of six 300-mm long slots centered between post slots, as shown in Figure 7. The slots were separated by 250-mm gaps, which provided three slots per valley between posts. Photographs of the assembled barrier are shown in Figures 8 through 9.

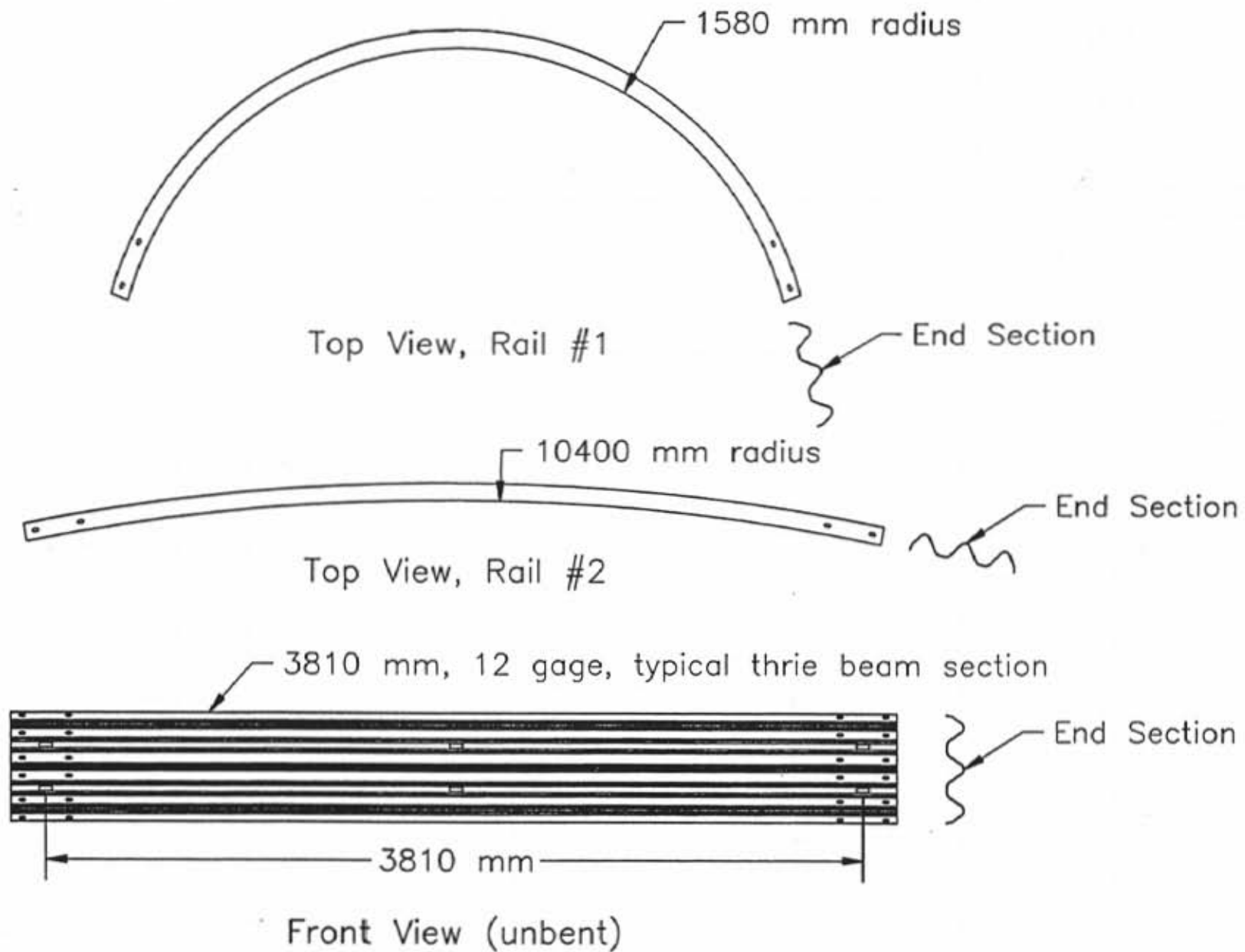
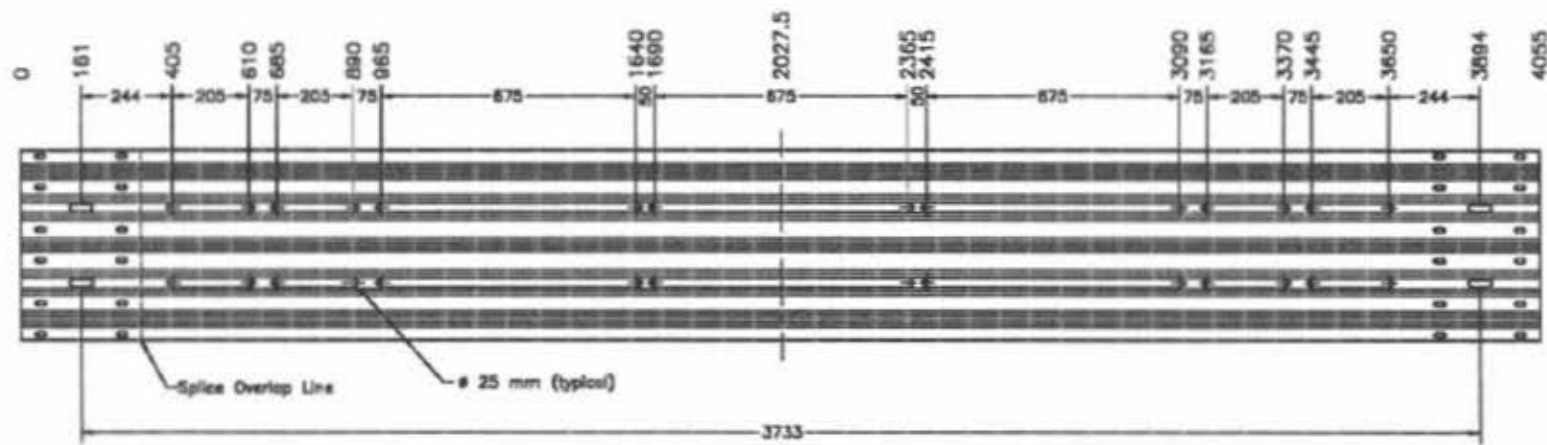
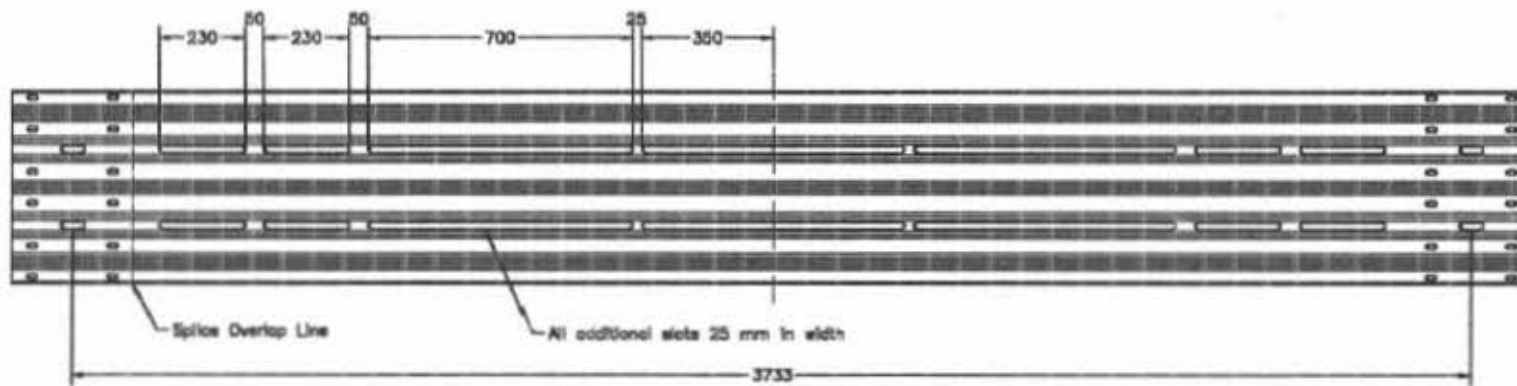


Figure 4. Layout of Bullnose Rails No. 1 and 2



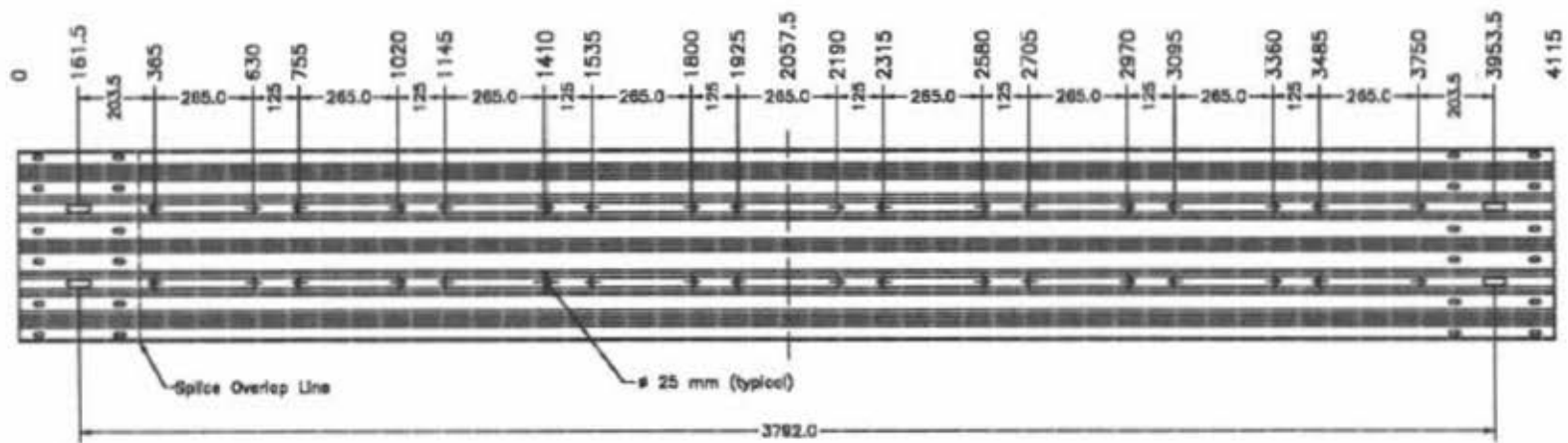
Rail Section 1 ("Nose" Section, MBN-2)

11

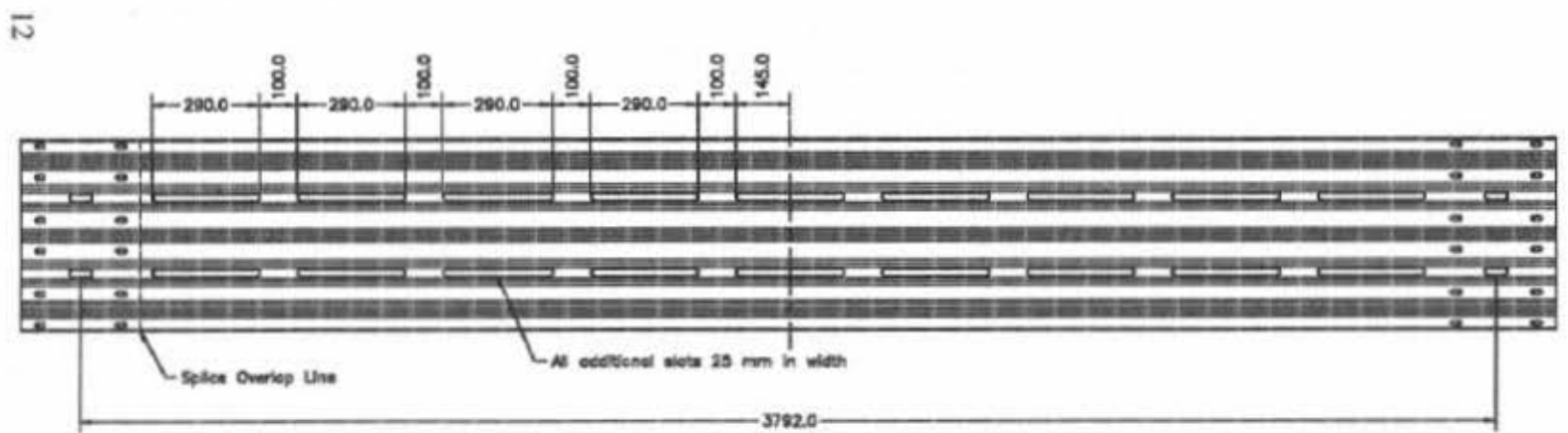


Rail Section 1 ("Nose" Section, MBN-2)

Figure 5. Rail Section No. 1 Detail

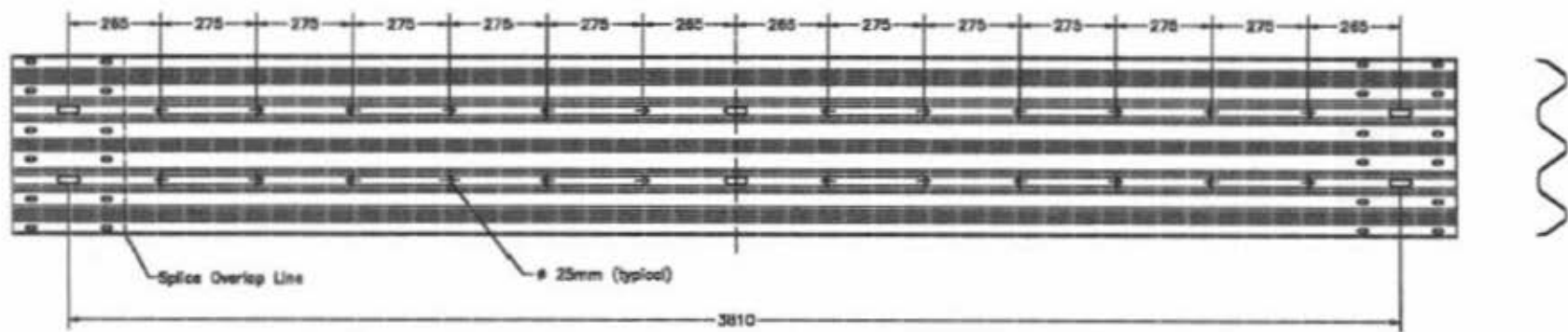


Rail Section 2 (MBN-2)



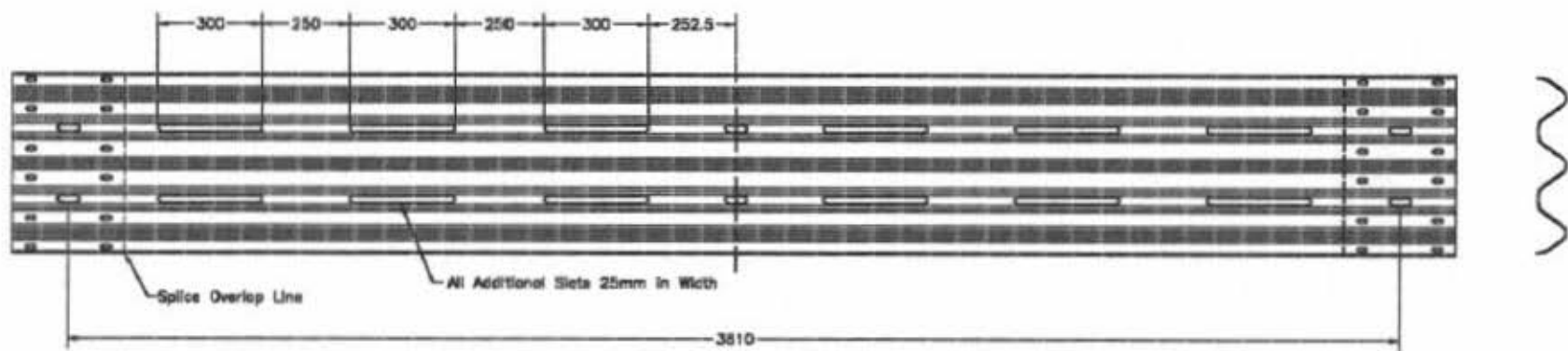
Rail Section 2 (MBN-2)

Figure 6. Rail Section No. 2 Detail



Rail Section 3 (MBN-2)

13



Rail Section 3 (MBN-2)

Figure 7. Rail Section No. 3 Detail



Figure 8. Bullnose Barrier Design



Figure 9. Bullnose Barrier Design

3 PERFORMANCE EVALUATION CRITERIA

3.1 Test Requirements

Terminals and crash cushions, such as bullnose barriers, must satisfy the requirements provided in NCHRP Report No. 350 (1) in order to be accepted for use on new construction projects or as a replacement for existing barriers not meeting current safety standards. The bullnose barrier is defined as a gated barrier and must fulfill the requirements for gated barriers. A gating device is one designed to allow controlled penetration of the vehicle when impacted between the beginning and the end of the length of need. According to NCHRP Report No. 350, terminals and crash cushions must be subjected to seven full-scale vehicle crash tests, four using a 2000-kg pickup truck and three using an 820-kg small car. The required 2000-kg pickup truck crash tests are: (1) Test 3-31, a 100 km/h impact at a nominal angle of 0 degrees on the tip of the barrier nose; (2) Test 3-33, a 100 km/h impact at a nominal angle of 15 degrees on the tip of the barrier nose; (3) Test 3-35, a 100 km/h impact at a nominal angle of 20 degrees on the beginning of the Length-of-Need (LON); and (4) Test 3-39, a 100 km/h impact at a nominal angle of 20 degrees on a point at the length of the terminal divided by two. The required 820-kg small car crash tests are: (1) Test 3-30, a 100 km/h impact at a nominal angle of 0 degrees on the tip of the barrier nose with a 1/4 point offset; (2) Test 3-32, a 100 km/h impact at a nominal angle of 15 degrees on the tip of the barrier nose; (3) Test 3-34, a 100 km/h impact at a nominal angle of 15 degrees on the Critical Impact Point (CIP). A diagram showing the impact location for the seven crash tests is shown in Figure 10.

Two full-scale crash tests of test designation no. 3-31 were conducted for this report. These tests were run in order to improve the original bullnose design to safely contain the head-on pickup truck impact. The results from these two tests would be used to obtain information for calibrating

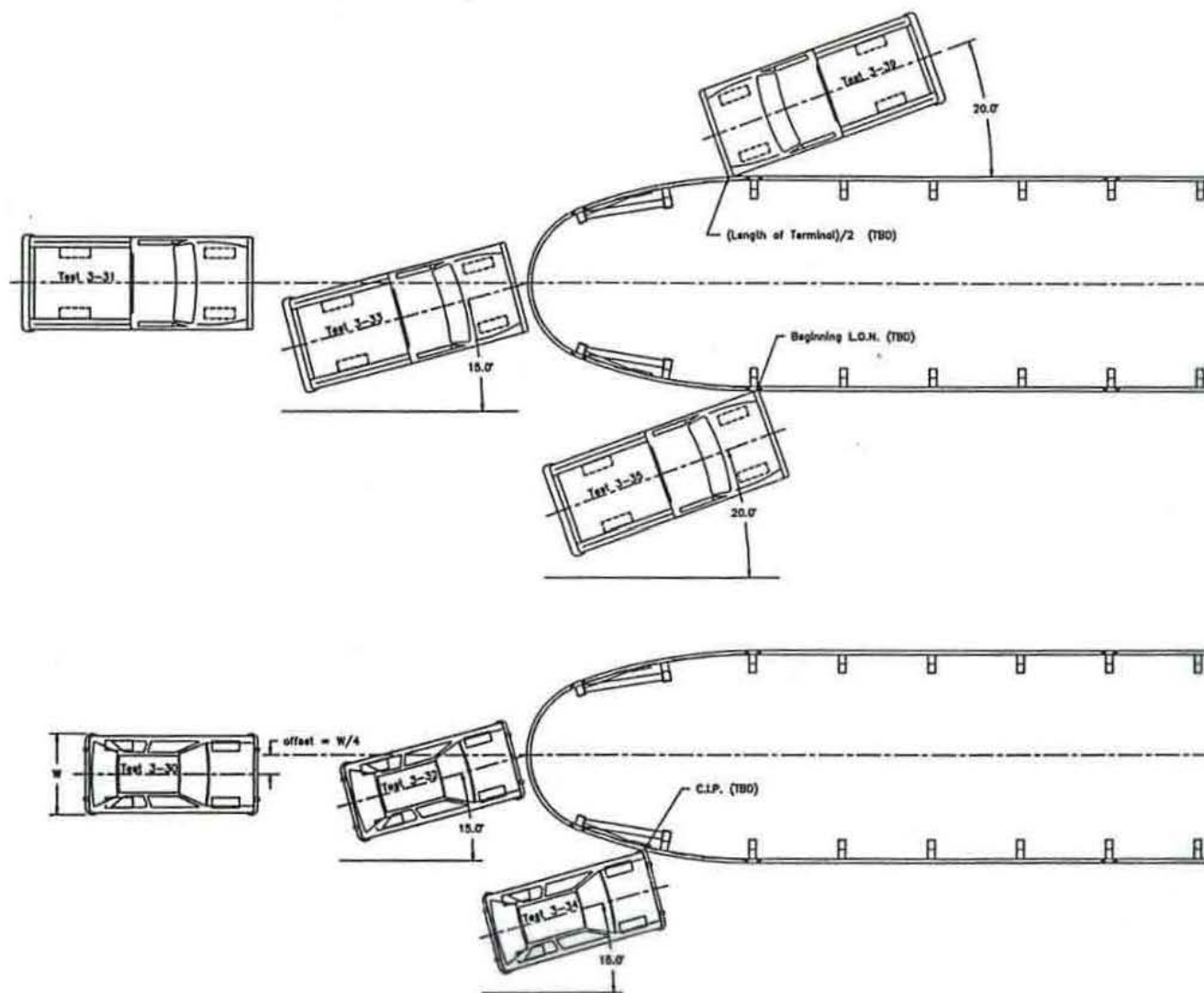


Figure 10. Proposed Full Scale Crash Tests for Bullnose Barrier Evaluation

computer models, evaluating the feasibility of the design concept for the other required impact conditions, and obtaining information for future design modifications and improvements.

3.2 Evaluation Criteria

Evaluation criteria for full-scale vehicle crash testing are based on three appraisal areas: (1) structural adequacy; (2) occupant risk; and (3) vehicle trajectory after collision. Criteria for structural adequacy are intended to evaluate the ability of the barrier to contain, redirect, or allow controlled vehicle penetration in a predictable manner. Occupant risk evaluates the degree of hazard to occupants in the impacting vehicle. Vehicle trajectory after collision is a measure of the potential for the post-impact trajectory of the vehicle to cause subsequent multi-vehicle accidents, thereby subjecting occupants of other vehicles to an undue hazard or to subject the occupants of the impacting vehicle to secondary collisions with other fixed objects. These three evaluation criteria are defined in Table 2. The full-scale vehicle crash tests were conducted and reported in accordance with the procedures provided in NCHRP Report No. 350.

Table 2. NCHRP Report 350 Evaluation Criteria for 2000P Pickup Truck (Test 3-31)

Structural Adequacy	C. Acceptable test article performance may be by redirection, controlled penetration, or controlled stopping of the vehicle.								
Occupant Risk	D. Detached elements, fragments or other debris from the test article should not penetrate or show potential for penetrating the occupant compartment, or present an undue hazard to other traffic, pedestrians, or personnel in a work zone. Deformations of, or intrusions into, the occupant compartment that could cause serious injuries should not be permitted.								
	F. The vehicle should remain upright during and after collision although moderate roll, pitching, and yawing are acceptable.								
	H. Occupant impact velocities should satisfy the following: Occupant Impact Velocity Limits (m/s)								
	<table><tr><td><u>Component</u></td><td>Preferred</td><td>Maximum</td></tr><tr><td>Longitudinal and Lateral</td><td>9</td><td>12</td></tr><tr><td>Longitudinal</td><td>3</td><td>5</td></tr></table>	<u>Component</u>	Preferred	Maximum	Longitudinal and Lateral	9	12	Longitudinal	3
<u>Component</u>	Preferred	Maximum							
Longitudinal and Lateral	9	12							
Longitudinal	3	5							
	I. Occupant ride down accelerations should satisfy the following: Occupant Ride down Acceleration Limits (G's)								
	<table><tr><td><u>Component</u></td><td>Preferred</td><td>Maximum</td></tr><tr><td>Longitudinal and Lateral</td><td>15</td><td>20</td></tr></table>	<u>Component</u>	Preferred	Maximum	Longitudinal and Lateral	15	20		
<u>Component</u>	Preferred	Maximum							
Longitudinal and Lateral	15	20							
Vehicle Trajectory	K. After collision it is preferable that the vehicle's trajectory not intrude into adjacent traffic lanes.								
	N. Vehicle trajectory behind the test article is acceptable.								

4 TEST CONDITIONS

4.1 Test Facility

The testing facility is located at the Lincoln Air-Park on the NW end of the Lincoln Municipal Airport and is approximately 8.0 km NW of the University of Nebraska-Lincoln. The site is protected by a 2.44-m high chain-link security fence.

4.2 Vehicle Tow and Guidance System

A reverse cable tow system with a 1:2 mechanical advantage was used to propel the test vehicles. The distance traveled and the speed of the tow vehicle are one-half that of the test vehicle. The test vehicle was released from the tow cable before impact with the bridge rail. A digital speedometer was located in the tow vehicle to increase the accuracy of the test vehicle impact speed.

A vehicle guidance system developed by Hinch ([15](#)) was used to steer the test vehicle. A guide-flag, attached to the front-left wheel and the guide cable, was sheared off before impact. The 9.5-mm diameter guide cable was tensioned to approximately 13.3 kN, and supported laterally and vertically every 30.48 m by hinged stanchions. The hinged stanchions stood upright while holding up the guide cable, but as the vehicle was towed down the line, the guide-flag struck and knocked each stanchion to the ground. The vehicle guidance system was approximately 457.2-m long.

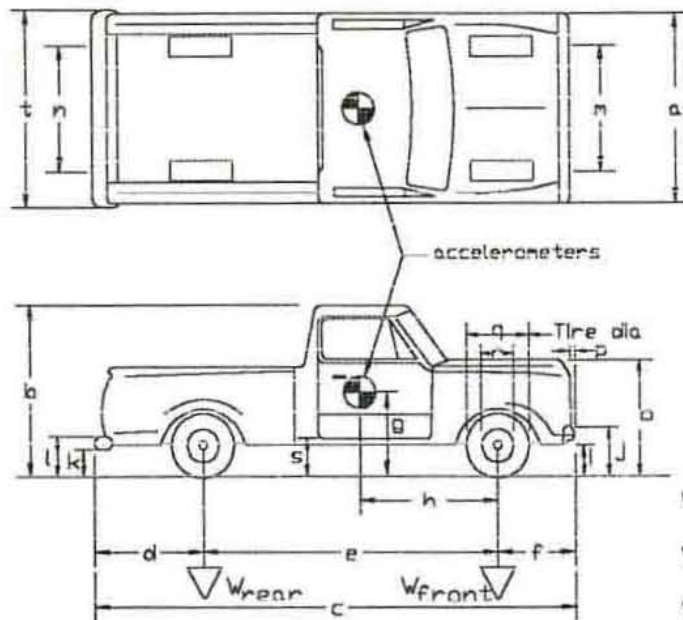
4.3 Test Vehicles

For test MBN-3, a 1990 Chevy 2500 $\frac{3}{4}$ -ton pickup truck was used as the test vehicle. The test inertial and gross static weights were 1,989 kg. The test vehicle and vehicle dimensions are shown in Figure 11.

For test MBN-4, a 1991 Chevy 2500 $\frac{3}{4}$ -ton pickup truck was used. The test inertial and gross static weights were 2,010-kg. The test vehicle and vehicle dimensions are shown in Figure 12.

Date: 5/6/98 Test Number: MBN-3 Model: 2500
 Make: CHEVY Vehicle I.D.#: 1GCFC24KXLE103250
 Tire Size: 245/75 R16 Year: 1990 Odometer: NA

*(All Measurements Refer to Impacting Side)



Vehicle Geometry - mm

a 1905 b 1778
 c 5550 d 1308
 e 3378 f 861
 g 737 h 1515
 i 406 j 622
 k 533 l 737
 m 1600 n 1613
 o 1029 p 76
 q 756 r 445
 s 413 t 1873

Wheel Center Height Front 371

Wheel Center Height Rear 371

Wheel Well Clearance (FR) 838

Wheel Well Clearance (RR) 883

Engine Type V-8

Engine Size 5.6 L

Transmission Type:

Automatic or Manual

FWD or RWD or 4WD

Weights - kg	Curb	Test Inertial	Gross Static
W _{front}	<u>1002</u>	<u>1083</u>	<u>1083</u>
W _{rear}	<u>826</u>	<u>906</u>	<u>906</u>
W _{total}	<u>1828</u>	<u>1989</u>	<u>1989</u>

Note any damage prior to test: Major cracks covering entire windshield.

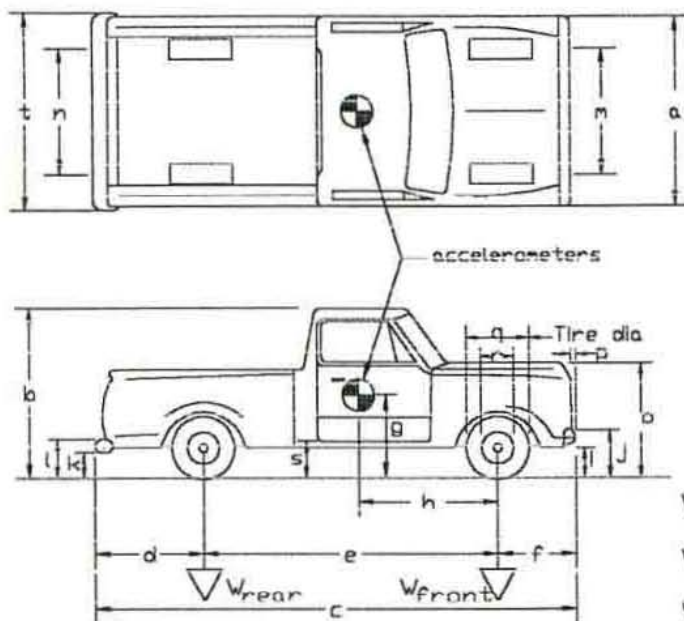
Figure 11. Vehicle Dimensions, Test MBN-3

Date: 7/9/98 Test Number: MBN-4 Model: 2500

Make: CHEVY Vehicle I.D.#: 1GCFC24K9ME1910916

Tire Size: LT 225/75 R16 Year: 1991 Odometer: 78341

*(All Measurements Refer to Impacting Side)



Vehicle Geometry - mm

a 1892 b 1778

c 5512 d 1295

e 3327 f 861

g 738 h 1454

i 413 j 629

k 527 l 724

m 1575 n 1616

o 1029 p 102

q 749 r 445

s 470 t 1848

Wheel Center Height Front 368

Wheel Center Height Rear 381

Wheel Well Clearance (FR) 851

Wheel Well Clearance (RR) 895

Engine Type V-8

Engine Size 5.7 L

Transmission Type:

Automatic or Manual

FWD or RWD or 4WD

Weights - kg	Curb	Test Inertial	Gross Static
W _{front}	<u>1101</u>	<u>1132</u>	<u>1132</u>
W _{rear}	<u>837</u>	<u>878</u>	<u>878</u>
W _{total}	<u>1938</u>	<u>2010</u>	<u>2010</u>

Note any damage prior to test: Minor dent along driver side door and fender

Figure 12. Vehicle Dimensions, Test MBN-4

The Suspension Method was used to determine the vertical component of the center of gravity for the test vehicles. This method is based on the principle that the center of gravity of any freely suspended body is in the vertical plane through the point of suspension. The vehicle was suspended successively in three positions, and the respective planes containing the center of gravity were established. The intersection of these planes pinpointed the location of the center of gravity. The longitudinal component of the center of gravity was determined using the measured axle weights. The locations of the final centers of gravity are shown in Figures 11 through 14.

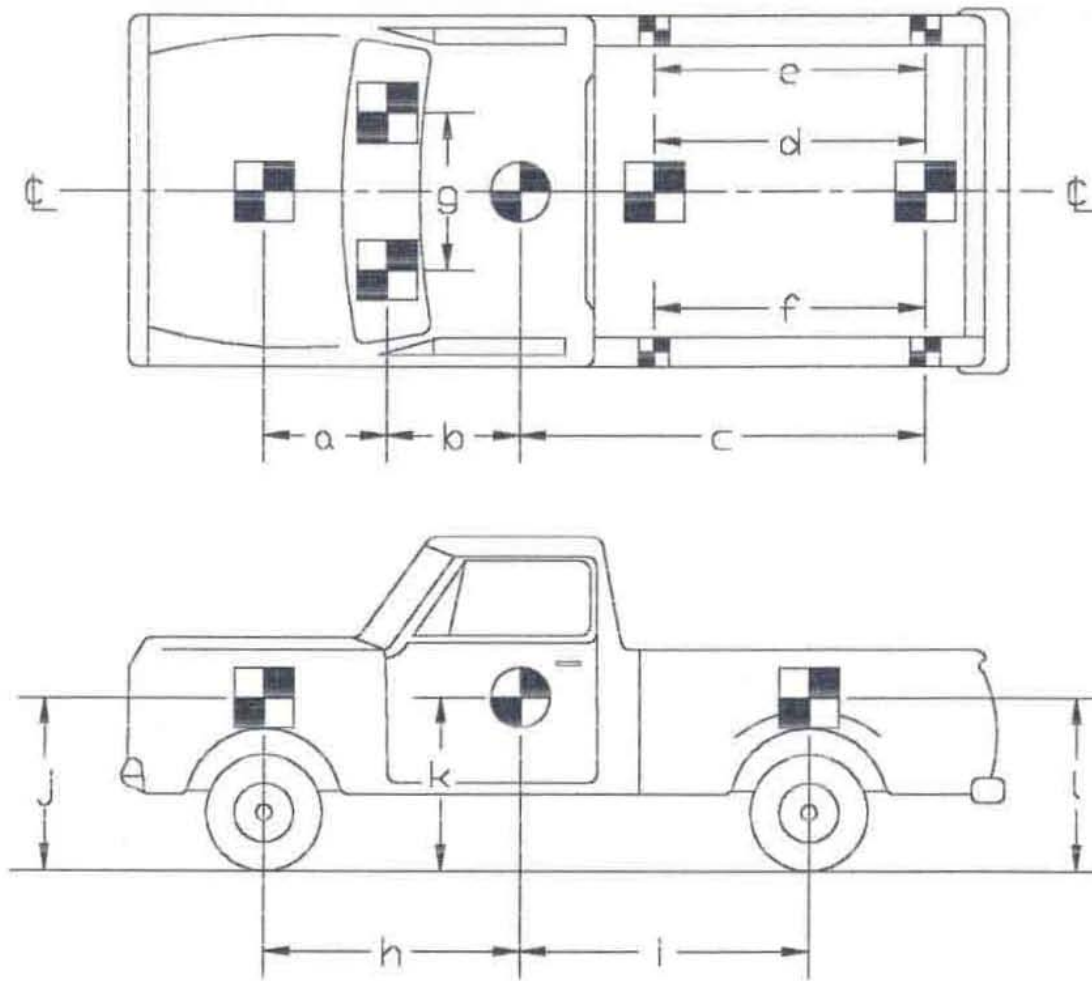
Square, black and white-checked targets were placed on the vehicle to aid in the analysis of the high-speed film, as shown in Figures 13 through 14. One target was placed on the center of gravity on the driver's side door, the passenger's side door, and on the roof of the vehicle. The remaining targets were located for reference so that they could be viewed from the high-speed cameras for film analysis.

The front wheels of the test vehicle were aligned for camber, caster, and toe-in values of zero so that the vehicles would track properly along the guide cable. Two 5B flash bulbs were mounted on both the hood and roof of the vehicles to pinpoint on high-speed film the time of impact with the bridge railing. The flash bulbs were fired by a pressure tape switch mounted on the front face of the bumper. A remote-controlled brake system was installed in the test vehicle so the vehicle could be brought safely to a stop after the test.

4.4 Data Acquisition Systems

4.4.1 Accelerometers

One triaxial piezoresistive accelerometer system with a range of ± 200 G's was used to

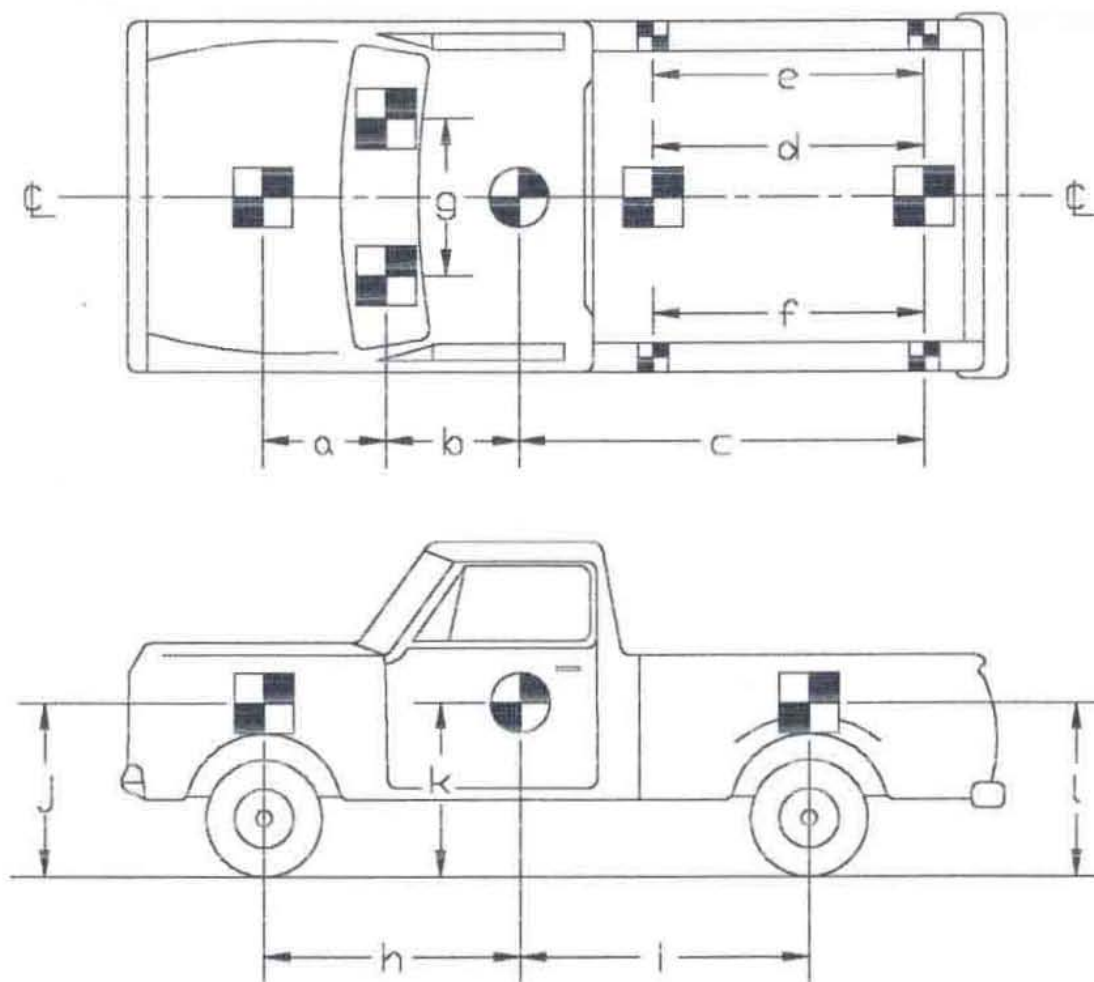


TEST #: MBN-3

TARGET GEOMETRY (mm)

a	<u>1397</u>	b	<u>648</u>	c	<u>2629</u>	d	<u>1918</u>
e	<u>2032</u>	f	<u>2013</u>	g	<u>902</u>	h	<u>1515</u>
i	<u>1863</u>	j	<u>940</u>	k	<u>737</u>	l	<u>800</u>

Figure 13. Vehicle Target Locations, Test MBN-3



TEST #1 MBN-4

TARGET GEOMETRY (mm)

a	<u>1207</u>	b	<u>648</u>	c	<u>2610</u>	d	<u>1724</u>
e	<u>2146</u>	f	<u>2150</u>	g	<u>959</u>	h	<u>1454</u>
i	<u>1095</u>	j	<u>953</u>	k	<u>738</u>	l	<u>1003</u>

Figure 14. Vehicle Target Locations, Test MBN-4

measure the acceleration in the longitudinal, lateral, and vertical directions at a sample rate of 10,000 Hz. The environmental shock and vibration sensor/recorder system, Model EDR-4M6, was developed by Instrumented Sensor Technology (IST) of Okemos, Michigan and includes three differential channels as well as three single-ended channels. The EDR-4 was configured with 6 Mb of RAM memory and a 1,500 Hz lowpass filter. Computer software, "DynaMax 1 (DM-1)" and "DADiSP" were used to digitize, analyze, and plot the accelerometer data.

A backup triaxial piezoresistive accelerometer system with a range of ± 200 G's was also used to measure the acceleration in the longitudinal, lateral, and vertical directions at a sample rate of 3,200 Hz. The environmental shock and vibration sensor/recorder system, Model EDR-3, was developed by Instrumented Sensor Technology (IST) of Okemos, Michigan. The EDR-3 was configured with 256 Kb of RAM memory and a 1,120 Hz lowpass filter. Computer software, "DynaMax 1 (DM-1)" and "DADiSP" were used to digitize, analyze, and plot the accelerometer data.

4.4.2 Rate Transducers

A Humphrey 3-axis rate transducer with a range of 250 deg/sec in each of the three directions (pitch, roll, and yaw) was used to measure the rates of motion of the test vehicle. The rate transducer was rigidly attached to the vehicles near the center of gravity of the test vehicle. Rate transducer signals, excited by a 28 volt DC power source, were received through the three single-ended channels located externally on the EDR-4M6 and stored in the internal memory. The raw data measurements were then downloaded for analysis and plotting. Computer software, "DynaMax 1 (DM-1)" and "DADiSP" were used to digitize, analyze, and plot the rate transducer data.

4.4.3 High Speed Photography

For test MBN-3, seven high-speed 16-mm Red Lake Locam cameras, with operating speeds

of approximately 500 frames/sec, were used to film the crash test. A Locam with a wide angle 12.5-mm lens was placed above the test installation to provide a field of view perpendicular to the ground. A Locam with a zoom lens was placed downstream from the impact point and had a field of view parallel to the barrier. Two Locams with zoom lenses were placed on both sides of the barrier at the nose and had a field of view perpendicular to the barrier. A Locam was placed 9.14 m upstream and offset 19.81 m to the right for a view of the front of the barrier. The two remaining Locams were placed 6.40 m and 37.80 m downstream offset 12.19 m and 21.34 m respectively to the left to provide additional viewing angles of the crash test. A schematic of all seven camera locations for test MBN-3 is shown in Figure 15.

For test MBN-4, five high-speed 16-mm Red Lake Locam cameras, with operating speeds of approximately 500 frames/sec, were used to film the crash test. A Locam with a wide-angle 12.5-mm lens was placed 17.17 m above the test installation to provide a field of view perpendicular to the ground. A Locam with a zoom lens was placed downstream from the impact point and had a field of view parallel to the barrier. Two Locams with zoom lenses were placed on both sides of the barrier perpendicular to post no. 3 for side views of the barrier. The remaining Locam was placed 37.80 m downstream and offset 21.33 m to the left to provide an additional viewing angle of the crash test. A schematic of the five high speed camera locations for test MBN-4 is shown in Figure 16.

The film was analyzed using the Vanguard Motion Analyzer. Actual camera speed and camera divergence factors were considered in the analysis of the high-speed film.

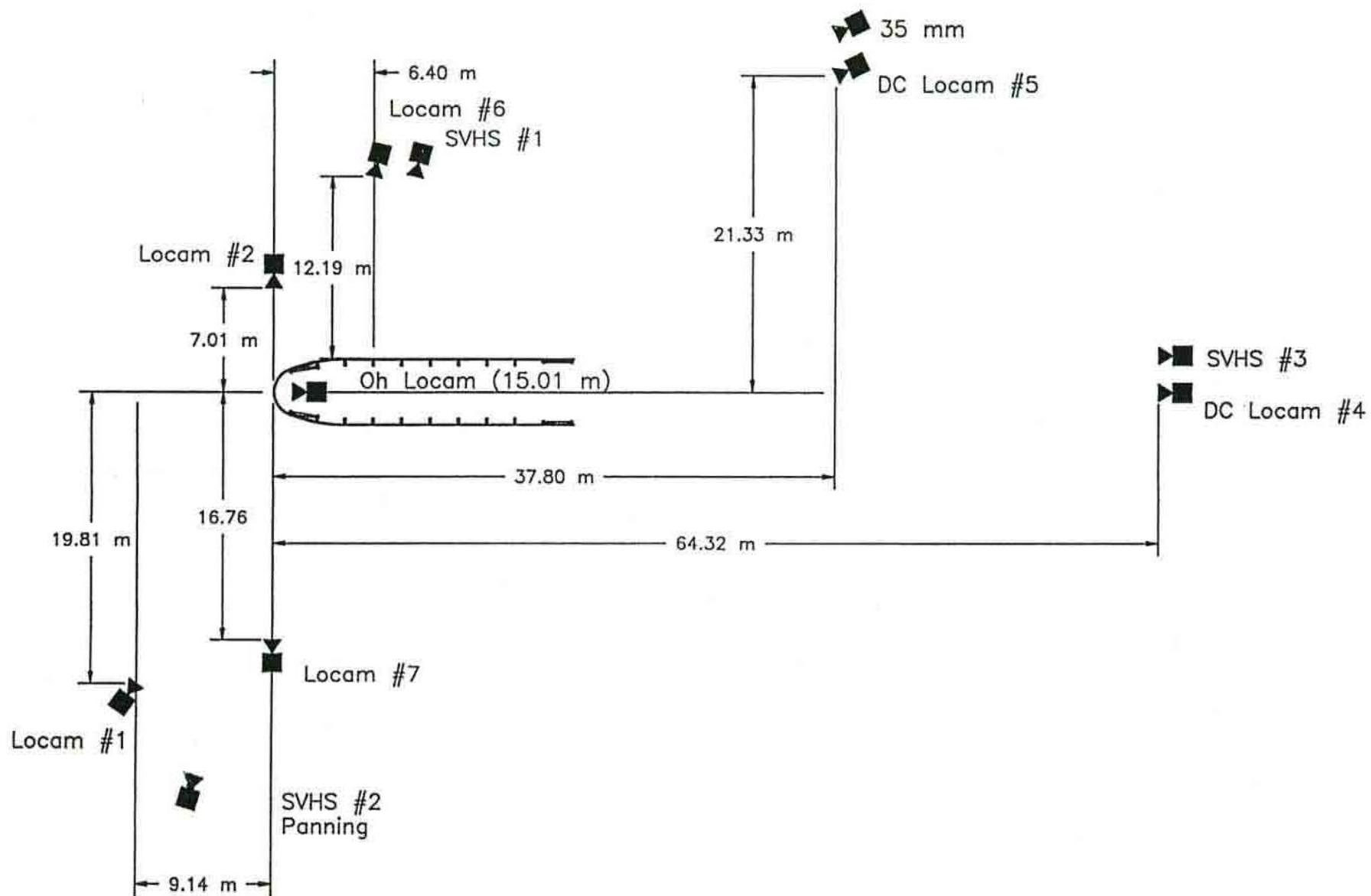


Figure 15. Location of High-Speed Cameras, Test MBN-3

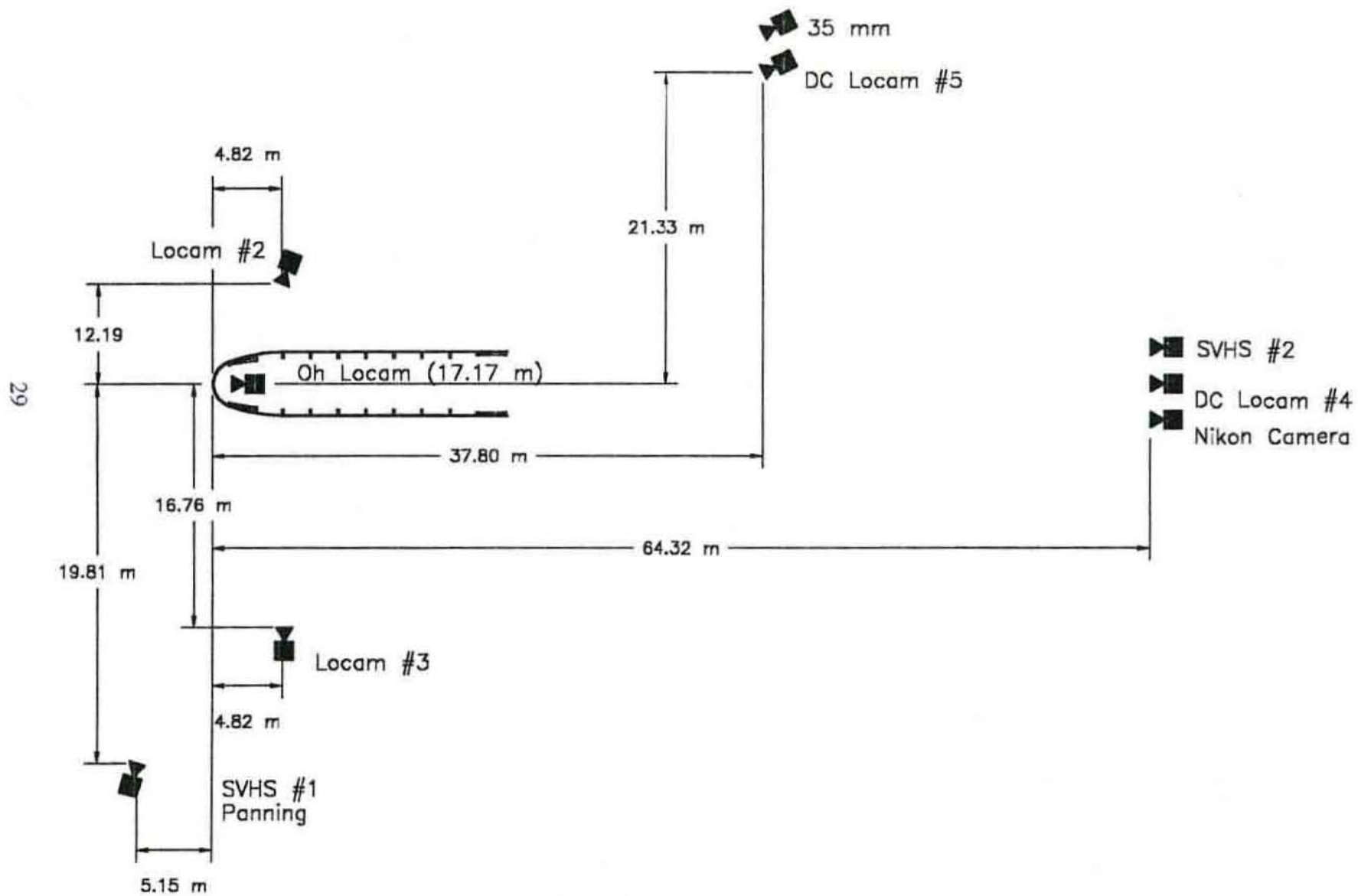


Figure 16. Location of High-Speed Cameras, Test MBN-4

4.4.4 Pressure Tape Switches

For tests MBN-3 and MBN-4, five pressure-activated tape switches, spaced at 2-m intervals, were used to determine the speed of the vehicle before impact. Each tape switch fired a strobe light which sent an electronic timing signal to the data acquisition system as the left front tire of the test vehicle passed over it. Test vehicle speeds were determined from electronic timing mark data recorded on "Test Point" software. Strobe lights and high-speed film analysis are used only as a backup in the event that vehicle speeds cannot be determined from the electronic data.

4.4.5 Strain Gauges

For test MBN-3, a series of strain gauges were installed on the thrie beam guardrail that consisted of eight gauges located the front side of the thrie beam rail. The strain gauge positions are given in Table 3, and photographs showing the gauges on the bullnose barrier are shown in Figure 17. Strain gauges were not used in the instrumentation for the small car test, test MBN-4.

For test MBN-3, weldable strain gauges were used and consisted of gauge type LWK-06-W250B-350. The nominal resistance of the gauges was 350.0 ± 1.4 ohms with a gauge factor equal to 2.02. The operating temperature limits of the gauges was -195 to +260 degrees Celsius. The strain limits of the gauges were 0.5% in tension or compression ($5000 \mu\epsilon$). The strain gauges were manufactured by the Micro-Measurements Division of Measurements Group, Inc. of Raleigh, North Carolina. The installation procedure required that the metal surface be clean and free from debris and oxidation. Once the surface had been prepared, the gauges were spot welded to the test surface.

A Measurements Group Vishay Model 2310 signal conditioning amplifier was used to condition and amplify the low-level signals to high-level outputs for multichannel, simultaneous dynamic recording on "Test Point" software. After each signal was amplified, it was sent to a Keithly

Metrabyte DAS-1802HC data acquisition board, and then stored permanently on the portable computer. The sample rate for all gauges was 5,000 samples per second (5,000 Hz), and the duration of sampling was 6 seconds.

Table 3. Strain Gauge Locations, Test MBN-3

STRAIN GAUGE INSTRUMENTATION		
GAUGE NUMBER	POSITION	DISTANCE
1	Middle Hump-Top Neutral Axis - Front Side	CL slot 216-mm Downstream Post # 2 CL
2	Middle Hump-Bottom Neutral Axis - Front Side	CL slot 216-mm Downstream Post # 2 CL
3	Middle Hump-Top Neutral Axis - Front Side	216-mm Downstream Post # 3 CL- 2" from Slot
4	Middle Hump-Bottom Neutral Axis - Front Side	216-mm Downstream Post # 3 CL- 2" from Slot
5	Top Hump-Top Neutral Axis - Front Side	210-mm Downstream Post # 4 CL- 2" from Slot
6	Middle Hump-Top Neutral Axis - Front Side	210-mm Downstream Post # 4 CL- 2" from Slot
7	Middle Hump-Bottom Neutral Axis - Front Side	210-mm Downstream Post # 4 CL- 2" from Slot
8	Bottom Hump-Bottom Neutral Axis - Front Side	210-mm Downstream Post # 4 CL- 2" from Slot

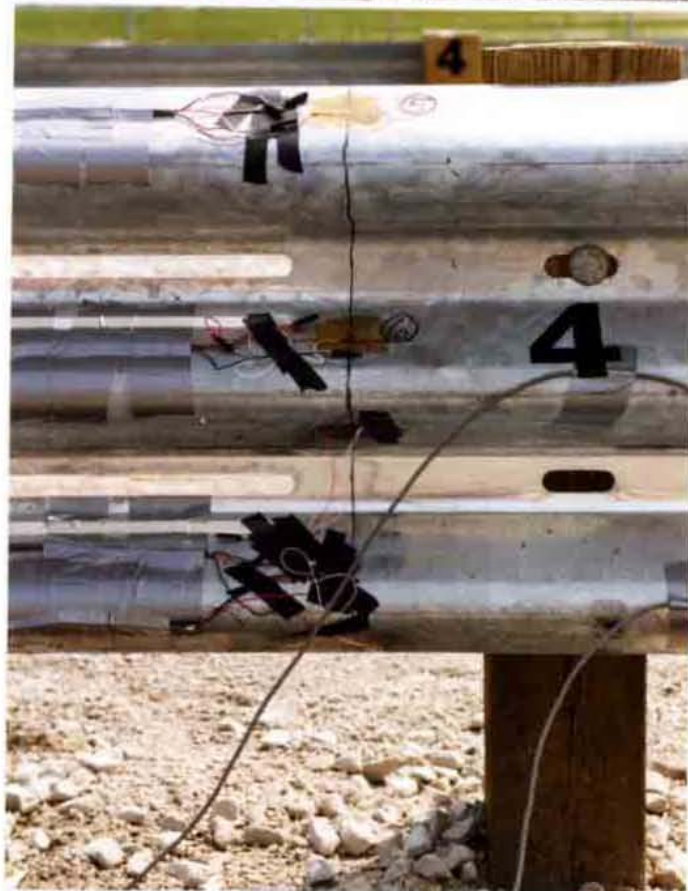
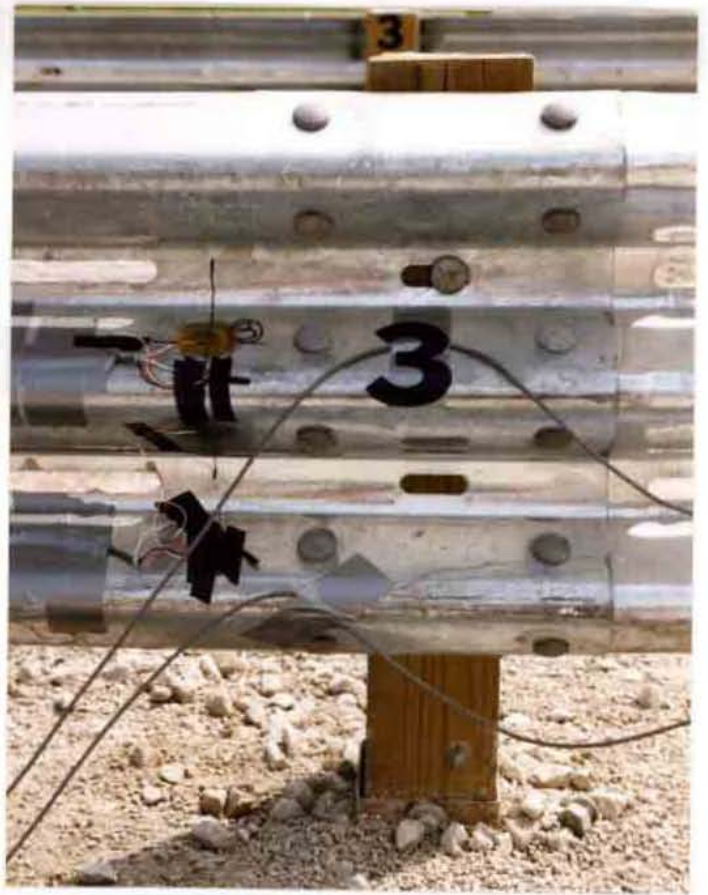


Figure 17. Strain Gauges for Full Scale Test MBN-3

5 CRASH TEST MBN-3

5.1 Test MBN-3

The 1,989-kg pickup truck impacted the bullnose barrier at a speed of 100.16 km/h and an angle of -1.08 degrees. A summary of the test results and the sequential photographs are shown in Figure 19. Additional sequential photographs are shown in Figure 20. Full-scale crash documentary photographs are shown in Figures 21 and 22.

5.2 Test Description

Following the initial impact with the pickup truck, the thrie beam rail immediately began to deform inward. At 0.054 sec after impact, a tear in the thrie beam rail began to occur in the middle hump just to the right of the centerline of the nose section. The middle hump was aligned directly with the bumper at impact and subsequently fractured. Unlike the middle hump, the upper hump of the rail did not fail immediately after impact. The bottom hump was impacted below the bumper and was pushed underneath the bumper and driven over by the front tires. As the pickup penetrated further into the barrier, post no. 1 on both sides was fractured as the beam wrapped around the posts at 0.076 sec. The first kink in the rail was formed downstream of the first rail splice on the right side of the barrier. At 0.200 sec, this kink impacted and dented the right-side door of the pickup. The pickup truck then continued to penetrate the system, kinking the rail at the cable box on the left side and forming a second kink at post no. 2 on the right side. As the rail wrapped around post no. 2 on both sides, high stresses in the top hump of the thrie beam, which was now carrying most of the impact load, caused the rail to tear. The tear occurred at 0.208 sec after impact at a location slightly to the left of the centerline of the bullnose. Post no. 2 on the left side of the barrier was also broken due to rail wrapping around the post. Following the rupture of the rail, the pickup truck proceeded

through the middle of the bullnose barrier and fractured post no. 11 at 0.876 sec as it exited the bullnose barrier. Figure 23 shows the trajectory of the pickup truck during the crash test and the final position of the vehicle.

5.3 Vehicle Damage

Vehicle damage was moderate, as shown in Figure 24. The front bumper and front end of the truck were crushed inward uniformly. The bumper was bent and flattened across the length of the pickup. The left-front fender of the pickup truck was crushed inward due to the barrier impact. The lower-front section of the left door was also crushed inward, and some of the sheet metal on the door was ripped and scratched. The left-front and left-rear tires were cut and deflated. There was no significant rim damage. The tires on the right side were not damaged and remained inflated. The right-front fender was crushed back toward the right door due to the barrier impact. The right door was crushed inward and a 152.8-mm cut was made near the center of the door. The window on the right door was also shattered. There was no crushing of the pickup truck's occupant compartment.

5.4 Barrier Damage

Barrier damage was extensive, as is shown in Figures 25 through 27. Three of the BCT posts fractured at the hole near the base of the post. Post no. 1 on both sides of the barrier was broken along with post no. 2 on the left side of the barrier. Post no. 11 on the left side of the barrier was contacted and broken as the truck exited through the middle of the barrier. The thrie beam buckled and bent around the cable box 813-mm upstream of post no. 2 on the left side of the barrier. The thrie beam also buckled at two locations on the right side of the barrier. The first buckle occurred at the start of the first set of slots downstream of the first rail splice, while the second buckle occurred around post no. 2.

The thrie beam tore in two places during the pickup truck impact. The first tear occurred 381-mm downstream and to the right of the nose of the barrier in the middle hump of the thrie beam. The second tear occurred 343-mm downstream and to the left of the nose of the barrier in the top hump of the beam. The lowest hump in the rail did not tear completely but did have partial rupture 381-mm downstream and to the right of the nose of the barrier. There were also some cuts in the rail on the right side of the barrier during impact. Major rips in the rail were found at 279-mm and at 178-mm upstream of post no. 1.

5.5 Occupant Risk Values

The normalized longitudinal and lateral occupant impact velocities (OIV) were determined to be 5.10 m/s and 1.36 m/s, respectively. The maximum 0.010-sec average occupant ridedown deceleration (ORD) in the longitudinal and lateral directions was 3.31 g's and 4.57 g's, respectively. It is noted that the occupant impact velocities and occupant ridedown decelerations were within the suggested limits provided in NCHRP Report No. 350. The results of the occupant risk data are summarized in Figure 19. Results are shown graphically in Appendix A.

5.6 Discussion

Following test MBN-3, a safety performance evaluation was conducted, and the bullnose barrier design was determined to be unacceptable for Test 3-31 according to NCHRP Report No. 350 criteria. The bullnose barrier did not contain or stop the test vehicle in a controlled manner due to the fracture of the thrie beam during the impact. However, it should be noted that the pickup truck did not override the thrie beam during the impact prior to the thrie beam fracture. Detached elements and debris from the test article did not penetrate or show potential for penetrating the occupant compartment. There was no deformation of, or intrusion into, the occupant compartment that could

have caused serious injury. The vehicle remained upright during and after collision and the vehicle's trajectory did not intrude into adjacent traffic lanes. Vehicle trajectory behind the test article was unacceptable as the test vehicle penetrated through the barrier and into the median area behind the bullnose. The occupant impact velocities and ridedown accelerations were within the suggested limits imposed by NCHRP Report No. 350.

The failure of the system to meet all of the safety performance criteria was directly attributed to the fracture of the thrie beam. The fracture of the thrie beam in test MBN-3 occurred more rapidly than during test MBN-1. This behavior was believed to be attributed to the direct alignment of the Chevrolet pickup truck's front bumper with the middle hump of the thrie beam in test MBN-3. It is believed that this impact condition caused high stresses and strains to be generated immediately in the middle hump of the thrie beam nose section, thus leading to rapid rupture of the middle hump. For test MBN-1, the Ford's front bumper was aligned to contact both the top and middle humps of the thrie beam. This impact condition resulted in a more gradual increase and distribution of stresses and strains in the middle and top humps. However, it was noted that rail rupture still occurred. It became obvious to the researchers that the middle and top thrie corrugations were inadequate to contain the impacting head-on pickup truck in the present configuration. The top mounting heights for the Ford and Chevrolet bumpers were 737-mm (test MBN-1) and 622-mm (test MBN-3), respectively. A comparison of the bumper heights is shown in Figure 28.

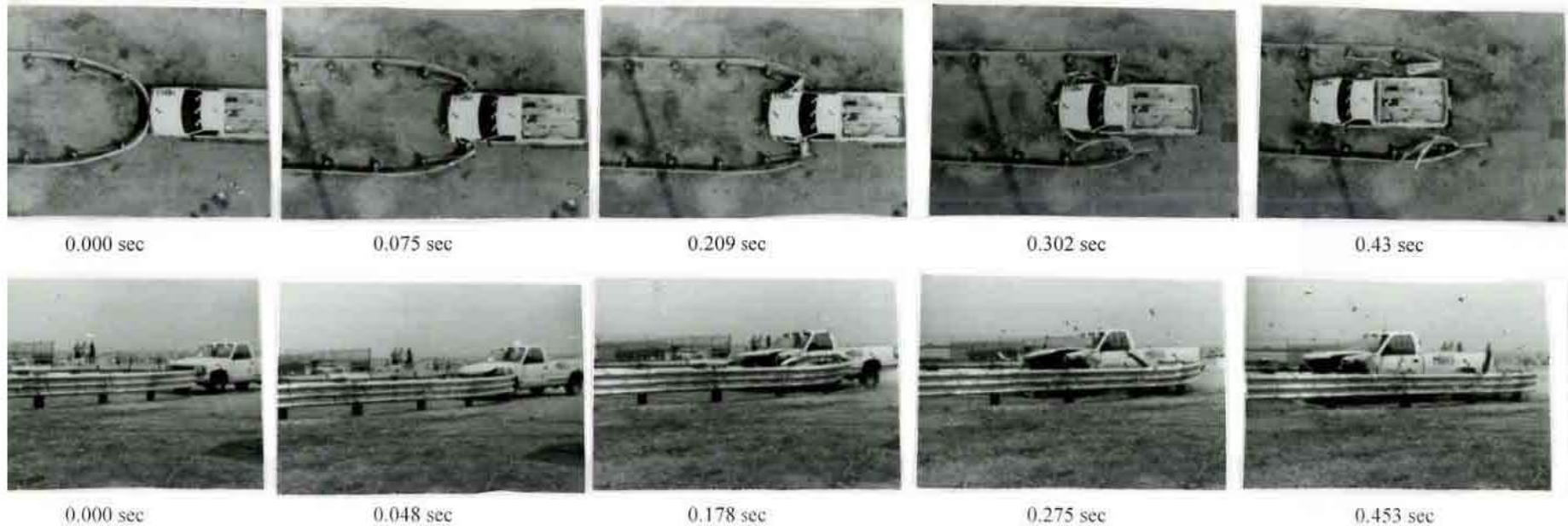
Design changes were therefore necessary to contain the pickup truck by preventing rail fracture or contain the pickup even if rail fracture occurred. However, these design modifications, intended to adequately contain the pickup truck impact, were to be incorporated without adversely affecting the small car's impact performance.

5.7 Barrier Instrumentation Results

For test MBN-3, strain gauges were located on the thrie beam rail. The results of the strain gauge analysis are provided in Table 4. Graphs of the data taken from gauge nos. 1 through 8 are located in the Appendix B (Figures B-1 through B-16).



Figure 18. Impact Location, Test MBN-3



- Test Number MBN-3
- Date 5/6/98
- Appurtenance Bullnose Median Barrier
- Total Length 20,144 mm
- Steel Thrie Beam (Nested)
 - Thickness 12 gauge (2.66 mm)
 - Top Mounting Height 804 mm
- Wood Posts
 - Post Nos. 1 - 2, 10 - 11 140 mm x 190.5 mm x 1080-mm long
 - Post Nos. 3 - 9 150 mm x 200 mm x 1980-mm long
- Wood Spacer Blocks
 - Post Nos. 1 - 8 150 mm x 200 mm x 320-mm long
- Soil Type Grading B - AASHTO M 147-65 (1990)
- Vehicle Model 1990 Chevy 2500 2WD
 - Curb 1,828 kg
 - Test Inertial 1,989 kg
 - Gross Static 1,989 kg
- Vehicle Speed
 - Impact 100.16 km/hr
 - Exit NA

- Vehicle Angle
 - Impact -1.08 deg
 - Exit NA
- Vehicle Snagging None
- Vehicle Stability Satisfactory
- Occupant Ridedown Deceleration (10 msec avg.)
 - Longitudinal 3.31 g's
 - Lateral (not required) 3.32/-4.57 g's
- Occupant Impact Velocity (Normalized)
 - Longitudinal 5.10 m/s
 - Lateral (not required) 1.36 m/s
- Vehicle Damage Moderate
 - TAD (17) 12-FD-4 // 3-RP-1
 - SAE (18) 12FDEW4
 - 03RPEW1
- Vehicle Stopping Distance 56.72 m downstream
20.54 m left of centerline
- Barrier Damage Extensive rail damage and
three fractured posts
- Maximum Deflections
 - Permanent Set NA
 - Dynamic NA

Figure 19. Summary and Sequential Photos, Test MBN-3



0.00 sec



0.054 sec



0.150 sec



0.208 sec



0.876 sec

Figure 20. Additional Sequential Photographs, Test MBN-3



Figure 21. Full-Scale Crash Test MBN-3



Figure 22. Full-Scale Crash Test MBN-3

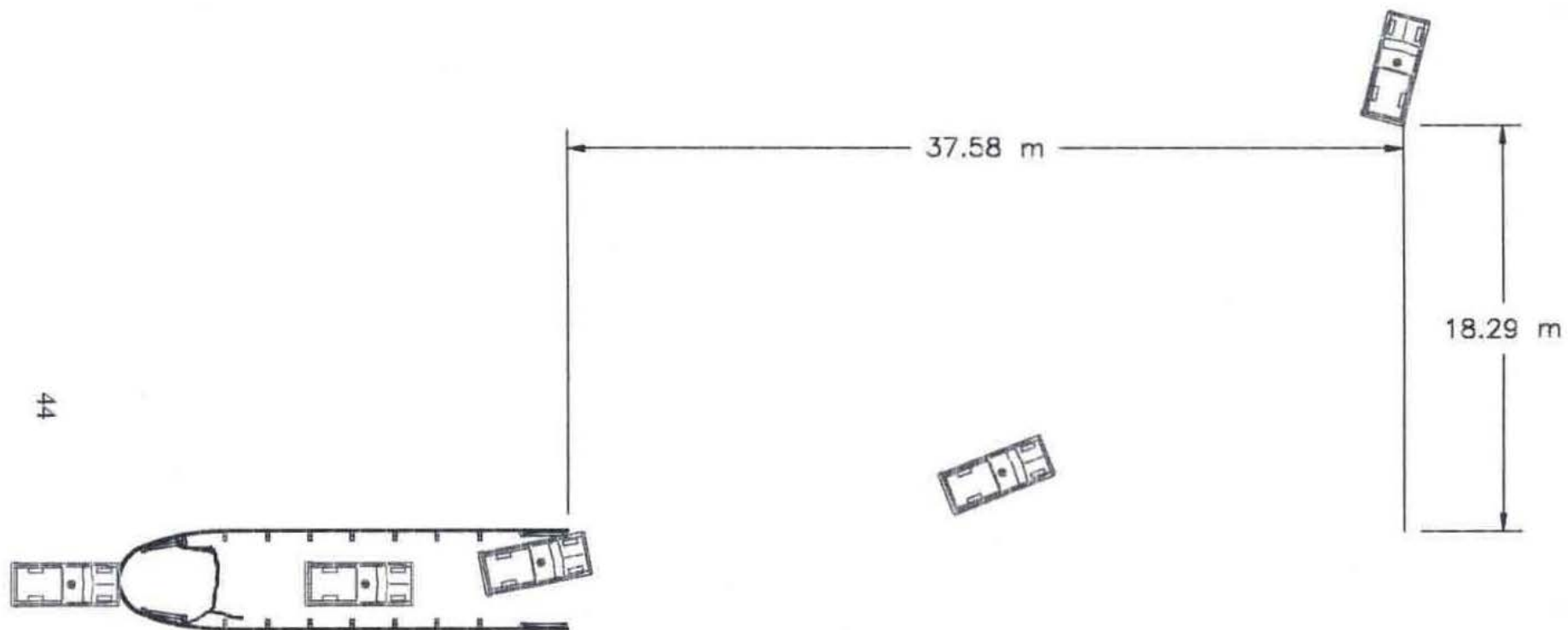


Figure 23. Vehicle Trajectory, MBN-3



Figure 24. Vehicle Damage, Test MBN-3



Figure 25. Barrier Damage, Test MBN-3



Figure 26. Barrier Damage, Test MBN-3



Figure 27. Barrier Damage, Test MBN-3



Figure 28. Front Bumper Impact Heights, Test MBN-1 and MBN-3

Table 4. Strain Gauge Data, Test MBN-3

Hardware type	Strain Gauge No.	Maximum μ Strain ¹ (mm/mm)	Maximum Stress ² (MPa)	Comments
Thrie Beam	1	923	190.16	None
	2	997	206.29	None
	3	269	55.71	None
	4	381	78.81	None
	5	312	64.47	None
	6	216	44.68	None
	7	227	46.95	None
	8	327	67.64	None

¹- All strain values are shown as the absolute value only

²- All elastic stress values are shown as the absolute value only and calculated by multiplying the strain by the modulus of elasticity equal to 30,000 ksi. Minimum yield stress for the thrie beam is 50 ksi.

NA- Not Available

6 COMPUTER SIMULATION OF TEST MBN-3

6.1 Simulation Objective

The computer simulation methods used in this project consisted of using nonlinear FEA to help determine the cause of the thrie beam fracture in test MBN-3 and to help determine possible solutions. LS-DYNA was the simulation code chosen to perform the simulation (21). Test MBN-3 was simulated to examine the failure of the bullnose barrier and to develop a validated model for future simulation.

6.2 Finite Element Model

To simulate test MBN-3, a vehicle model and a bullnose model were needed. FHWA had previously contracted model development of the C2500 pickup truck to the National Crash Analysis Center (NCAC) (22). NCAC subsequently developed two models, a large detailed model (approximately 50,000 elements) and a reduced model (approximately 10,000 elements). The truck models were primarily developed for frontal impact scenarios. For the bullnose project, the reduced truck model was deemed appropriate.

6.2.1 Bullnose Model

The bullnose is composed of many components, including wood posts, cable anchor bracket assemblies, guardrail, ground-line struts, foundation tubes and various brackets and attachment bolts. The modeling of the guardrail component in the simulation was critical for proper model results. The guardrail model consists of two important elements. First, the mesh size of the rail is important to ensure accuracy and to ensure efficient computer simulation times. These criteria are somewhat in conflict in that a refined mesh often improves accuracy while at the same time increases computer requirements. Second, failure of the rail material must be reasonably accurate in order to replicate

test MBN-3. A subsequent study was done of the rail mesh size, including considerations for internal energy absorption, peak forces, quality of kinks, and CPU execution time. It was decided that a mesh with 42 elements in the cross section and a 50-mm length along the rail was appropriate for the bullnose model.

The wood posts were also considered an important component of the model. Fortunately, a previous study on the SKT end terminal had already investigated appropriate modeling techniques for the wood posts in the bullnose system (23).

Since the goal of the simulation was to determine the cause of the bullnose failure and to investigate potential design fixes, detailed modeling would only be added as needed. This meant that several components were modeled without extreme detail, such as (1) splices modeled by doubling the rail thickness at splice locations; (2) slots made in the rail by removing elements without rounding out the corners; (3) a cable anchor box was not modeled; (4) the post connections modeled with spot welds with failure set at loads determined from previous component testing; and (5) the model extended to the location of post no. 5 but included only the first 3 posts.

These modeling techniques were justified for four reasons: (1) test results indicated that those components listed above did not greatly influence the performance; (2) positive results with previous modeling using the stated techniques; (3) the sponsors of the project wanted timely results and modeling details for every component would slow the project down; and (4) the CPU time needed for simulation was to be controlled as much as possible, detailed component modeling often requires many more elements.

6.2.2 Truck Model

Version 7 of the NCAC reduced truck model was downloaded from the NCAC web site and was modified for this study. Changes made to the model included: (1) the units of the model were converted to kg, mm and ms, (2) the format was changed from structured to keyword, (3) the material properties were reduced to a minimal set using the capabilities of the part and material keywords available in LS-DYNA, (4) the vehicle was translated and rotated to match with the bullnose location, (5) and various control parameters were changed to be consistent with the bullnose model. Once the modifications were made, the vehicle model was impacted into a rigid wall and compared to results from simulation of the unmodified truck model. The results indicated that the modifications made no significant changes from the unmodified truck simulation results.

6.3 Material Failure

Initial simulation of the model described above did not accurately simulate test MBN-3, because the guardrail material did not tear during the simulation. This required a more detailed investigation into material failure. A component test and corresponding component simulation were set-up to mimic the tab tearing between the slots in the center section of the rail. Two different tab sizes were investigated, one 25 mm in length and the other 50 mm in length. Using a Material Testing Systems (MTS) machine, the right ends of the samples were pulled apart until the tabs failed and the force levels were recorded. Four static component tests were completed with each tab size. Photographs of the slot tab testing are shown in Figure 29.

During component testing, the 25-mm length tab tore at an average maximum force of 23.7 kN, while the 50-mm tab tore at an average of 27.2 kN, resulting in approximately a 15 percent increase in strength. Computer simulation of the component testing, using an effective plastic strain



Figure 29. Physical Testing of Slot Tabs

failure of 0.2, failed the tabs at 24.7 kN for the 25-mm tab and 27.1 kN for the 50-mm tab. Simulation results compared very well with component testing results, and thus, the material properties from the component simulation could be used with confidence. One item of note was the required mesh density. In order to get reasonable tearing, the mesh density had to be relatively fine compared to the initial bullnose guardrail mesh. Thus, the bullnose guardrail mesh was refined by a factor of four to obtain the correct failure behavior.

6.4 Rotating Tires

Using the material properties obtained from the component study and the refined rail mesh, the bullnose model was again simulated. This time, the tabs connecting the peaks of the thrie beam tore, allowing the rail to wrap around the front of the truck, as seen in Figure 30. However, as shown in Figure 30, the lower peak of the rail caught on the front tires. In the physical test, the rail was pushed down, and the front tires rolled over the lower rail section. It was thought that the difference between test and simulation results was due to the absence of a rotating tire in the model. Thus, capabilities for a rotating tire were added to the model.

The initial wheel assembly on the truck model consisted of four parts that were rigidly attached together, thus preventing tire rotation. These four parts are the knuckle, spindle (which is actually a combination of the brake rotor and spindle), wheel and tire. A fifth part, referred to as an axle, was added to the model to efficiently add rotation capabilities. These parts are depicted in Figure 31.

The knuckle and spindle are defined as rigid materials and are combined using the merge rigid bodies function. These two parts move with the body of the vehicle. The axle is a rigid material and is located such that its two center end nodes coincide with nodes on the spindle shaft.

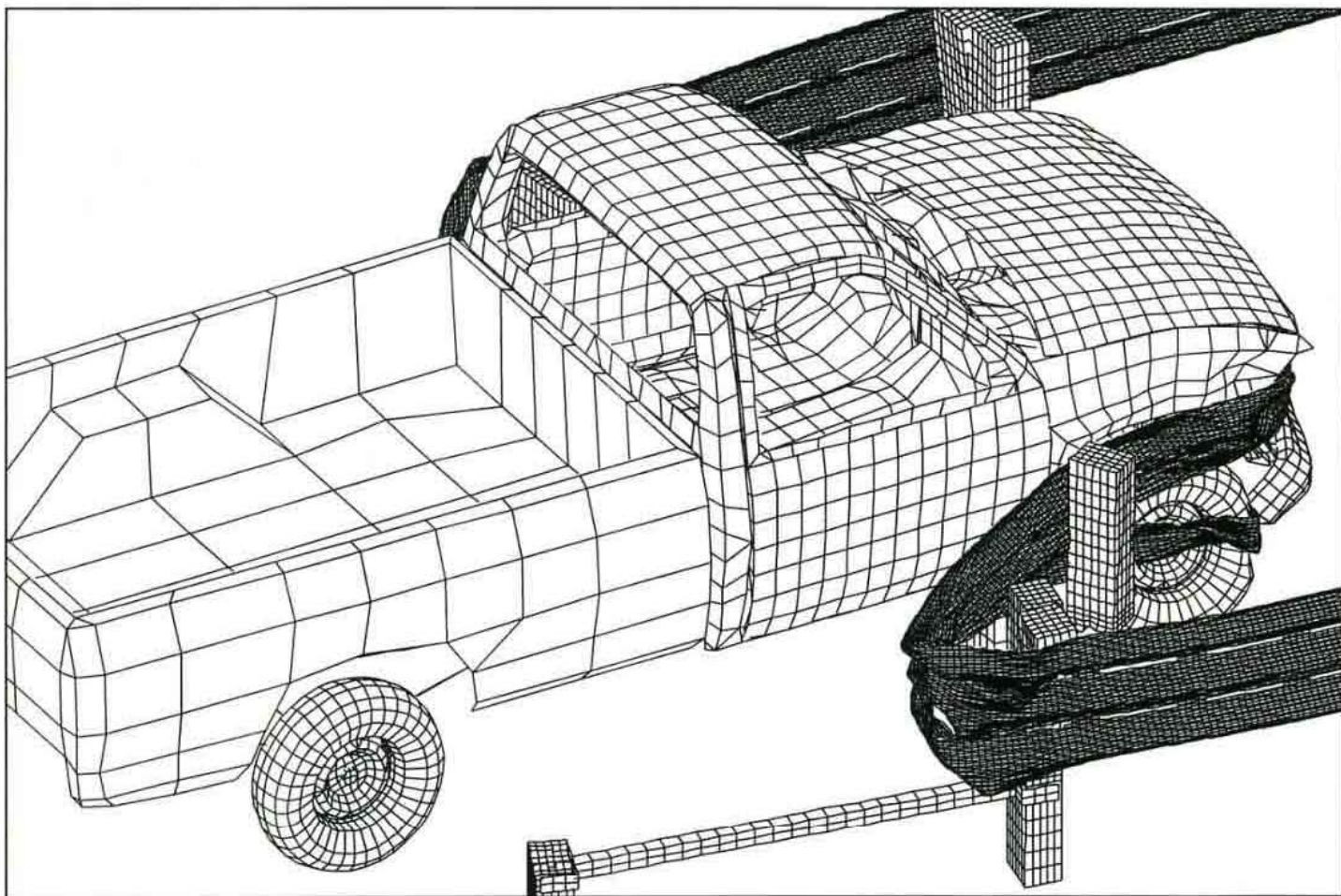
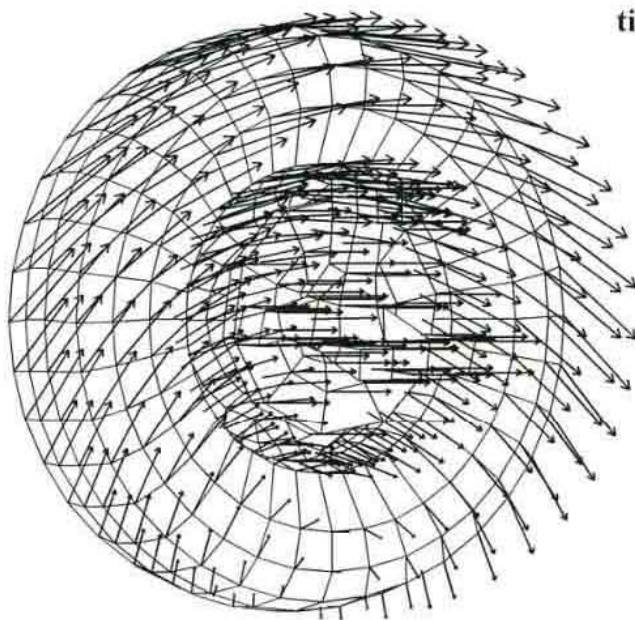
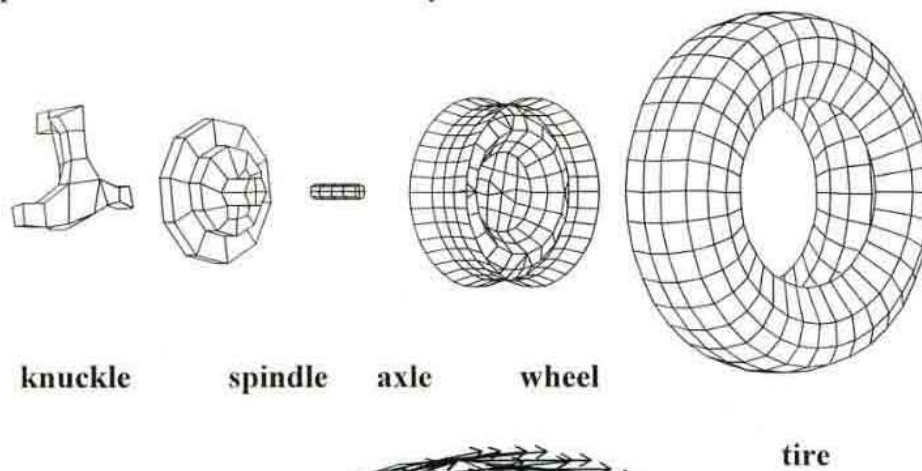


Figure 30. Lower Rail Catches on Tire

Exploded View of Wheel Assembly



Velocity Vectors

Figure 31. Rotating Tire

These coincident nodes are used to define a revolute joint in LS-DYNA. Thus, the axle is allowed to rotate relative to the spindle about the center line of the spindle. The wheel is attached to the axle by assigning nodes around the center of the wheel as extra nodes on the axle rigid body. The wheel is defined as a deformable metal. The tire is defined using an airbag so that it is a pressurized deformable structure. The mesh of the tire and wheel are such that they are connected at common nodes. Because the wheel and tire are connected to the axle, they also rotate relative to the spindle and the rest of the vehicle body.

The rotating tire model was then added to both front tires of the truck model, and the bullnose simulation was repeated. Contact snagging occurred between the rotating tire and the lower rail as the rail was indeed pushed below the tire due to the rotation of the tire. In order to eliminate the contact troubles, the tire mesh was refined in order to provide more uniform contact forces between the tire and the rail.

6.5 MBN-3 Bullnose Simulation

With material failure and rotating tires defined, simulation of test MBN3 was repeated. This time the results were very encouraging, as shown in Figures 32 and 33. As the truck impacted the rail, the three peaks separated, wrapping themselves around the front of the truck. The lower peak contacted the tires and was pushed down and driven over by the front tires. As the rail wrapped around post no. 1, the upper two peaks of the rail tore just before the first splice in the rail. The vehicle then proceeded to penetrate behind the bullnose system. The velocity comparison between test and simulation is shown in Figure 33. After 200 ms, the vehicle was essentially rolling unconstrained and thus, not of concern.

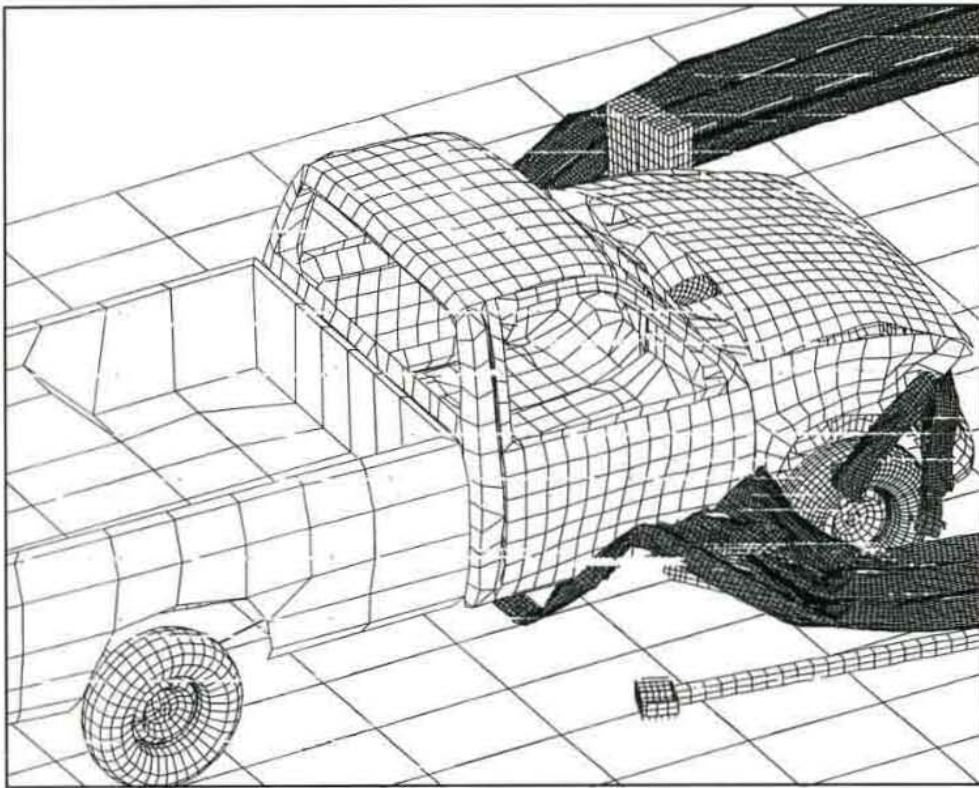
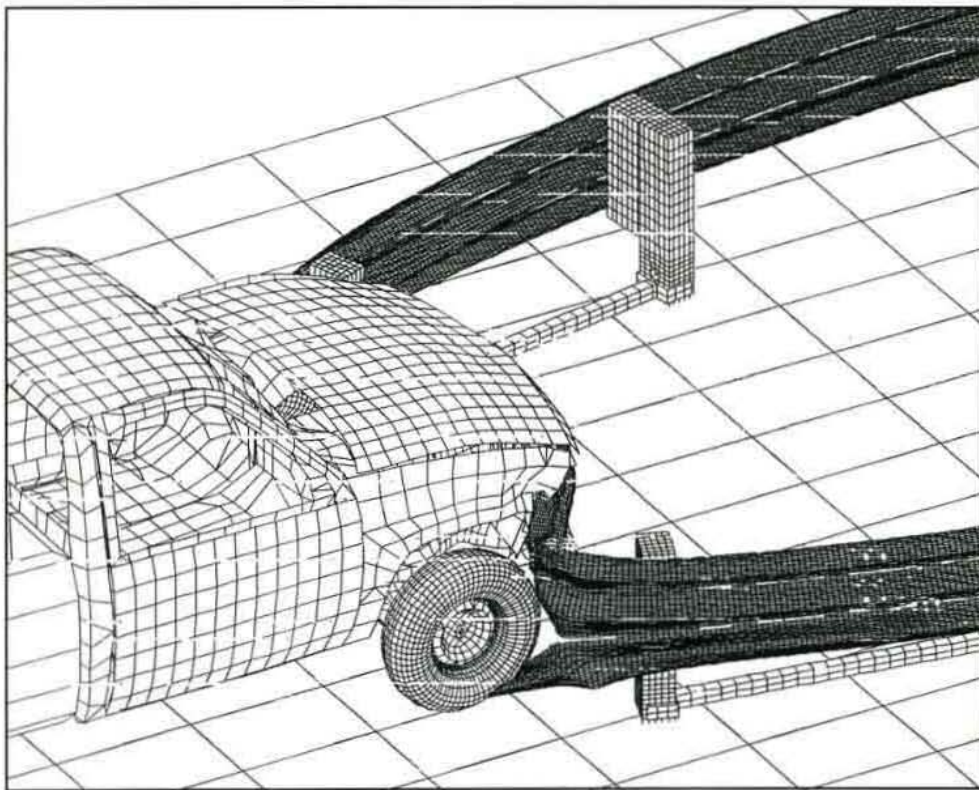


Figure 32. MBN-3 Simulation - Truck Tears Through Guardrail

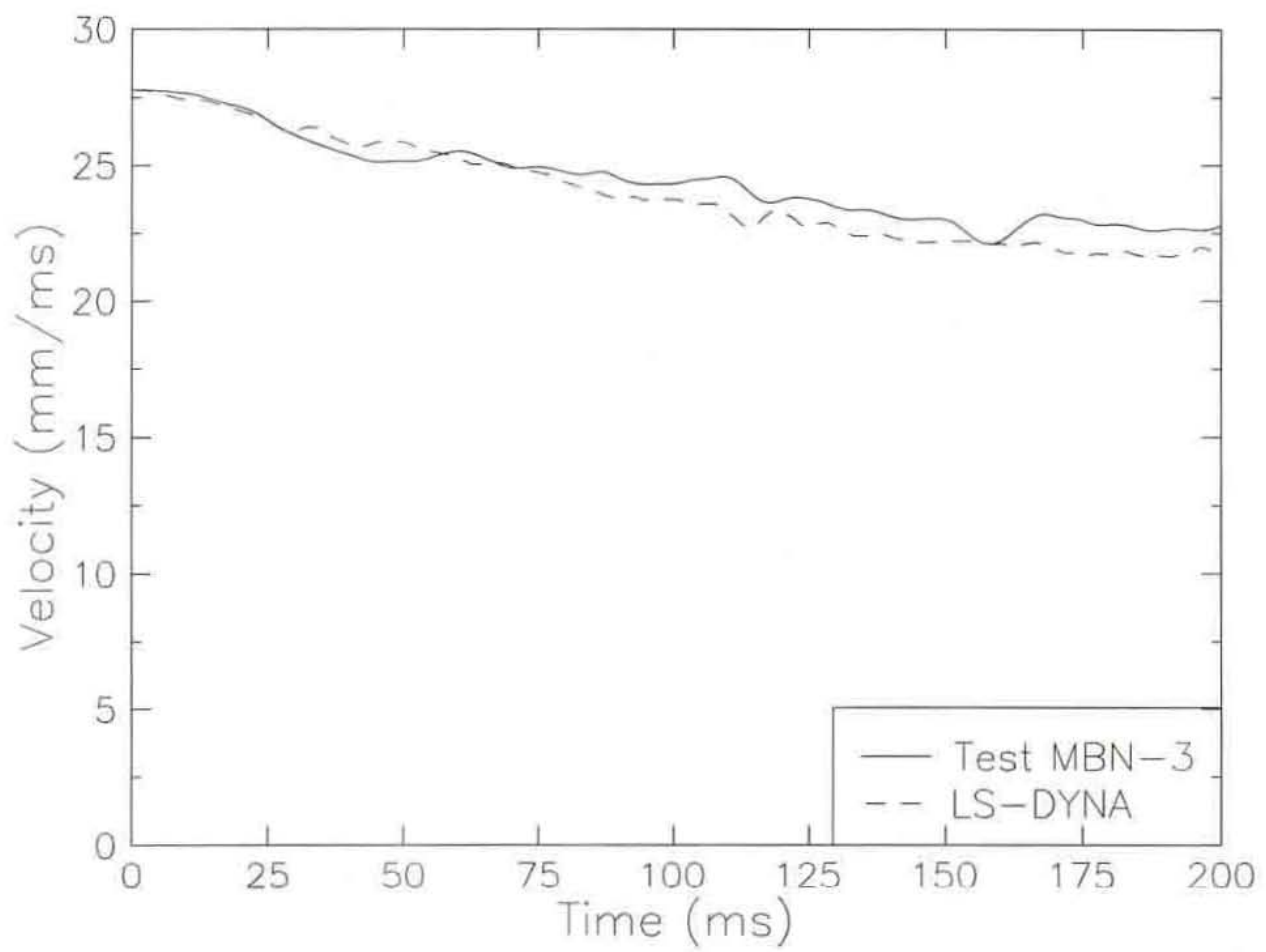


Figure 33. Velocity Comparison for MBN-3

7 BARRIER MODIFICATIONS (DESIGN FOR MBN-4)

7.1 Modification of Bullnose Design

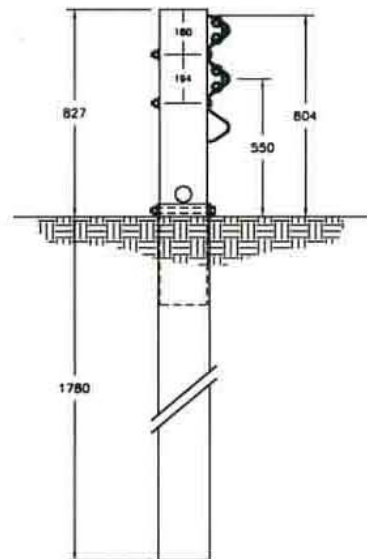
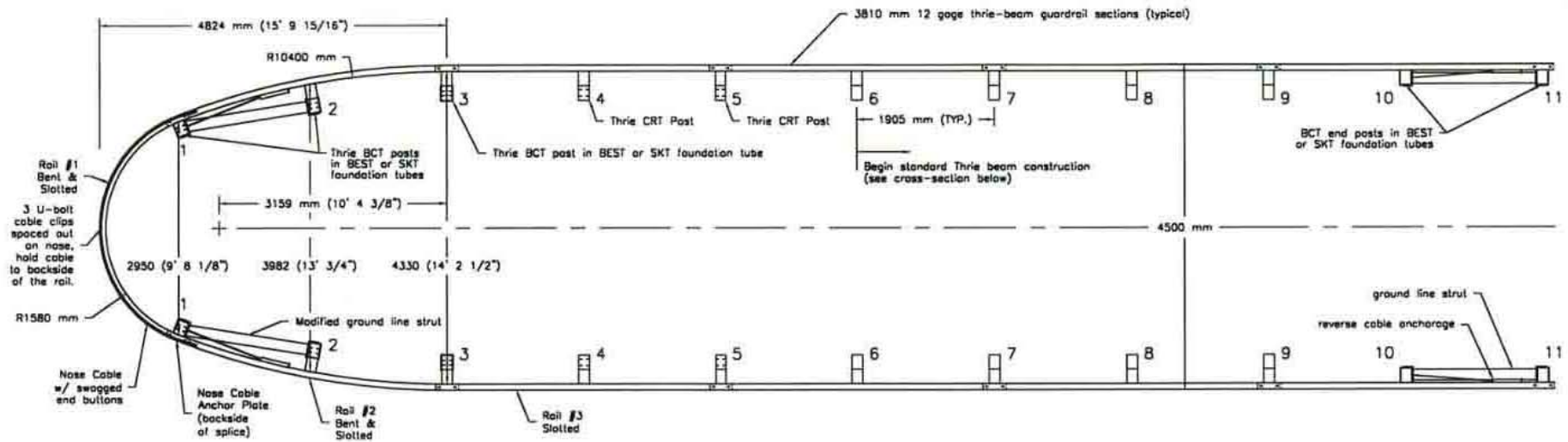
The bullnose barrier system was modified prior to conducting the second full-scale crash test, test MBN-4. The full-scale test results of MBN-3 as well as the LS-DYNA modeling of test MBN-3 demonstrated that it would be very difficult to ensure that a single three beam rail with slots would be capable of containing a pickup truck impact without rail fracture. Therefore, it was deemed necessary to reinforce the first rail section of the bullnose barrier. It was initially suggested that reinforcing or strengthening the nose section be done by nesting two pieces of rail. This idea was discarded because it was feared that increasing the rail thickness and strength would cause the nose to be too stiff and adversely affect the small car's impact performance. A second suggestion was to place a second three beam section at an offset behind the nose section. This design was rejected based on complexity and a desire by the project supporters to have an open area inside the bullnose to allow for easy mowing. A third idea was to weld steel straps to the back of the rail at key locations in an attempt to eliminate the initial rail fracture. The final suggestion was to incorporate a set of steel cables along the backside of the three beam section that would serve to contain the truck in the event of three beam failure, but that would not increase the impact stiffness of the system for the small car impact. A computer simulation model was used to test the feasibility of the cable modification. A more detailed discussion of the computer simulation of the cable modified design is covered in the next section.

A schematic of the modified bullnose design is shown in Figure 34, and photographs are provided in Figures 35 through 36. The only modification to the bullnose barrier system was the addition of the cables and steel retention devices. A 4.38-m long by 15.9-mm diameter cable was

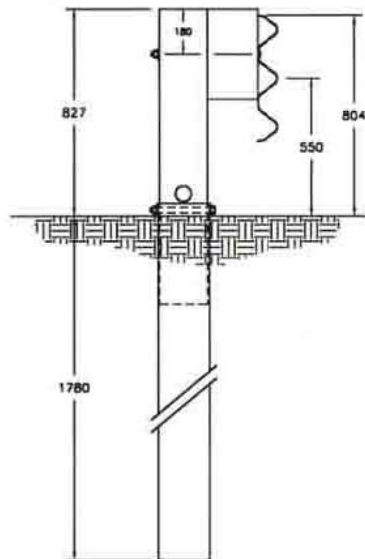
added behind the top and middle humps of the nose section of the beam rail. A 7 x 19 cable was chosen such that one of the two cables was capable of containing the impacting vehicle. Cables were only placed behind the first rail section because it was the only section that had failed in previous testing. It was believed that the rail sections after the nose section would be active in containing the vehicle, and therefore, the use of longer cable lengths was not deemed necessary. The cables were attached to the guardrail using three U-bolts per cable to fix the cables behind the top and middle humps of the beam. The ends of each cable were fitted with "Cold Tuff" buttons and clamped between formed steel plates located at the guardrail splice at post no. 1 on each side. The cable plate and the cable detail are shown in Figure 37.

It was decided that the fourth test be a repeat of test MBN-3 in order to prove that the modified design was capable of capturing the head-on impact with a 2000-kg pickup truck. A rerun of the small car, 1/4-point offset test was deemed unnecessary: since, the barrier modification did not stiffen the nose section of the bullnose barrier in such a way that the small car test would be adversely affected.

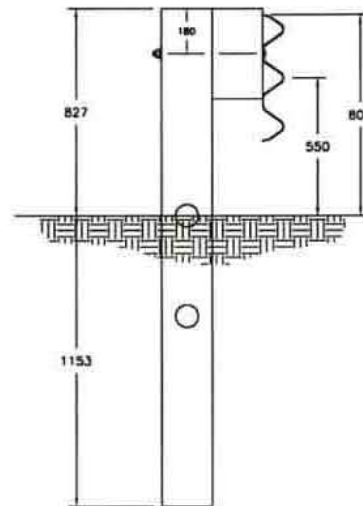
Bull-Nose 350 Test Layout MBN-4 Test



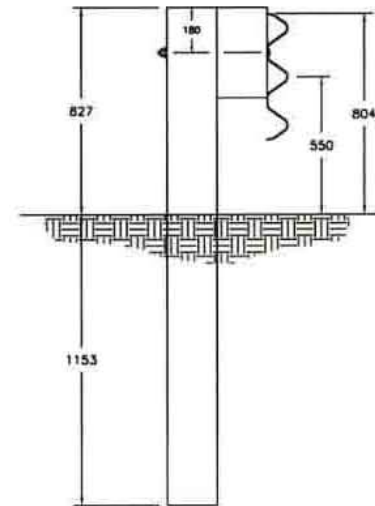
Thrie Beam BCT Post
w/ 1830mm Foundation Tube
Post 1 (as shown)
Posts 10,11 (w/o nose
cables and plates)



Thrie Beam BCT Post
w/ 1830mm Foundation Tube
& 360mm Block
Posts 2,3



Thrie Beam CRT Post
1980mm long
w/ 360mm Block
Posts 4,5



Thrie Beam Post
1980mm long
w/ 360mm Block
Posts 6,7,8,9

Figure 34. Bullnose Barrier Design, Test MBN-4

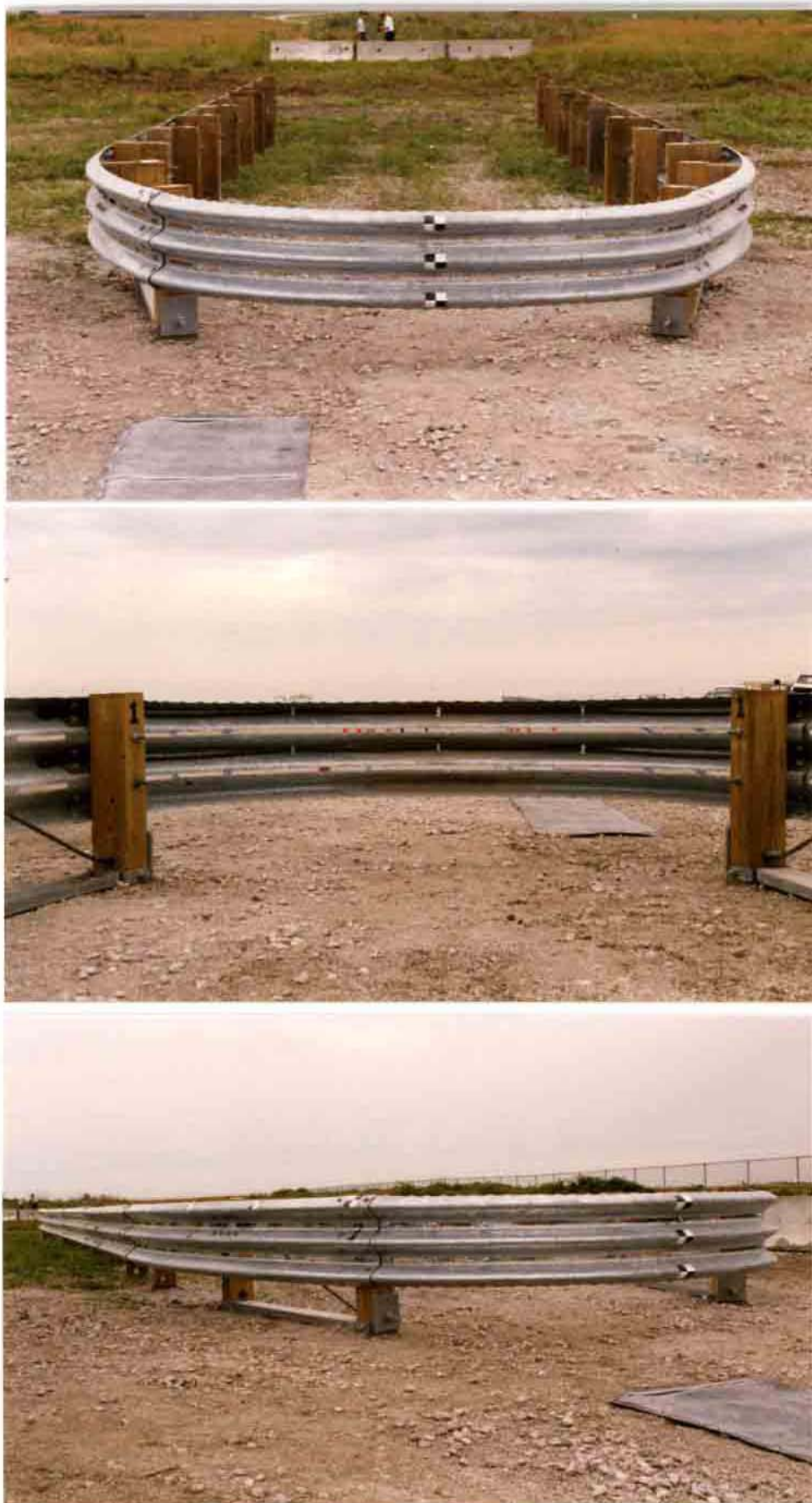
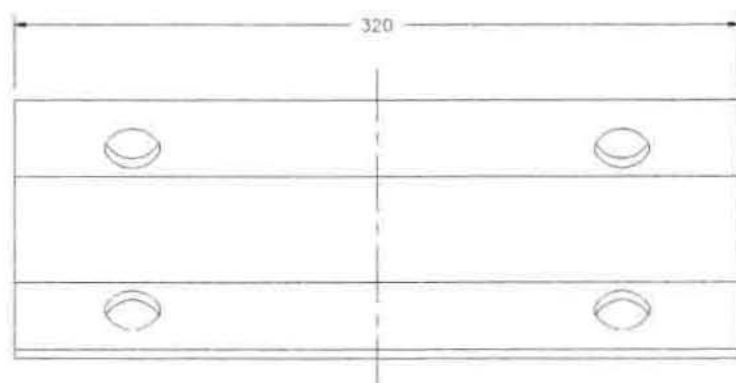
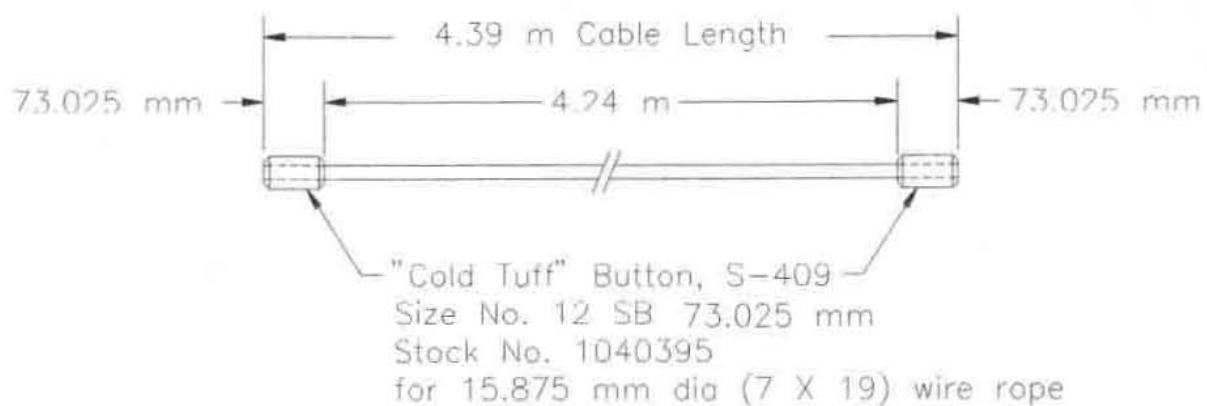


Figure 35. Bullnose Design, Test MBN-4



Figure 36. Bullnose Design, Test MBN-4



Steel Plate, A306
 320mm x 150mm x 5mm

Figure 37. Cable Detail and Cable Plate, Test MBN-4

8 SIMULATION OF MODIFIED DESIGN FOR TEST MBN-4

The modified bullnose barrier with the addition of cables behind the nose section was simulated in LS-DYNA in order to predict the performance of the new design. The simulation was created for a head-on pickup truck impact on the modified barrier design.

A cable, as described previously, was added to the final bullnose model developed after test MBN-3. Beam elements were used to model the cable along with the cable material available in LS-DYNA. The cable material is an elastic material. The size of the cable used in the design was large enough that the cable should remain elastic during impact. Therefore, the cable material was applicable. The contact algorithm for beam elements in LS-DYNA assumes a circular cross section for determining contact. Since the cable is circular, the contact algorithm should be fairly accurate.

Results of the simulation indicated that the cable design would adequately contain the truck during the frontal impact test, as shown in Figure 38. The bullnose simulation took 220 hours for 367 ms of simulation on an SGI Octane. It is noted that the simulation was stopped at 367 ms due to a power outage. The model contained approximately 60,000 deformable elements. Because of the long simulation times, the permission for construction to proceed was given with only partial simulation results available. The permission for testing given after it was clear no further useful information could be gathered from simulation in regards to the proposed design.

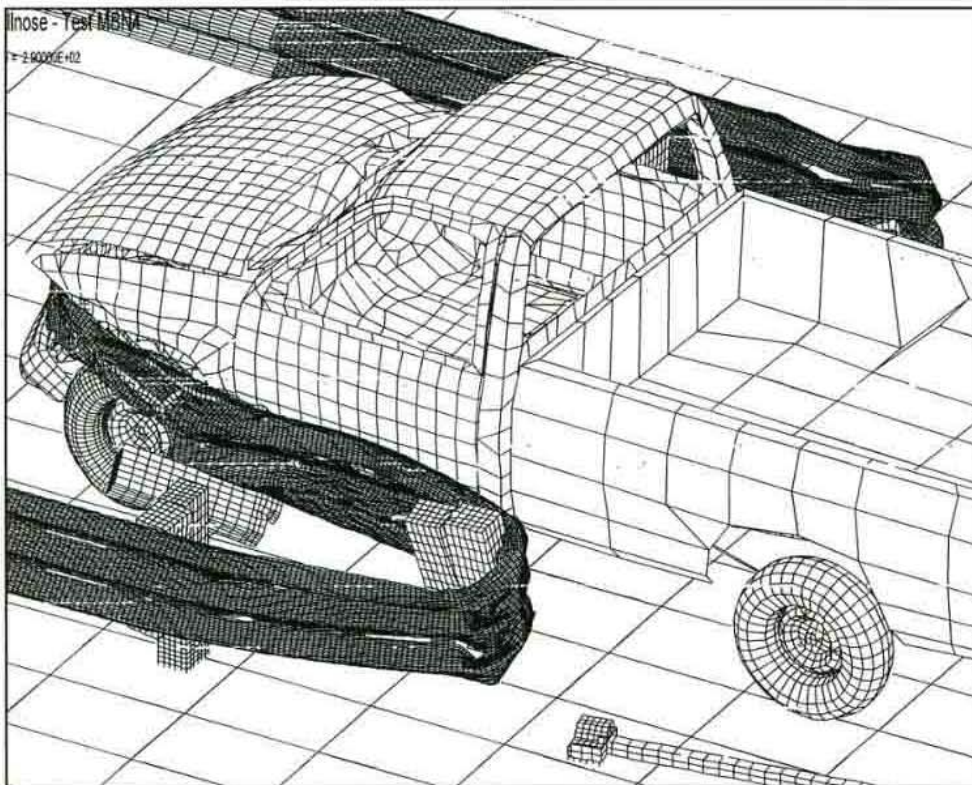
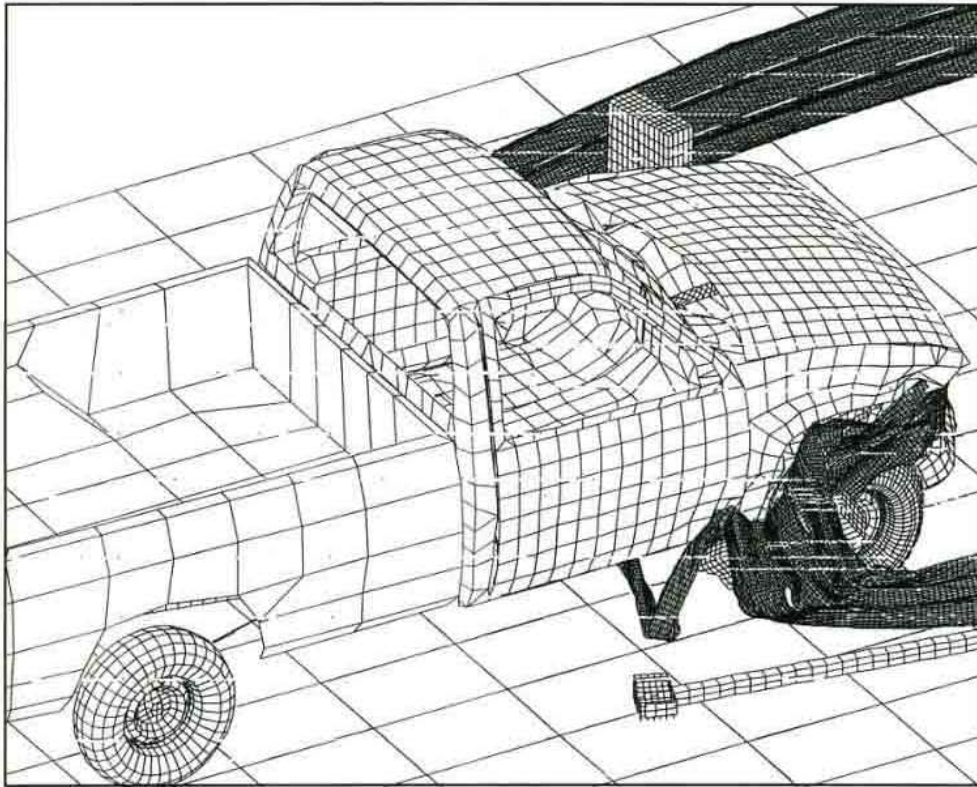


Figure 38. Simulation Results, Test MBN-4

9 CRASH TEST MBN-4

9.1 Test MBN-4

The 2,010-kg pickup truck impacted the bullnose barrier at a speed of 103.50 km/h and an angle of 0.58 degrees. A summary of the test results and the sequential photographs are shown in Figure 40. Additional sequential photographs are shown in Figure 41. Full-scale crash documentary photographs are shown in Figures 42 and 43.

9.2 Test Description

The nose section of the bullnose barrier began to deform immediately after the initial impact. The bottom hump of the thrie beam rail impacted below the bumper of the truck and was pushed under the front tires at 0.052 sec. As the pickup continued to penetrate the bullnose system, the top hump of the rail began to tear at 0.076 sec. Subsequently, at 0.082 sec, the rail wrapped around post no. 1 on both sides, causing the BCT posts to fracture. After the fracture of both post nos. 1, the nose section of thrie beam rail had ruptured completely, leaving the cables to contain the impact. The pickup truck then continued to penetrate the bullnose past post no. 1, deforming the rail inward without the formation of large, sharp kinks in the thrie beam rail. Smaller kinks formed when the rail deformed around the posts, cable boxes, and rail splices. Post nos. 2 on both sides were broken at 0.247 sec when the front of the pickup extended past post no. 3. As the vehicle proceeded, a kink formed between post nos. 2 and 3 on the right side of the system. At 0.301 sec, a rail kink impacted and dented the right side of the pickup truck box between the cab and the rear wheel. Later, the pickup truck moved forward and caused the thrie beam rail to wrap around post nos. 3 and 4 on both sides, resulting in fracture of the posts. At 1.102 sec, the vehicle was then brought to a complete stop as the rail wrapped around post no. 5 with the front wheels of the vehicle even with post no. 9. The

vehicle trajectory is shown in Figure 44.

9.3 Vehicle Damage

Vehicle damage was moderate, as shown in Figure 45. The front end of the pickup truck was crushed, including the bumper, engine compartment, and front quarter panels. The front bumper of the pickup was crushed inward and flattened along the top half. All of the front sheet metal on the truck was crushed uniformly inward as well. The engine, hood, and several engine components such as the alternator, belts, and pulleys were undamaged. A small dent occurred to the ride side of the truck box due to contact with the kinked thrie beam. The right-side front fender was crushed downward and inward while the right-side door showed signs of contact with the rail. The left side of the vehicle was damaged similarly to the right side, except that no dent was found on the truck box. No damage occurred to the vehicle tires or the rims. There was no crushing of the pickup truck's occupant compartment.

9.4 Barrier Damage

Barrier damage was extensive, as shown in Figures 46 through 48. Post nos. 1 through 4 on each side of the system were completely fractured as well as post no. 5 on the right side of the system. The remaining six posts on each side showed only small amounts of deflection in the soil due to the impact. Post no. 5 on the left side had pieces of the top of the post broken off. The thrie beam tore completely through with a vertical tear 203-mm upstream of post no. 1. The thrie beam rail also tore vertically on the right side of the system 305-mm downstream of post no. 1. The left-side thrie beam also tore minimally between post nos. 1 and 2 as well as between post nos. 2 and 3.

The thrie beam rail buckled in several locations. The thrie beam on the left side of the system buckled 381-mm upstream of post no. 5 with no tearing of the slots and also 381-mm upstream of

post no. 4 with slight tearing of slots. On the right side, the thrie beam buckled 305-mm upstream of post no. 5 with only a small amount of tearing, 178-mm downstream of post no. 5, and 1,016-mm downstream of post no. 5. Deformation of the thrie beam occurred to the nose piece as well as rail section nos. 2 through 4 on both sides of the system. The cables attached to the nose section as well as the cable anchor plates remained functional after impact. Five of the U-bolts holding the cables remained intact, while the center U-bolt on the middle hump pulled through. The maximum permanent rail deflection, as measured longitudinally into the bullnose system, was 16.33 m.

9.5 Occupant Risk Values

The normalized longitudinal and lateral occupant impact velocities (OIV) were determined to be 5.39 m/s and 1.06 m/s, respectively. The maximum 0.010-sec average occupant ridedown decelerations (ORD) in the longitudinal and lateral directions were 9.18 g's and 4.39 g's, respectively. It is noted that the occupant impact velocities and occupant ridedown decelerations were within the suggested limits provided in NCHRP Report No. 350. The results of the occupant risk, determined from the accelerometer, are summarized in Figure 40. Results are shown graphically in Appendix A.

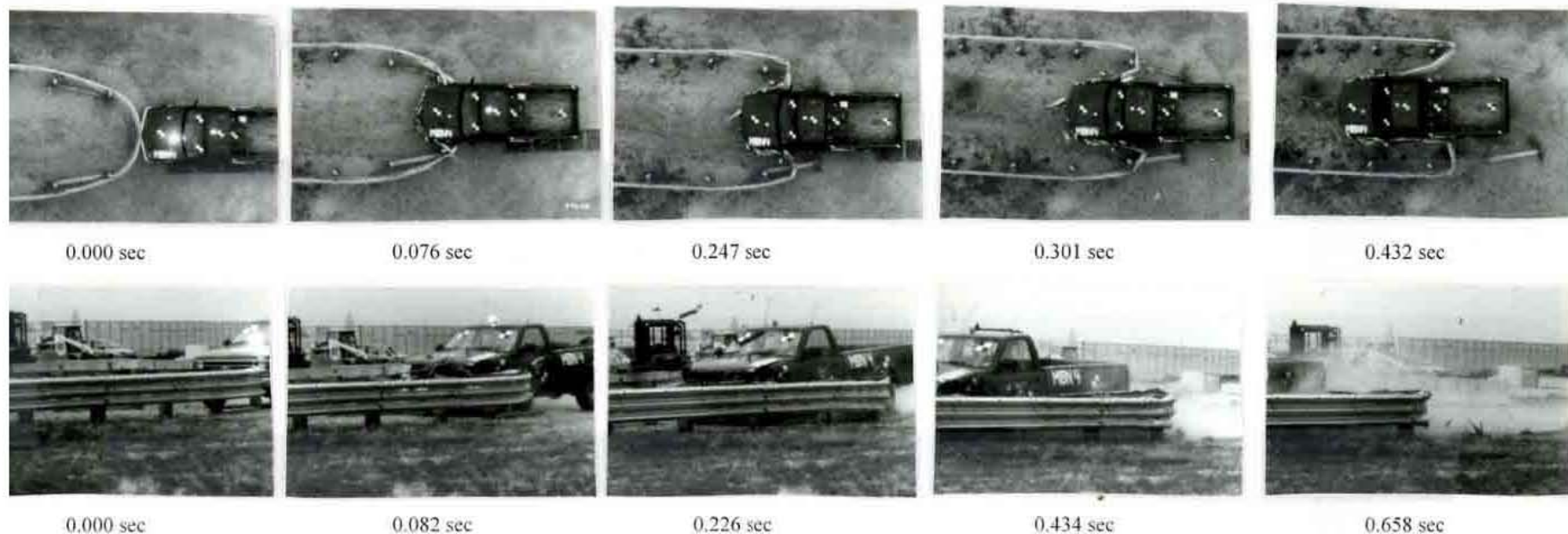
9.6 Discussion

Following test MBN-4, a safety performance evaluation was conducted, and the bullnose barrier design was determined to be acceptable for Test 3-31 according to NCHRP Report No. 350 criteria. The bullnose barrier contained and stopped the test vehicle in a controlled manner. It should be noted that the thrie beam captured the pickup truck with no overriding or under riding of the rail. Detached elements and debris from the test article did not penetrate or show potential for penetrating the occupant compartment. There was no deformation of, or intrusion into, the occupant

compartment that could have caused serious injury. The vehicle remained upright during and after collision and the vehicle's trajectory did not intrude into adjacent traffic lanes. Vehicle trajectory behind the impact area was acceptable as the test vehicle did not penetrate through the barrier. The occupant impact velocities and ridedown accelerations were within the suggested limits imposed by NCHRP Report No. 350.



Figure 39. Impact Location, Test MBN-4



74

- Test Number MBN-4
- Date 7/9/98
- Appurtenance Bullnose Median Barrier
- Total Length 20,144 m
- Steel Thrie Beam (Nested)
 - Thickness 12 gauge (2.66 mm)
 - Top Mounting Height 804 mm
- Wood Posts
 - Post Nos. 1 - 2, 10 - 11 140 mm x 190.5 mm x 1080-mm long
 - Post Nos. 3 - 9 150 mm x 200 mm x 1980-mm long
- Wood Spacer Blocks
 - Post Nos. 1 - 8 150 mm x 200 mm x 320-mm long
- Soil Type Grading B - AASHTO M 147-65 (1990)
- Vehicle Model 1991 Chevy 2500 2WD
 - Curb 1,938 kg
 - Test Inertial 2,010 kg
 - Gross Static 2,010 kg
- Vehicle Speed
 - Impact 103.50 km/hr
 - Exit 0.0 km/hr

- Vehicle Angle
 - Impact 0.58 deg
 - Exit NA
- Vehicle Snagging None
- Vehicle Stability Satisfactory
- Occupant Ridedown Deceleration (10 msec avg.)
 - Longitudinal 9.18 g's
 - Lateral (not required) 4.39 g's
- Occupant Impact Velocity (Normalized)
 - Longitudinal 5.39 m/s
 - Lateral (not required) 1.06 m/s
- Vehicle Damage Moderate
 - TAD(17) 12-FD-5//3-RP-1//3-RBQ-2
 - SAE(18) 12FDEW5//03RBMD2//03RPLD1
- Vehicle Stopping Distance 16.33 m downstream
1.01 m west of centerline
- Barrier Damage Extensive rail damage and
nine fractured posts
- Maximum Deflections
 - Permanent Set 16.33 m downstream
0.97 m west of centerline
 - Dynamic NA

Figure 40. Summary and Sequential Photographs, Test MBN-4



0.000 sec



0.052 sec



0.076 sec



0.574 sec



1.102 sec

Figure 41. Additional Sequential Photographs, Test MBN-4



Figure 42. Full-Scale Crash Test, Test MBN-4



Figure 43. Full-Scale Crash Test, Test MBN-4

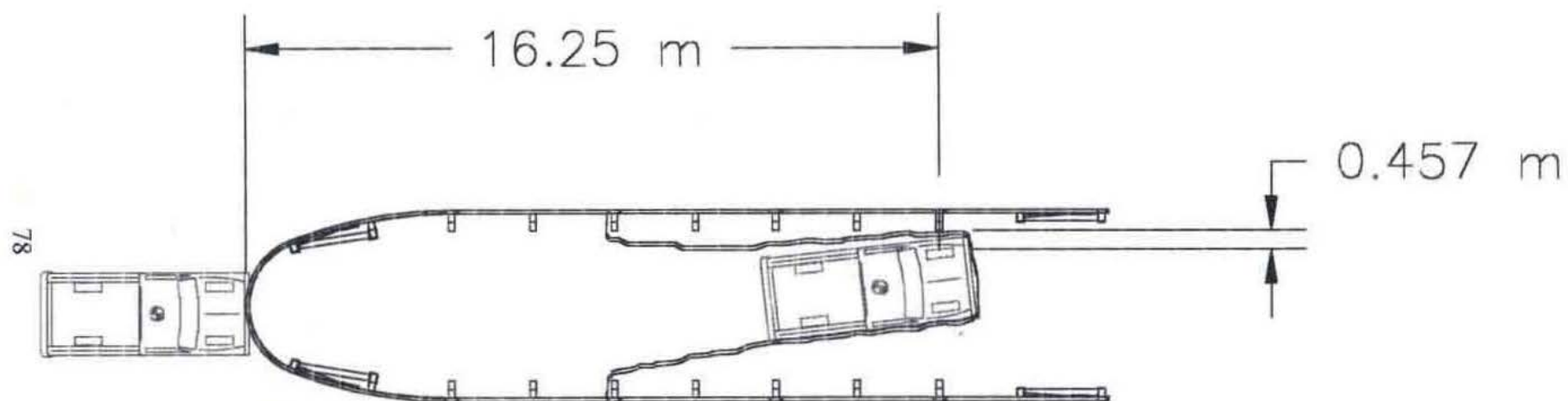


Figure 44. Vehicle Trajectory, Test MBN-4



Figure 45. Vehicle Damage, Test MBN-4



Figure 46. Barrier Damage, Test MBN-4



Figure 47. Barrier Damage, Test MBN-4



Figure 48. Barrier Damage, Test MBN-4

10 SUMMARY AND CONCLUSIONS

A bullnose median barrier was developed and full-scale crash tested to further develop the design concept and to provide compliance testing according to federal standards. Two crash tests were performed according to Test Level 3 (TL-3) of NCHRP Report No. 350. The results of the tests are summarized in Table 5. Test MBN-3 used a 1,989-kg pickup truck while test MBN-4 used a 2,010-kg pickup truck. The first test, test MBN-3, failed after the thrie beam fractured, resulting in an uncontrolled penetration of the vehicle behind the barrier. However, it is noted that the pickup truck did not show any potential for override of the thrie beam. Following this crash test, the results were analyzed and used along with LS-DYNA computer simulation modeling to determine the cause of the fracture.

An analysis of the crash test and simulation results suggested that the bullnose system be redesigned to contain the truck impact without increasing the stiffness of the barrier for a small car impact. Therefore, the bullnose barrier was modified using cables to reinforce the first section of thrie beam between post no. 1 on each side. Two cables, one behind each of the top two humps of the thrie beam, were fitted to the nose section of the bullnose to contain the impact of a pickup truck in the event of a rail fracture. Since cables only develop tensile loads and have virtually no bending stiffness, the researchers believed that the cables would not adversely stiffen the barrier or reduce the ability of the design to safely contain a small car impact. LS-DYNA computer simulation of the modified design suggested that the cables would be capable of containing the truck if the rail failed. The second test, test MBN-4, was performed on the modified barrier and was determined to be acceptable according to the TL-3 crash test criteria of NCHRP Report No. 350. The pickup truck did not show any potential for underride or override of the thrie beam.

The Phase II development of the bullnose barrier end terminal was successfully completed. The initial design concept was further developed and successfully tested for head-on pickup truck impacts. Computer simulation was successfully used to analyze and predict the behavior of the bullnose barrier system. The data gathered during the testing provided valuable information that will be used in further modification and compliance testing of the bullnose design as well as in computer simulation of the bullnose barrier terminal.

Table 5. Summary of Safety Performance Evaluation

Evaluation Factors	Evaluation Criteria	Test MBN-3	Test MBN-4
Structural Adequacy	C. Acceptable test article performance may be by redirection, controlled penetration, or controlled stopping of the vehicle.	U	S
Occupant Risk	D. Detached elements, fragments or other debris from the test article should not penetrate or show potential for penetrating the occupant compartment, or present an undue hazard to other traffic, pedestrians, or personnel in a work zone. Deformations of, or intrusions into, the occupant compartment that could cause serious injuries should not be permitted.	S	S
	F. The vehicle should remain upright during and after collision although moderate roll, pitching, and yawing are acceptable.	S	S
	H. Occupant impact velocities should satisfy the following: Occupant Impact Velocity Limits (m/s) <u>Component</u> Preferred Maximum Longitudinal and Lateral 9 12	S	S
	I. Occupant ride down accelerations should satisfy the following: Occupant Ride down Acceleration Limits (G's) <u>Component</u> Preferred Maximum Longitudinal and Lateral 15 20	S	S
Vehicle Trajectory	K. After collision it is preferable that the vehicle's trajectory not intrude into adjacent traffic lanes.	S	S
	N. Vehicle trajectory behind the test article is acceptable.	U	S

S - (Satisfactory)

U - (Unsatisfactory)

11 RECOMMENDATIONS

The bullnose barrier system described in this report was successfully tested for a 2000P pickup truck subjected to a head-on impact. Based on the success demonstrated by the bullnose system in this report, it is recommended that the five remaining tests for NCHRP Report No. 350 compliance be performed. The remaining tests using a 2000-kg pickup truck include: (1) Test 3-33, a 100 km/h impact at a nominal angle of 15 degrees on the tip of the barrier nose; (2) Test 3-35, a 100 km/h impact at a nominal angle of 20 degrees on the beginning of the Length-of-Need (LON); and (3) Test 3-39, a 100 km/h impact at a nominal angle of 20 deg on a point at the length of the terminal divided by two. The remaining tests using a 820-kg small car are: (1) Test 3-32, a 100 km/h impact at a nominal angle of 15 degrees on the tip of the barrier nose; and (2) Test 3-34, a 100 km/h impact at a nominal angle of 15 degrees on the Critical Impact Point (CIP).

12 REFERENCES

1. Ross, H.E., Sicking, D.E., Zimmer, R.A. and Michie, J.D., *Recommended Procedures for the Safety Performance Evaluation of Highway Features*, National Cooperative Highway Research Program (NCHRP) Report No. 350, Transportation Research Board, Washington, D.C., 1993.
2. Bielenberg, B. W., Faller, R. K., Reid, J. D., Rohde, J. R., Sicking, D.L., Keller, E.A., *Concept Development of a Bullnose Guardrail System for Median Applications*, MwRSF Report No. TRP-03-73-98, Final Report, Submitted to the Missouri Department of Transportation, Midwest Roadside Safety Facility, May 22, 1998.
3. Button, J.W., Buth, E. and Olson, R.M., *Crash Tests of Five Foot Radius Plate Beam Guardrail*, Submitted to the Department of Highways, State of Minnesota, Performed by Texas Transportation Institute, Texas A & M University, June 1975.
4. Task Force 13, *A Guide to Standardized Highway Barrier Hardware*, AAHSTO-AGC-ARTBA Joint Cooperative Committee Subcommittee on New Highway Materials, Task force 13, 1995.
5. Robertson, R.G. and Ross, H.E. Jr., *Colorado Median Barrier End Treatment Tests*, TTI Research Report No. 4179-1F, Submitted to the Colorado Department of Highways, Performed by Texas Transportation Institute, Texas A&M University, May 1981.
6. Bronstad, M.E., Ray, M.H., Mayer, J.B. Jr. and Brauer, S.K., *Median Barrier Terminals and Median Treatments. Volume 1 Research Reports and Appendix A*, Report No. FHWA/RD-088/004, Final Report to the Federal Highway Administration, Southwest Research Institute, October 1987.
7. Bronstad, M.E., Ray, M.H., Mayer, J.B. Jr. and Brauer, S.K., *Median Barrier Terminals and Median Treatments. Volume 2 Appendices B and C*, Report No. FHWA/RD-088/005, Final Report to the Federal Highway Administration, Southwest Research Institute, October 1987.
8. Bronstad, M.E., Calcote, L.R., Ray, M.H., and Mayer, J.B., *Guardrail-Bridge Rail Transition Designs - Volume 1 - Research Report*, Report No. FHWA/RD-86/178, Final Report to the Safety Design Division, Federal Highway Administration, Performed by Southwest Research Institute, April 1988.
9. Bronstad, M.E., Ray, M.H., Mayer, J.B., Jr., and McDevitt, C.F., *W-Beam Approach Treatment at Bridge Rail Ends Near Intersecting Roadways*, Transportation Research Record No. 1133, Transportation Research Board, National Research Council, Washington, D.C., 1987.

10. Mayer, J.B., *Full-Scale Crash Testing of Approach Guardrail for Yuma County Public Works Department*, Final Report, Project No. 06-2111, Southwest Research Institute, San Antonio Texas, 1989.
11. *Curved W-Beam Guardrail Installations at Minor Roadway Intersections*, Federal Highway Administration (FHWA), U.S. Department of Transportation, Technical Advisory T 5040.32, April 13, 1992.
12. Ross, H.E., Jr., Bligh, R.P., and Parnell, C.B., *Bridge Railing End Treatments at Intersecting Streets and Drives*, Report No. FHWA TX-91/92-1263-1F, Final Report to the Texas Department of Transportation, Performed by Texas Transportation Institute, Texas A&M University, November 1992.
13. Bligh, R.P., Ross, H.E., Jr., and Alberson, D.C., *Short-Radius Thrie Beam Treatment for Intersecting Streets and Drives*, Report No. FHWA/TX-95/1442-1F, Final Report to the Texas Department of Transportation, Performed by Texas Transportation Institute, Texas A&M University, November 1994.
14. Sicking, D. L., Reid, J. D., and Rohde, J. R., *Development of a Sequential Kinking Terminal for W-Beam Guardrails*, TRB Paper 980614, Transportation Research Board, January 1998.
15. Hinch, J., Yang, T-L, and Owings, R., *Guidance Systems for Vehicle Testing*, ENSCO, Inc., Springfield, VA, 1986.
16. Bronstad, M. E., Michie, J. D., *Recommended Procedures for Vehicle Crash Testing of Highway Appurtenances*, National Cooperative Highway Research Program Report 153, 1974.
17. *Recommended Procedures for Vehicle Crash Testing of Highway Appurtenances*, Transportation Research Circular Number 191, February 1978.
18. Michie, J.D., *Recommended Procedures for the Safety Performance Evaluation of Highway Appurtenances*, NCHRP Report 230, National Research Council, Washington, D.C., March 1981.
19. *Vehicle Damage Scale for Traffic Investigators*, Second Addition, Technical Bulletin No. 1, Traffic Accident Data (TAD) Project, National Safety Council, Chicago, Illinois, 1971.
20. *Collision Deformation Classification - Recommended Practice J224 March 1980*, Handbook Volume 4, Society of Automotive Engineers (SAE), Warrendale, Pennsylvania, 1985.
21. Hallquist, J.O., *LS-DYNA Keyword User's Manual*, Livermore Software Technology Corporation, California, 1997.

22. Zaouk, A., Bedewi, N., and Meczowski, L., "Development and Validation of Detailed Chevrolet C-1500 Pickup Truck for Multiple Impact Applications," TRB Paper 980419, Transportation Research Board, January 1998.
23. Reid, J.D., "Tracking the Energy in an Energy Absorbing Guardrail terminal," *International Journal of Crashworthiness*, Vol. 3, No. 2, 1998, pp. 135-146.

APPENDIX A

ACCELEROMETER DATA

Figure A-1. Graph of Longitudinal Deceleration, Test MBN-3

Figure A-2 Graph of Longitudinal Occupant Impact Velocity, Test MBN-3

Figure A-3. Graph of Longitudinal Occupant Displacement, Test MBN-3

Figure A-4. Graph of Lateral Deceleration, Test MBN-3

Figure A-5. Graph of Lateral Occupant Impact Velocity, Test MBN-3

Figure A-6. Graph of Lateral Occupant Displacement, Test MBN-3

Figure A-7. Graph of Longitudinal Deceleration, Test MBN-4

Figure A-8. Graph of Longitudinal Occupant Impact Velocity, Test MBN-4

Figure A-9. Graph of Longitudinal Occupant Displacement, Test MBN-4

Figure A-10. Graph of Lateral Deceleration, Test MBN-4

Figure A-11. Graph of Lateral Occupant Impact Velocity, Test MBN-4

Figure A-12. Graph of Lateral Occupant Displacement, Test MBN-4

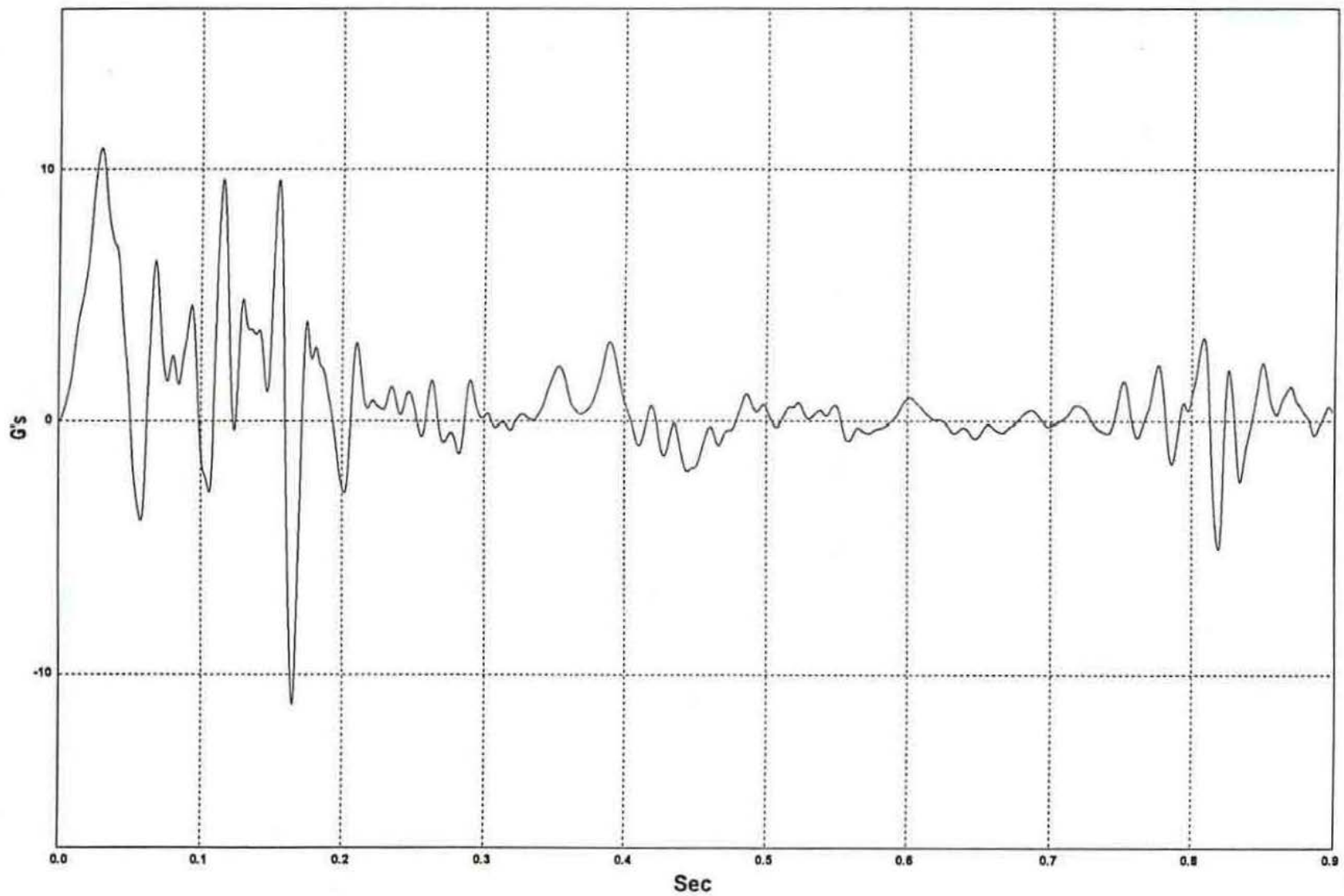
W5: Longitudinal Deceleration - Test MBN-3 (EDR-4)

Figure A-1. Graph of Longitudinal Deceleration, Test MBN-3

W6: Longitudinal Occupant Impact Velocity - Test MBN-3 (EDR-4)

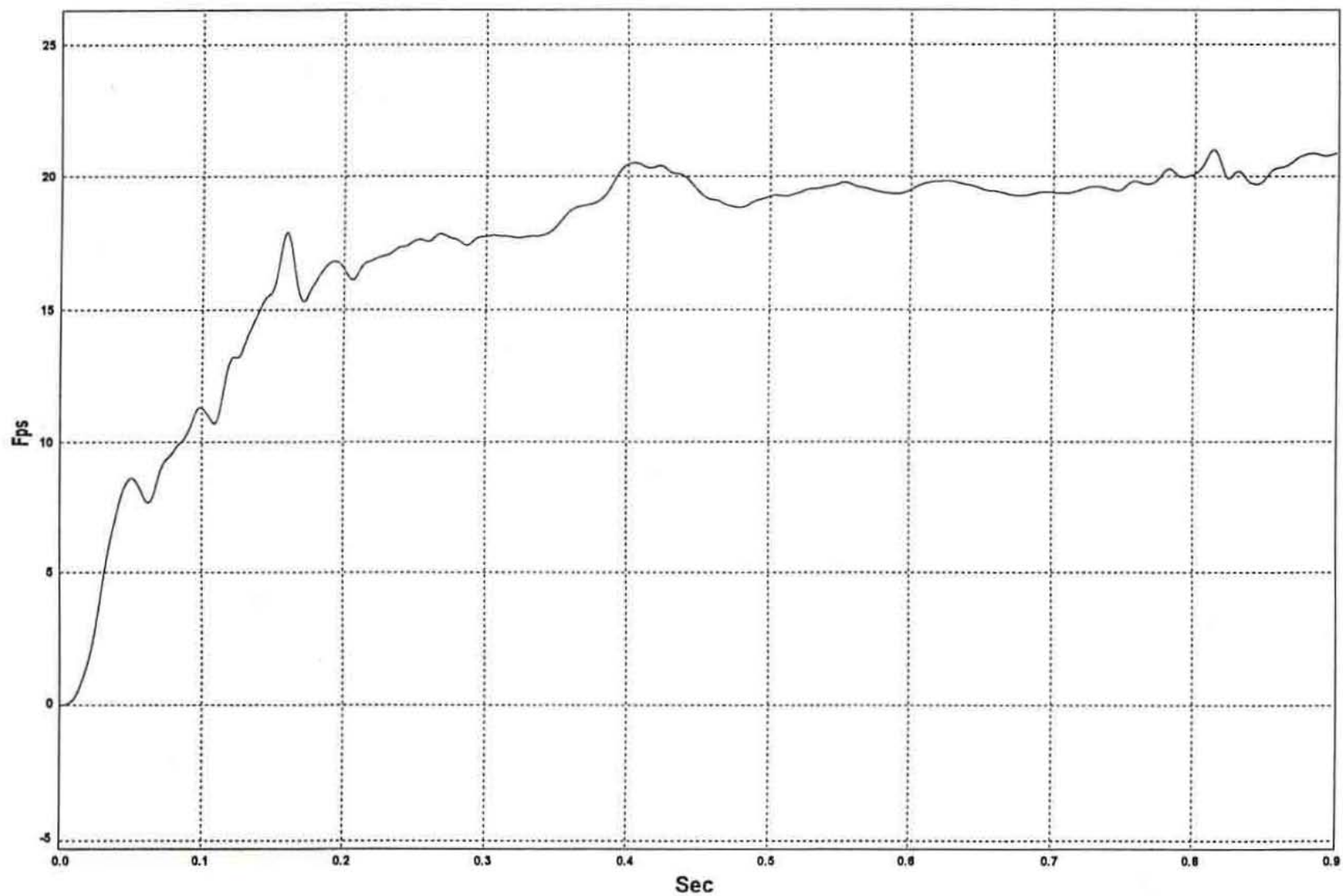


Figure A-2. Graph of Longitudinal Occupant Impact Velocity, Test MBN-3

W12: Longitudinal Occupant Displacement - Test MBN-3 (EDR-4)

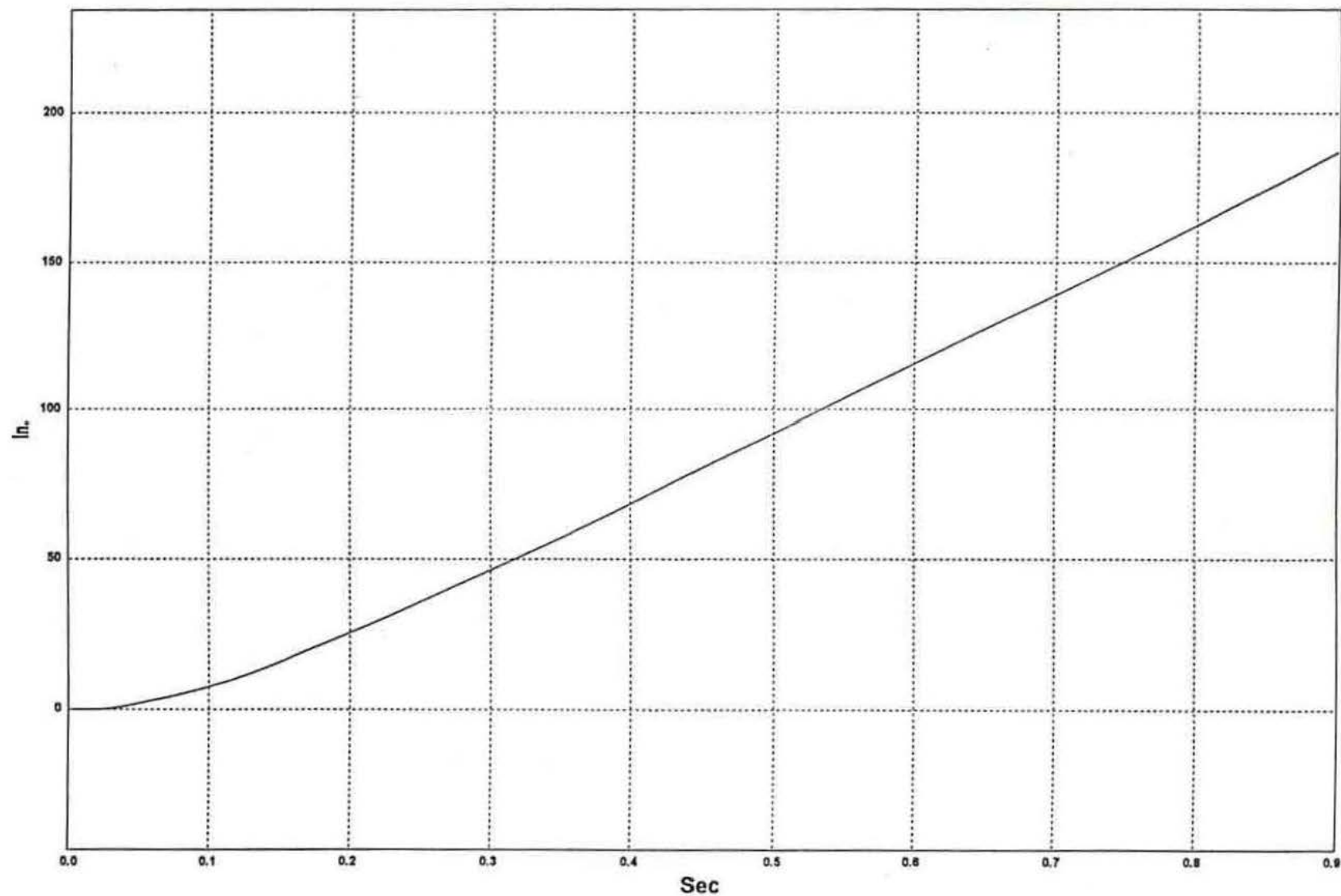


Figure A-3. Graph of Longitudinal Occupant Displacement, Test MBN-3

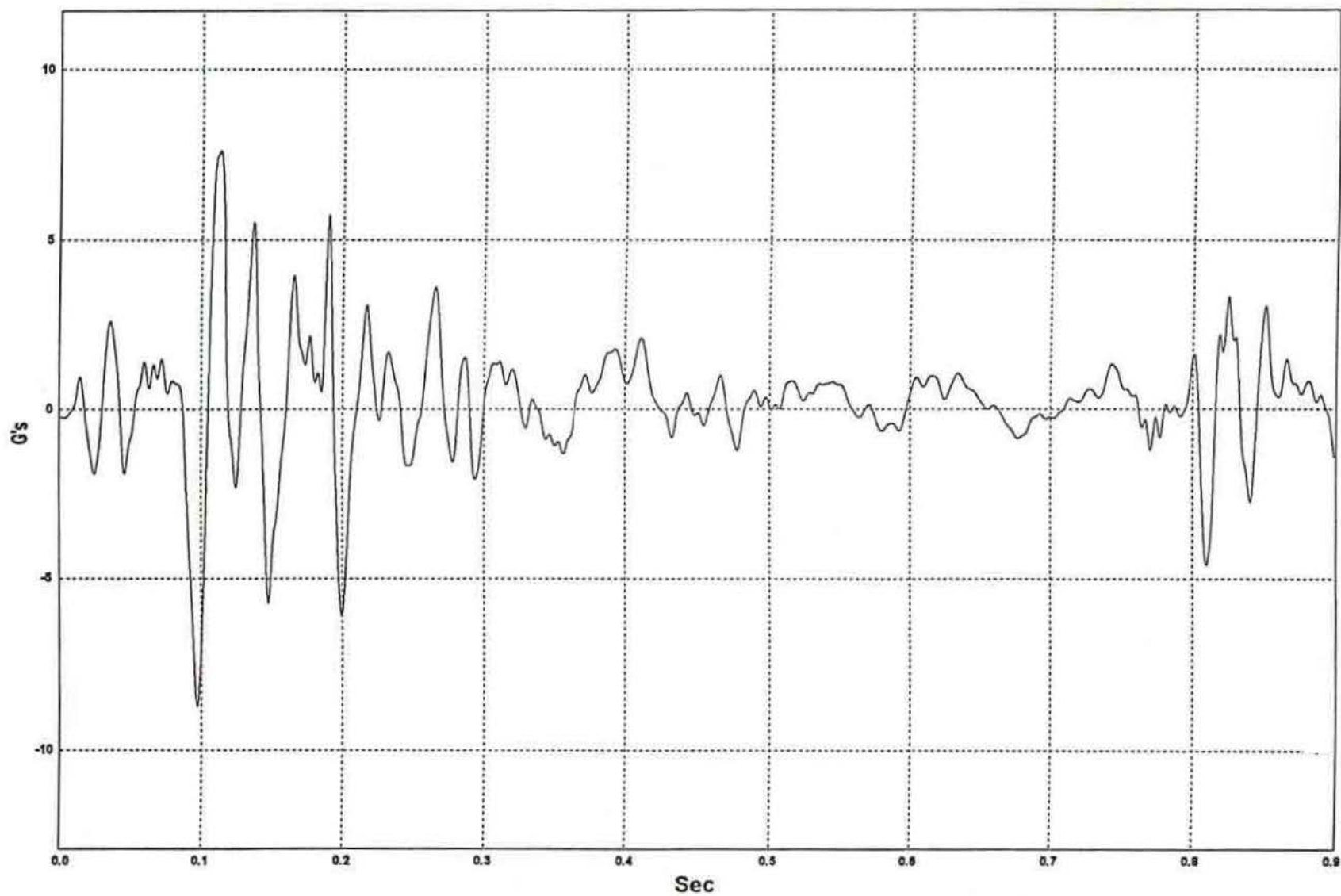
W5: Lateral Deceleration - Test MBN-3 (EDR-4)

Figure A-4. Graph of Lateral Deceleration, Test MBN-3

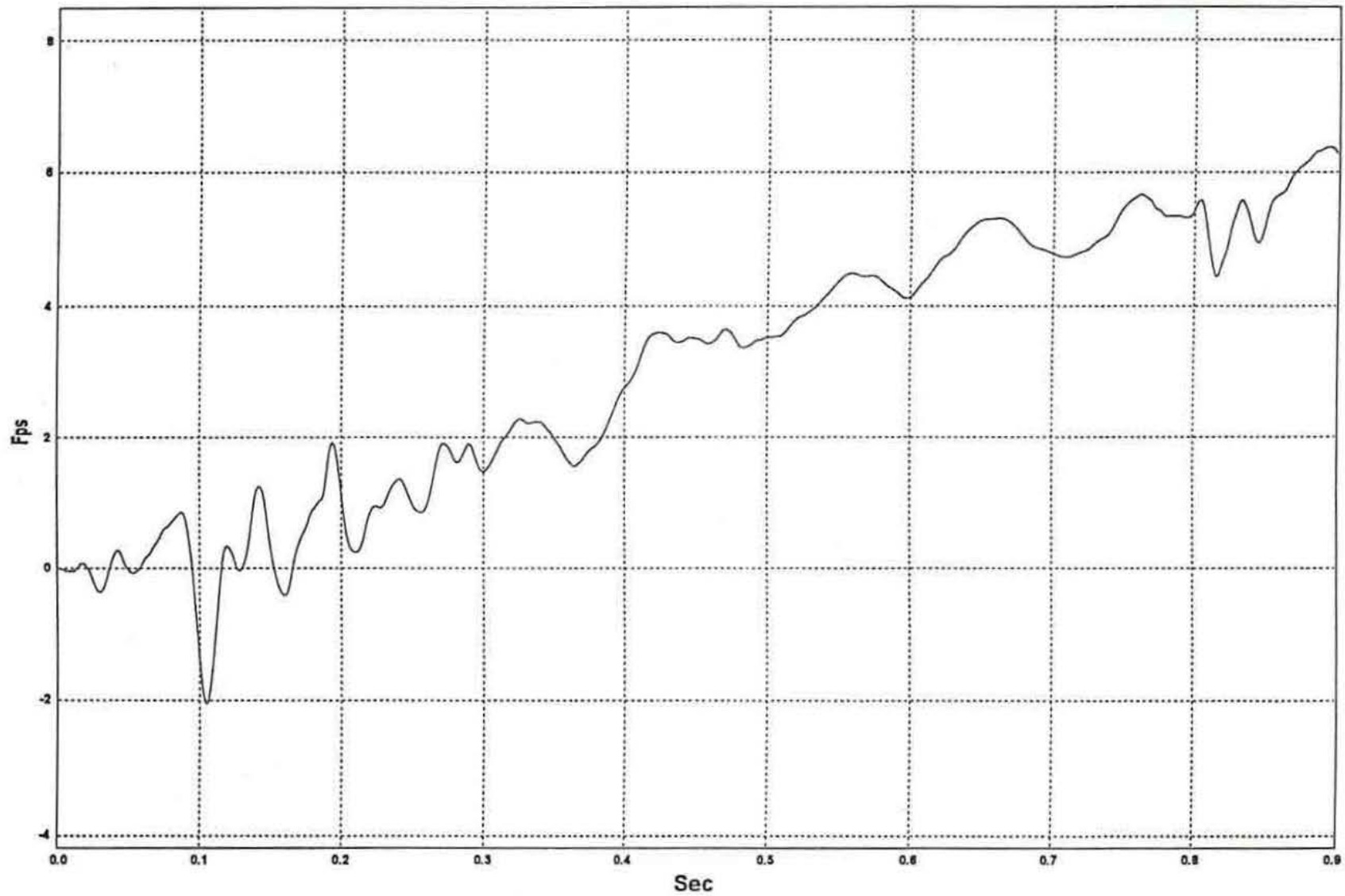
W6: Lateral Occupant Impact Velocity - Test MBN-3 (EDR-4)

Figure A-5. Graph of Lateral Occupant Impact Velocity, Test MBN-3

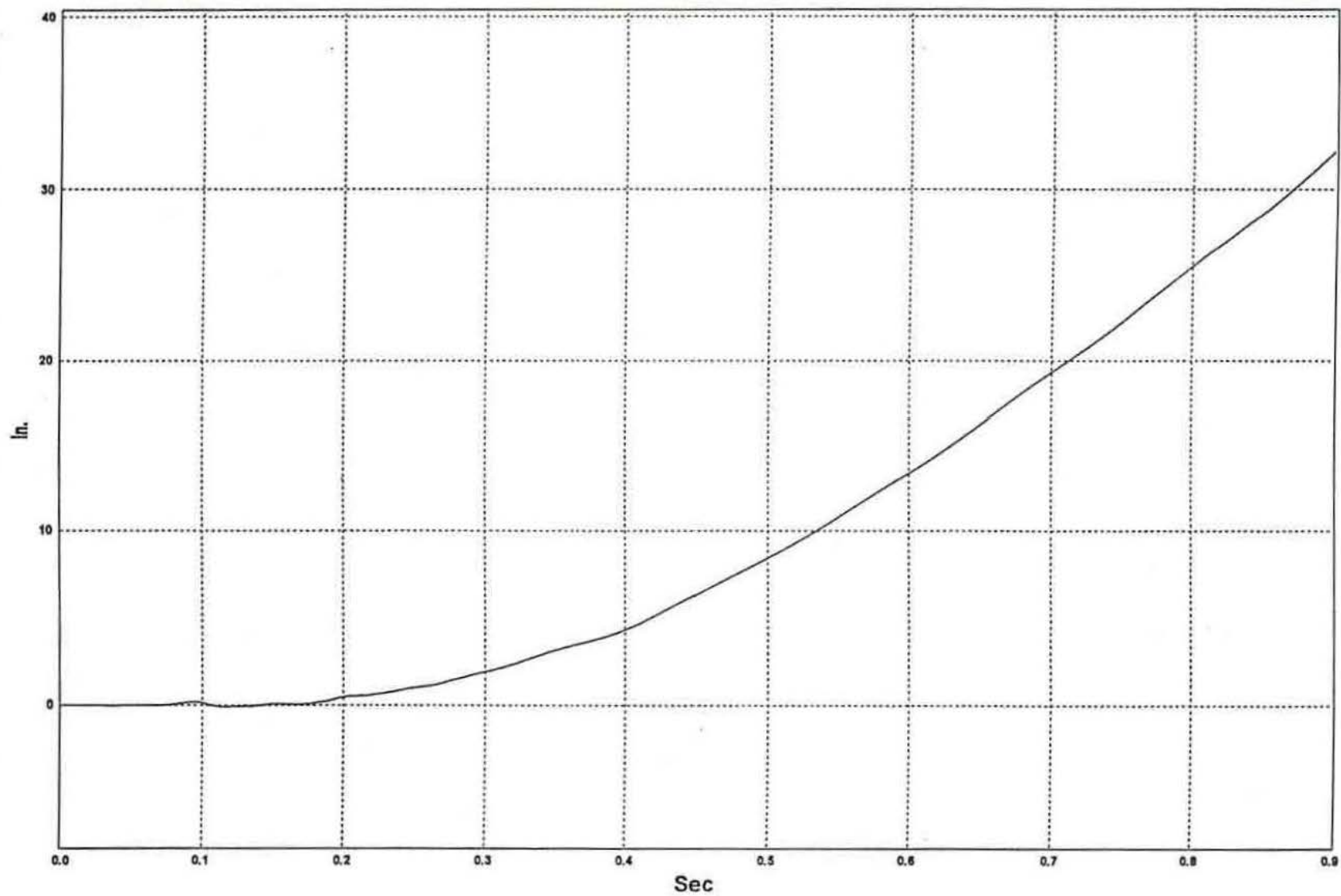
W7: Lateral Occupant Displacement - Test MBN-3 (EDR-4)

Figure A-6. Graph of Lateral Occupant Displacement, Test MBN-3

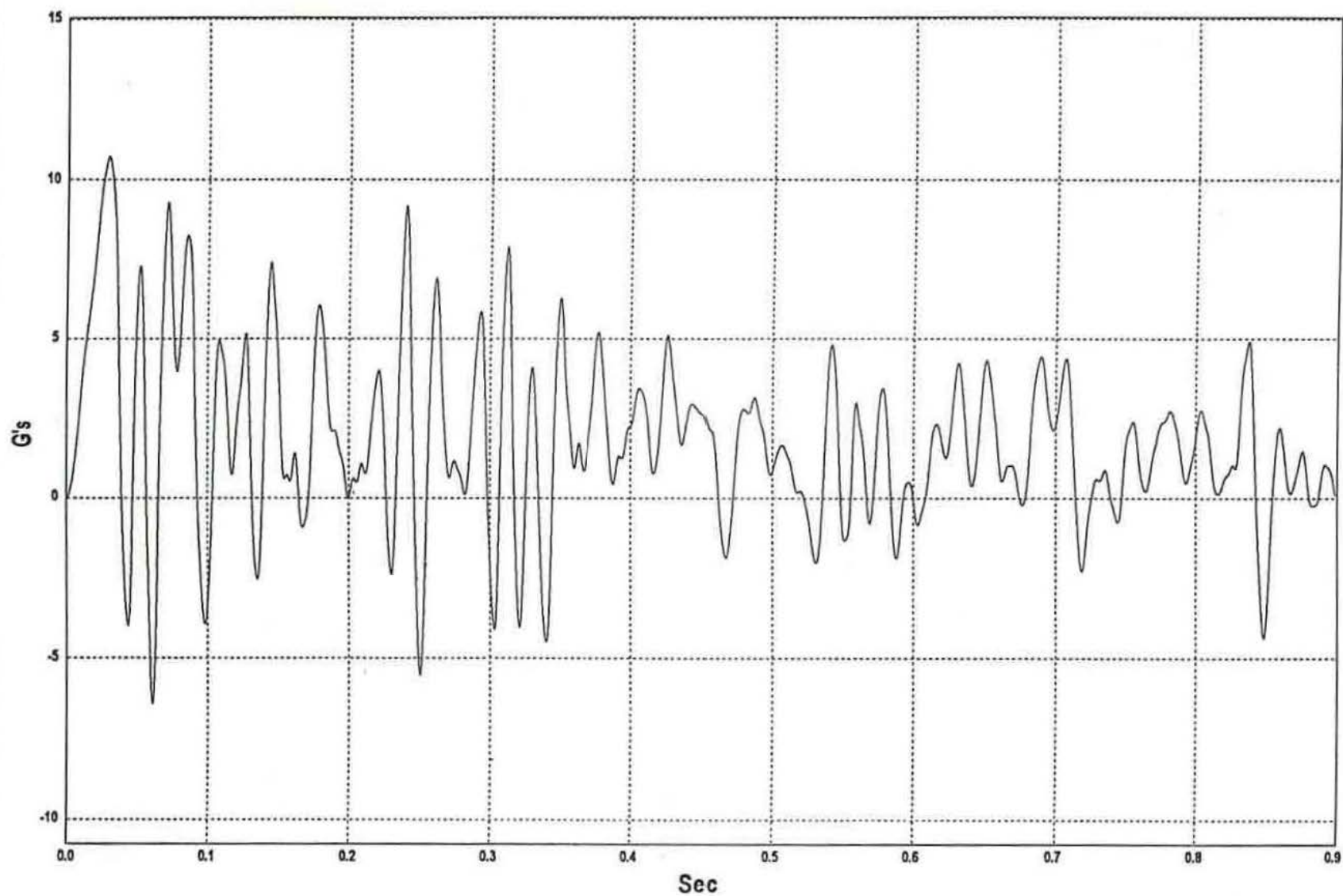
W5: Longitudinal Deceleration - Test MBN-4 (EDR-4)

Figure A-7. Graph of Longitudinal Deceleration, Test MBN-4

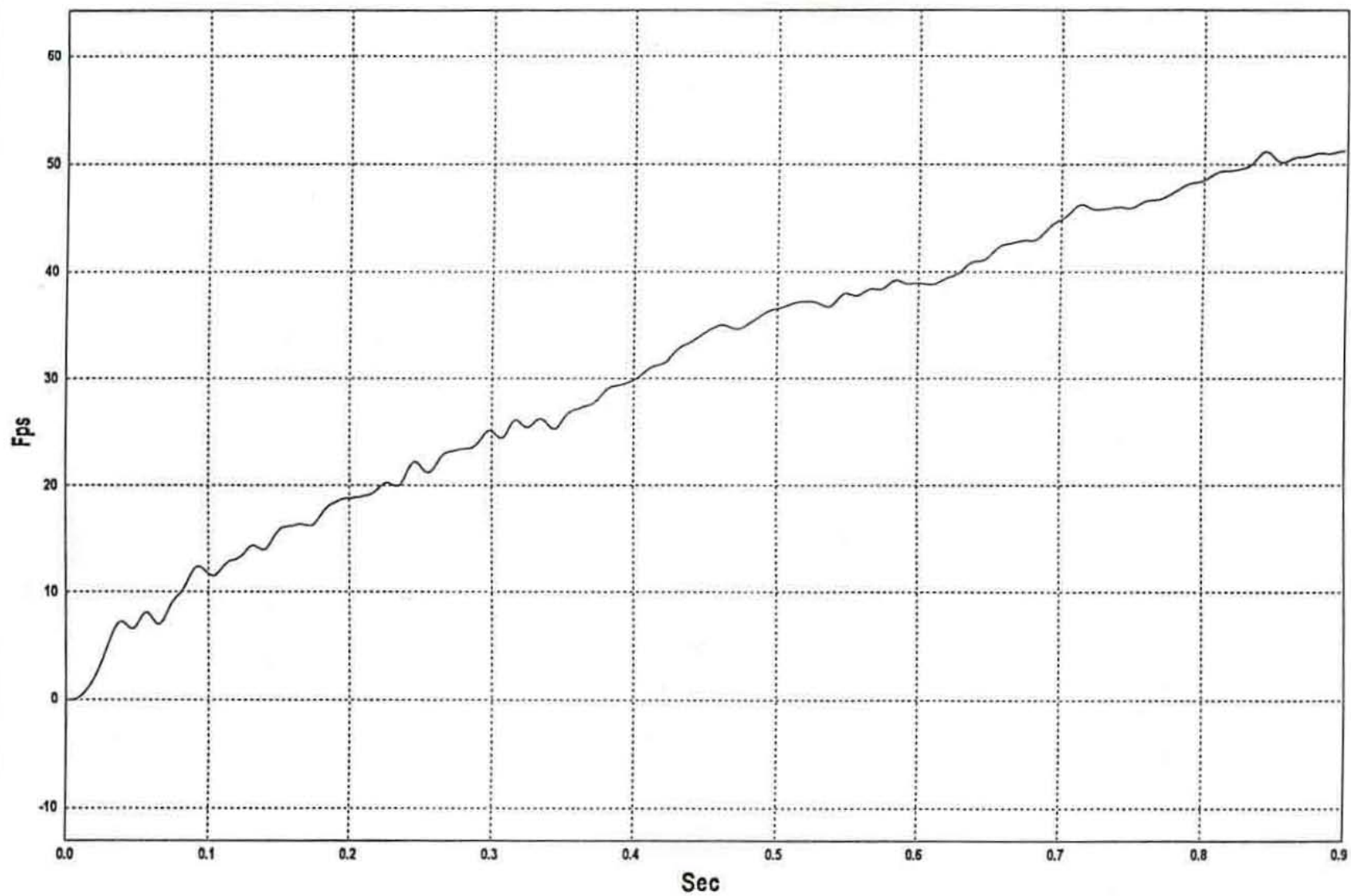
W6: Longitudinal Occupant Impact Velocity - Test MBN-4 (EDR-4)

Figure A-8. Graph of Longitudinal Occupant Impact Velocity, Test MBN-4

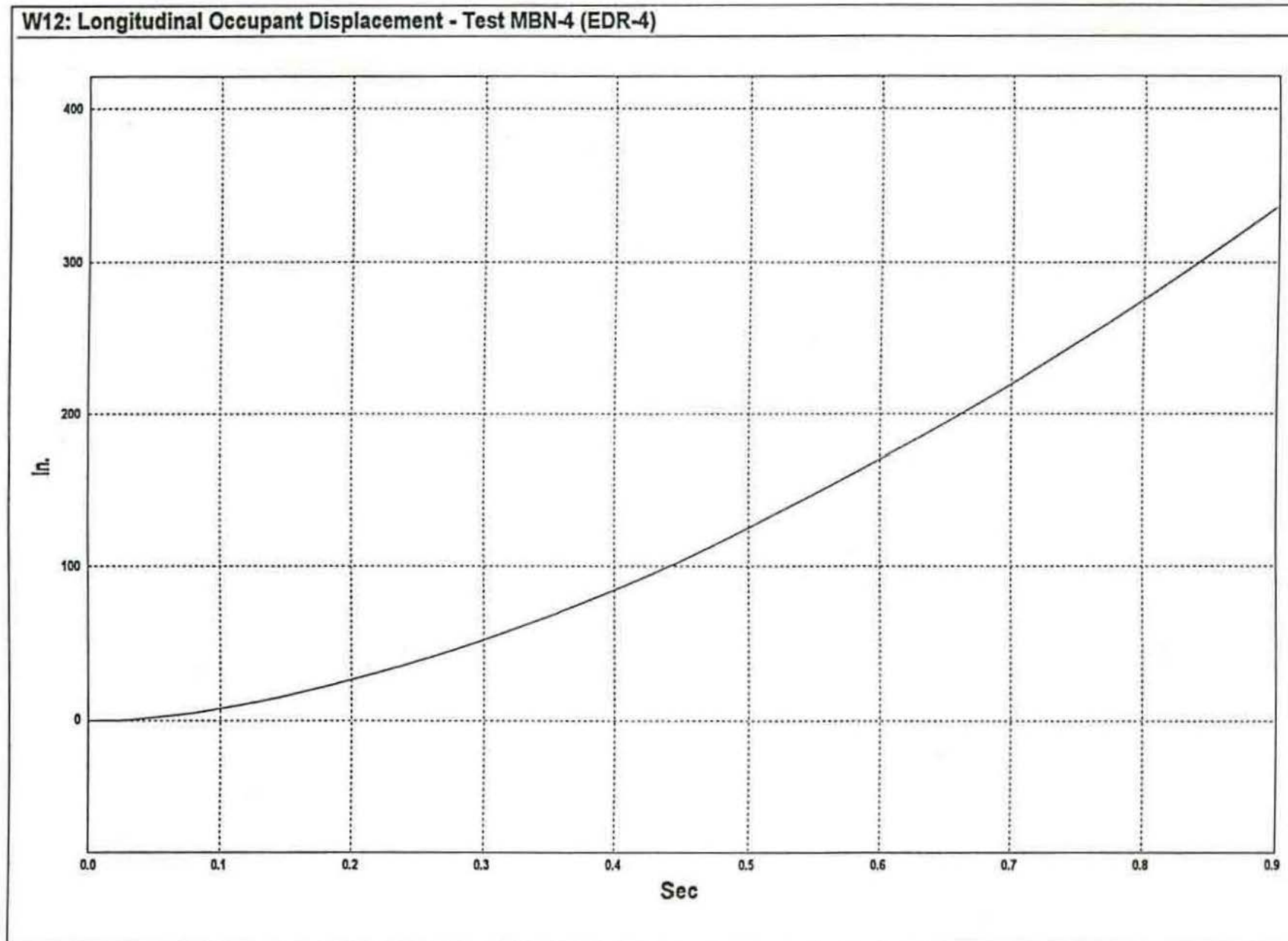


Figure A-9. Graph of Longitudinal Occupant Displacement, Test MBN-4

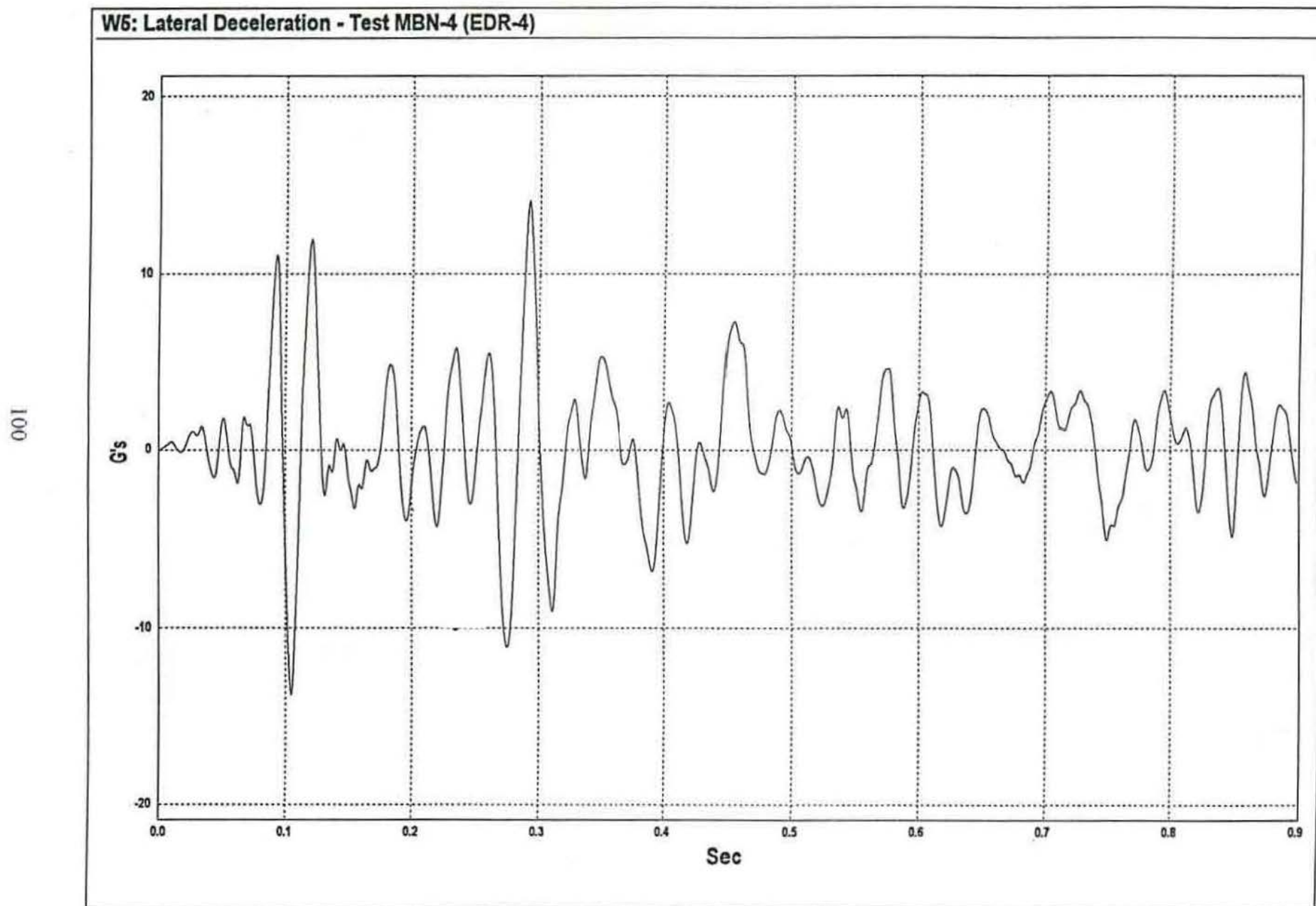


Figure A-10. Graph of Lateral Deceleration, Test MBN-4

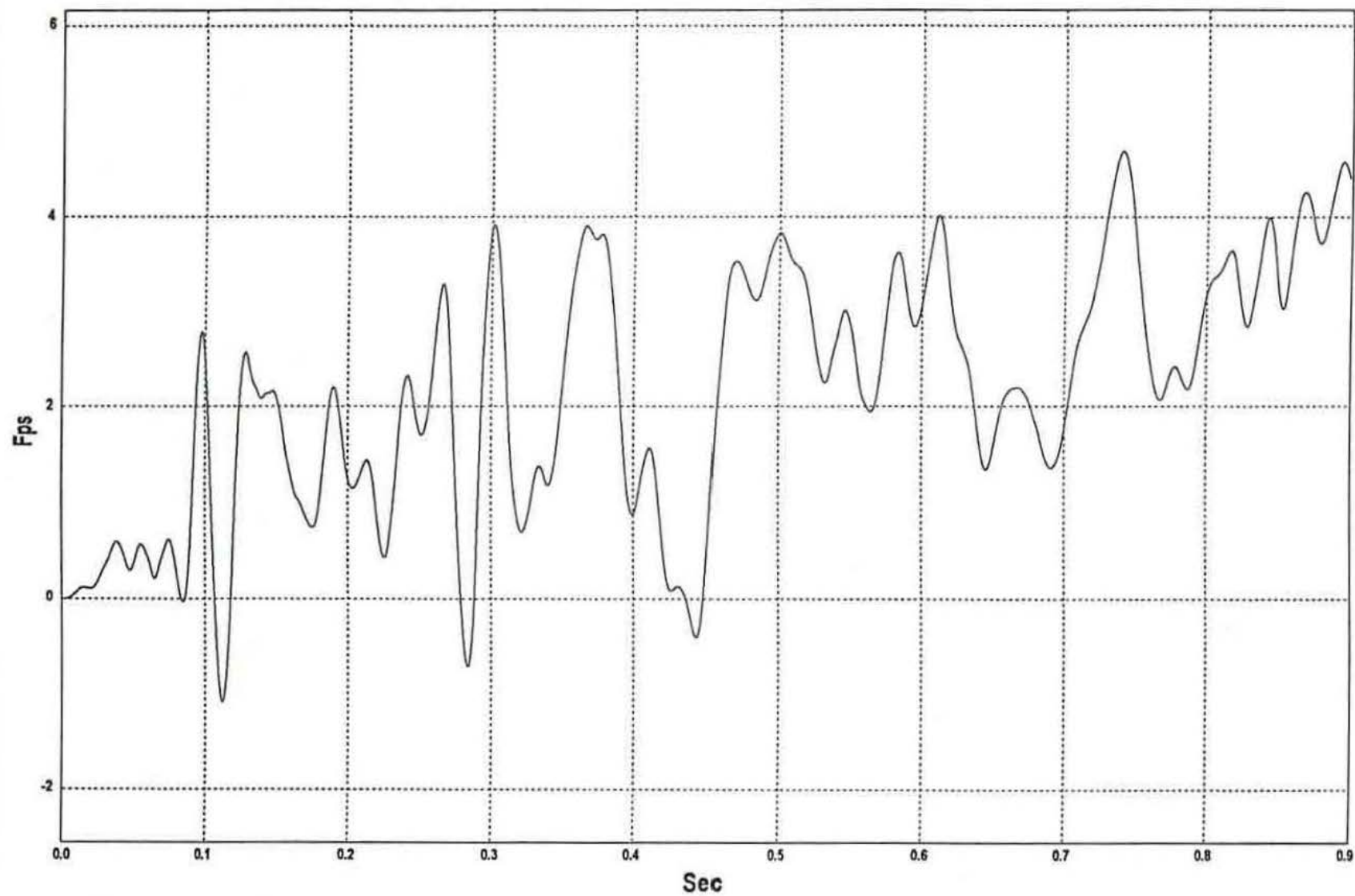
W6: Lateral Occupant Impact Velocity - Test MBN-4 (EDR-4)

Figure A-11. Graph of Lateral Occupant Impact Velocity, Test MBN-4

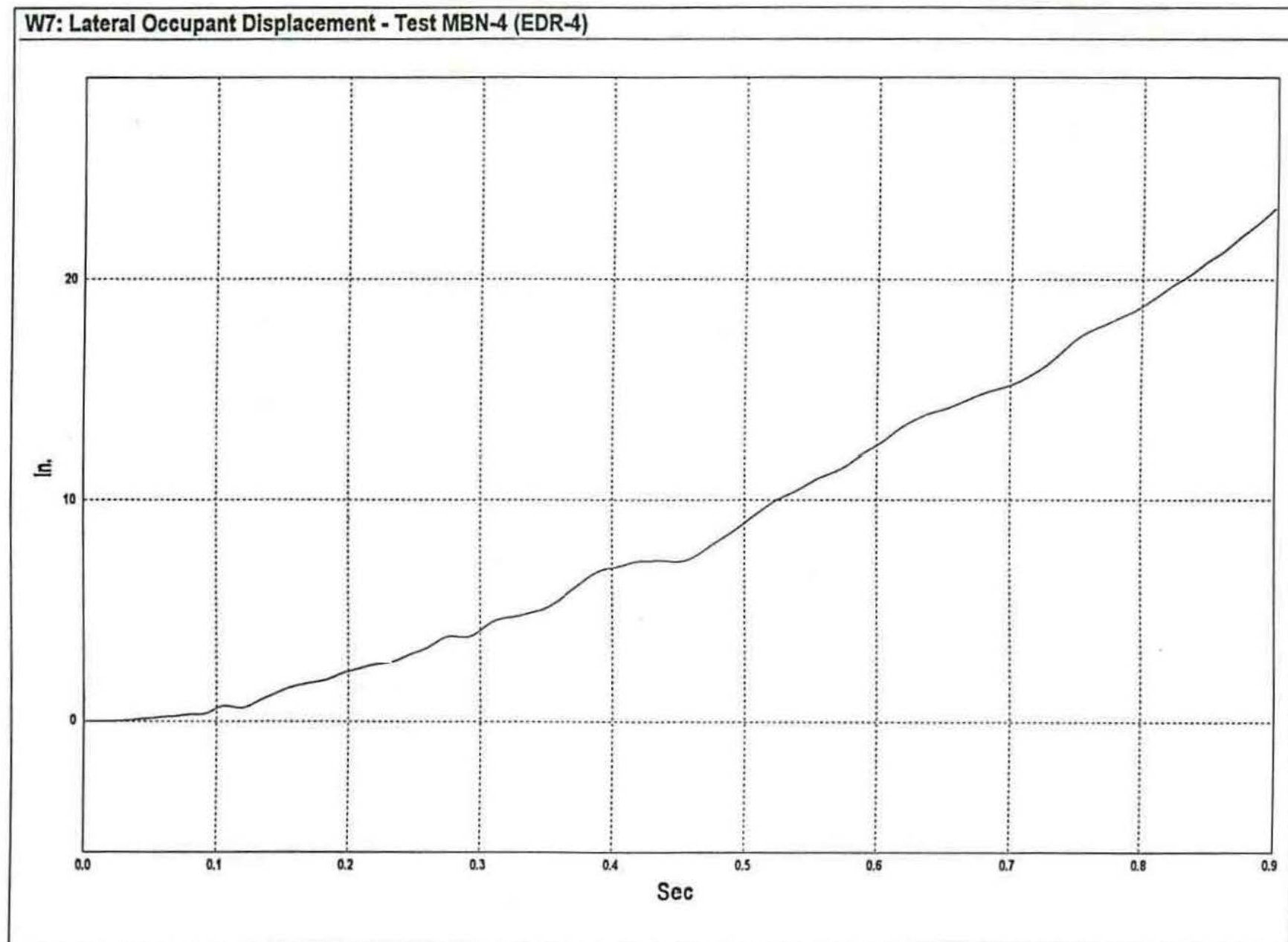


Figure A-12. Graph of Lateral Occupant Displacement, Test MBN-4

APPENDIX B

STRAIN GAUGE DATA

Figure B-1. Strain Gauge No. 1 Data, Strain Data, Test MBN-3

Figure B-2. Strain Gauge No. 1 Data, Stress Data, Test MBN-3

Figure B-3. Strain Gauge No. 2 Data, Strain Data, Test MBN-3

Figure B-4. Strain Gauge No. 2 Data, Stress Data, Test MBN-3

Figure B-5. Strain Gauge No. 3 Data, Strain Data, Test MBN-3

Figure B-6. Strain Gauge No. 3 Data, Stress Data, Test MBN-3

Figure B-7. Strain Gauge No. 4 Data, Strain Data, Test MBN-3

Figure B-8. Strain Gauge No. 4 Data, Stress Data, Test MBN-3

Figure B-9. Strain Gauge No. 5 Data, Strain Data, Test MBN-3

Figure B-10. Strain Gauge No. 5 Data, Stress Data, Test MBN-3

Figure B-11. Strain Gauge No. 6 Data, Strain Data, Test MBN-3

Figure B-12. Strain Gauge No. 6 Data, Stress Data, Test MBN-3

Figure B-13. Strain Gauge No. 7 Data, Strain Data, Test MBN-3

Figure B-14. Strain Gauge No. 7 Data, Stress Data, Test MBN-3

Figure B-15. Strain Gauge No. 8 Data, Strain Data, Test MBN-3

Figure B-16. Strain Gauge No. 8 Data, Stress Data, Test MBN-3

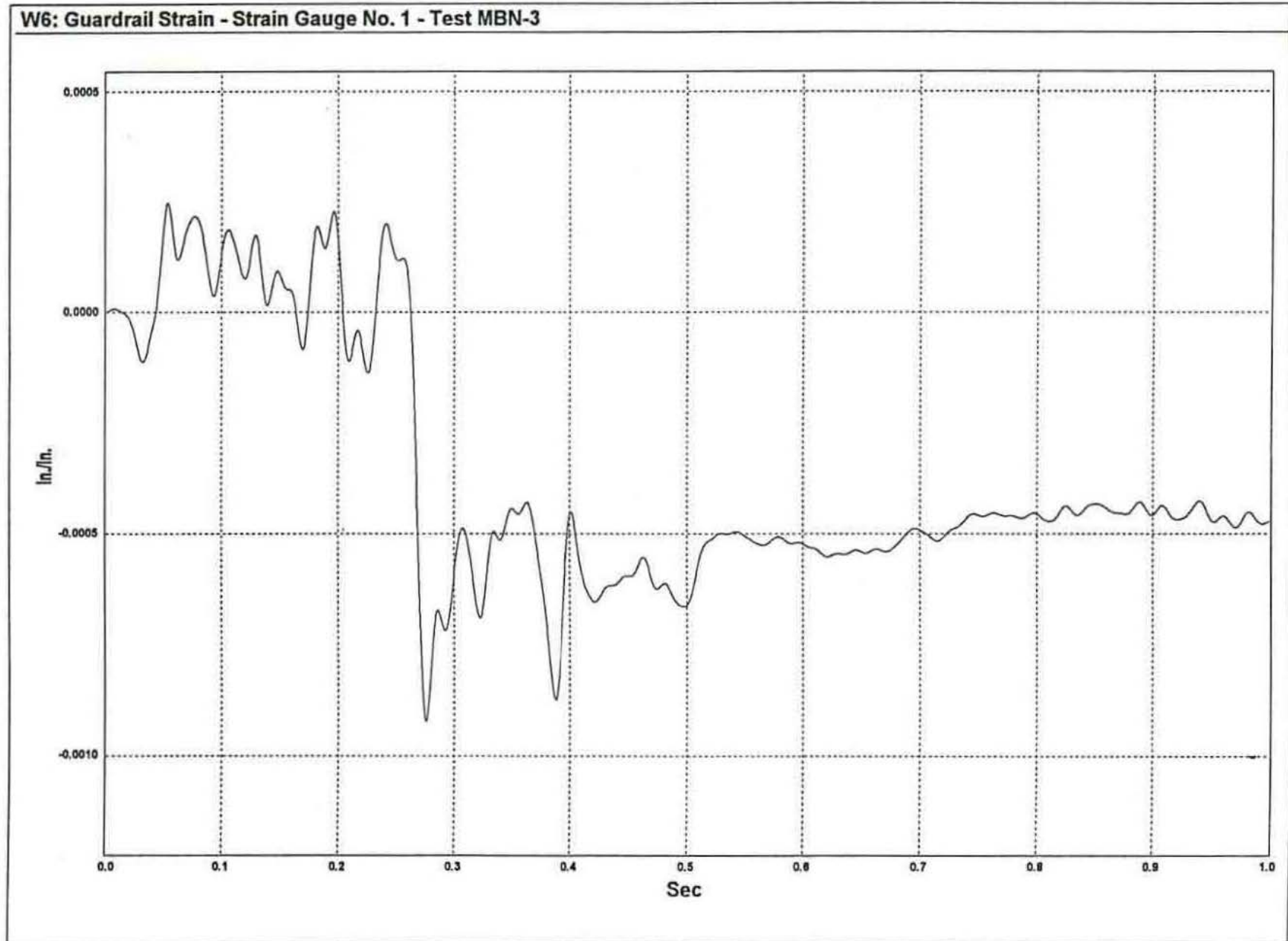


Figure B-1. Strain Gauge No. 1, Strain Data, Test MBN-3

W7: Guardrail Stress - Strain Gauge No. 1 - Test MBN-3

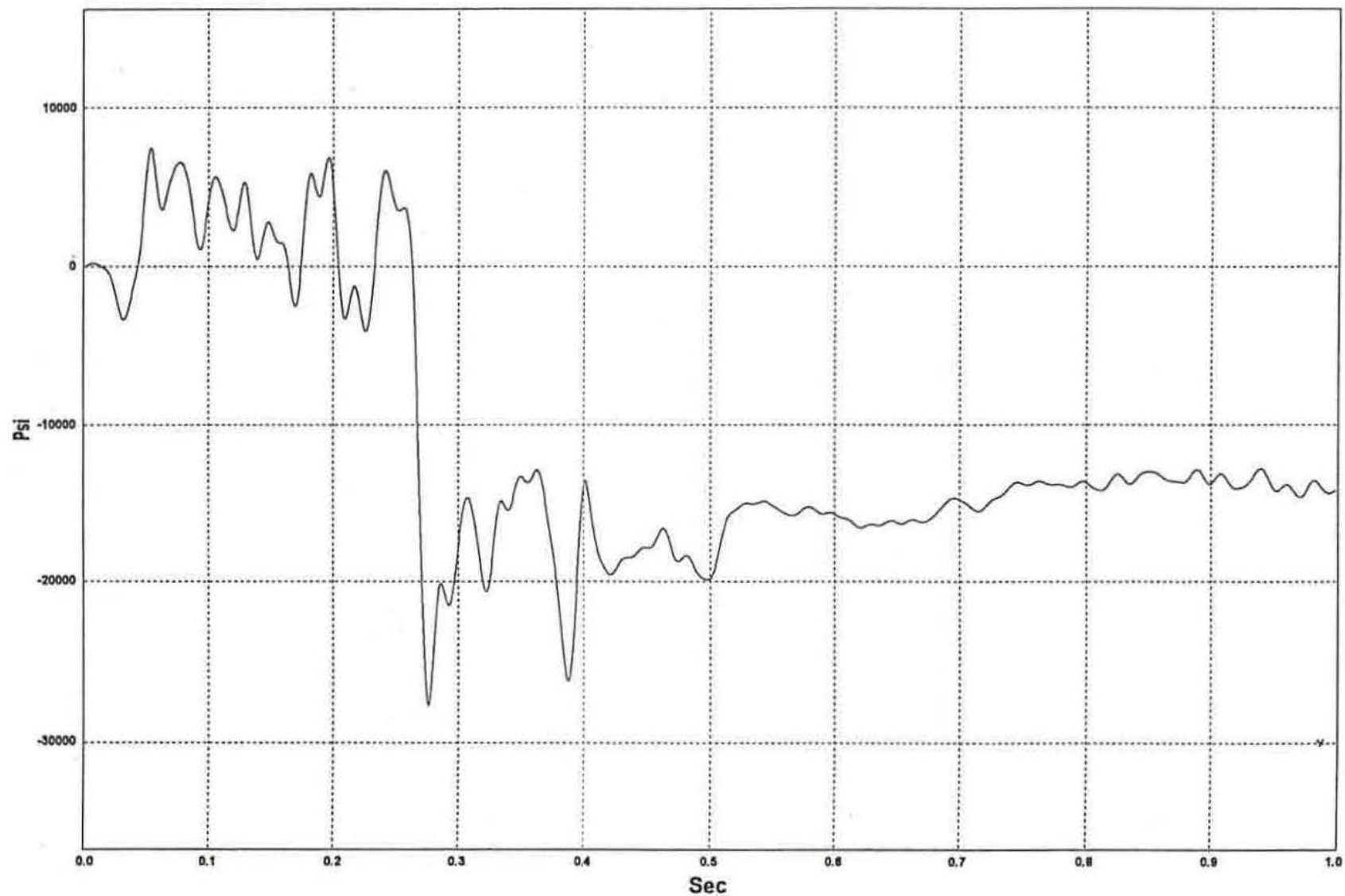


Figure B-2. Strain Gauge No. 1, Stress Data, Test MBN-3

W6: Guardrail Strain - Strain Gauge No. 2 - Test MBN-3

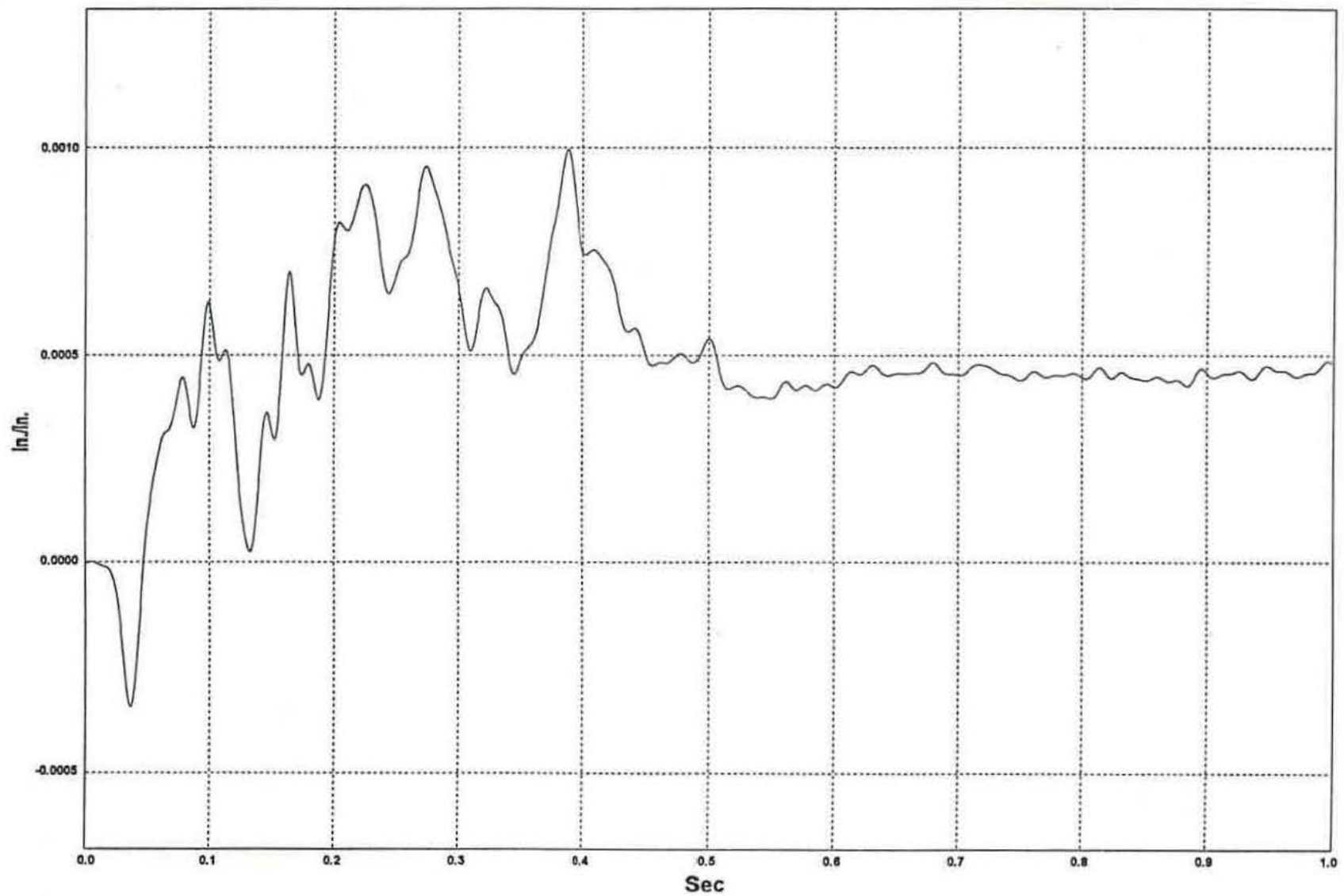


Figure B-3. Strain Gauge No. 2 Data, Strain Data, Test MBN-3

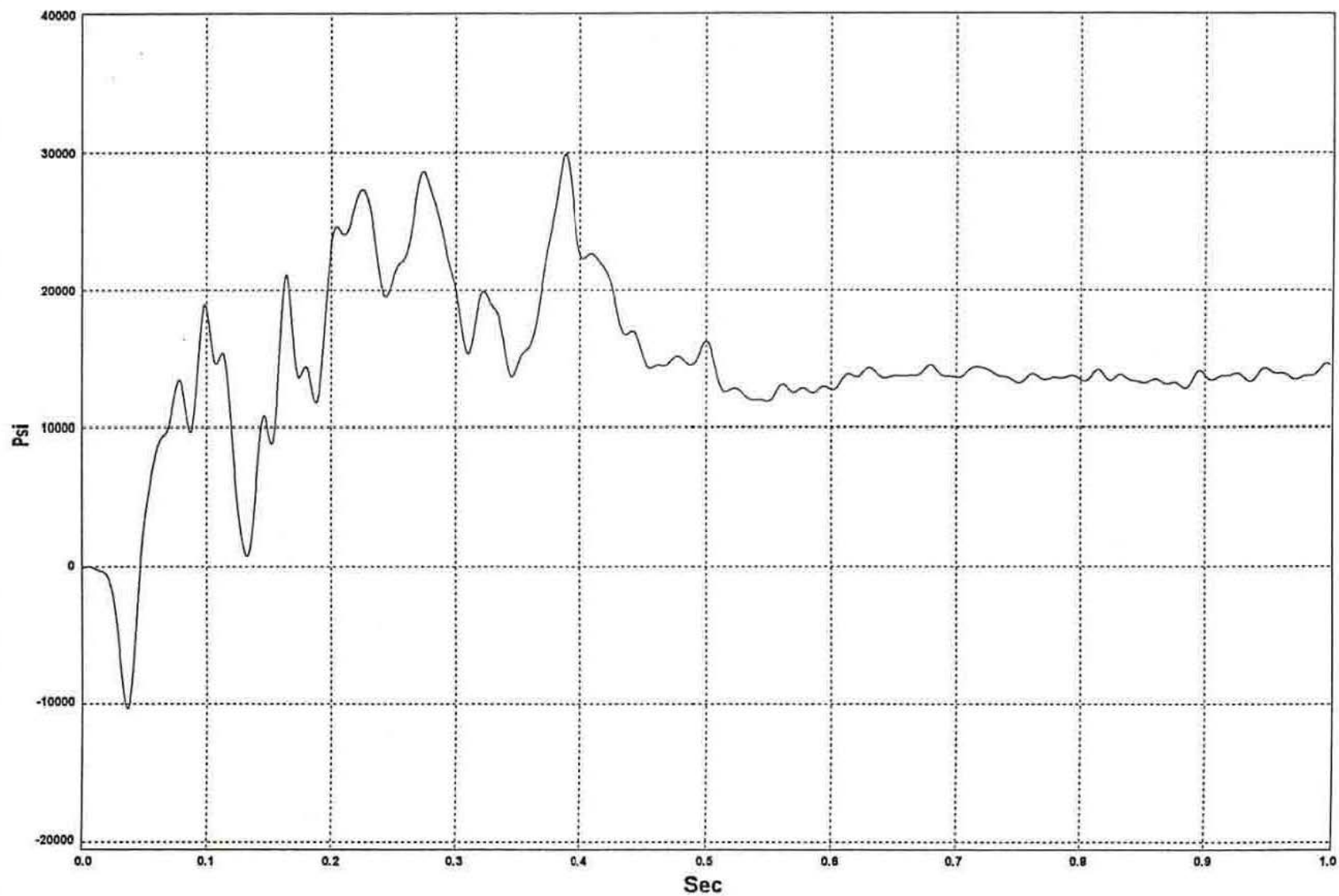
W7: Guardrail Stress - Strain Gauge No. 2 - Test MBN-3

Figure B-4. Strain Gauge No. 2 Data, Stress Data, Test MBN-3

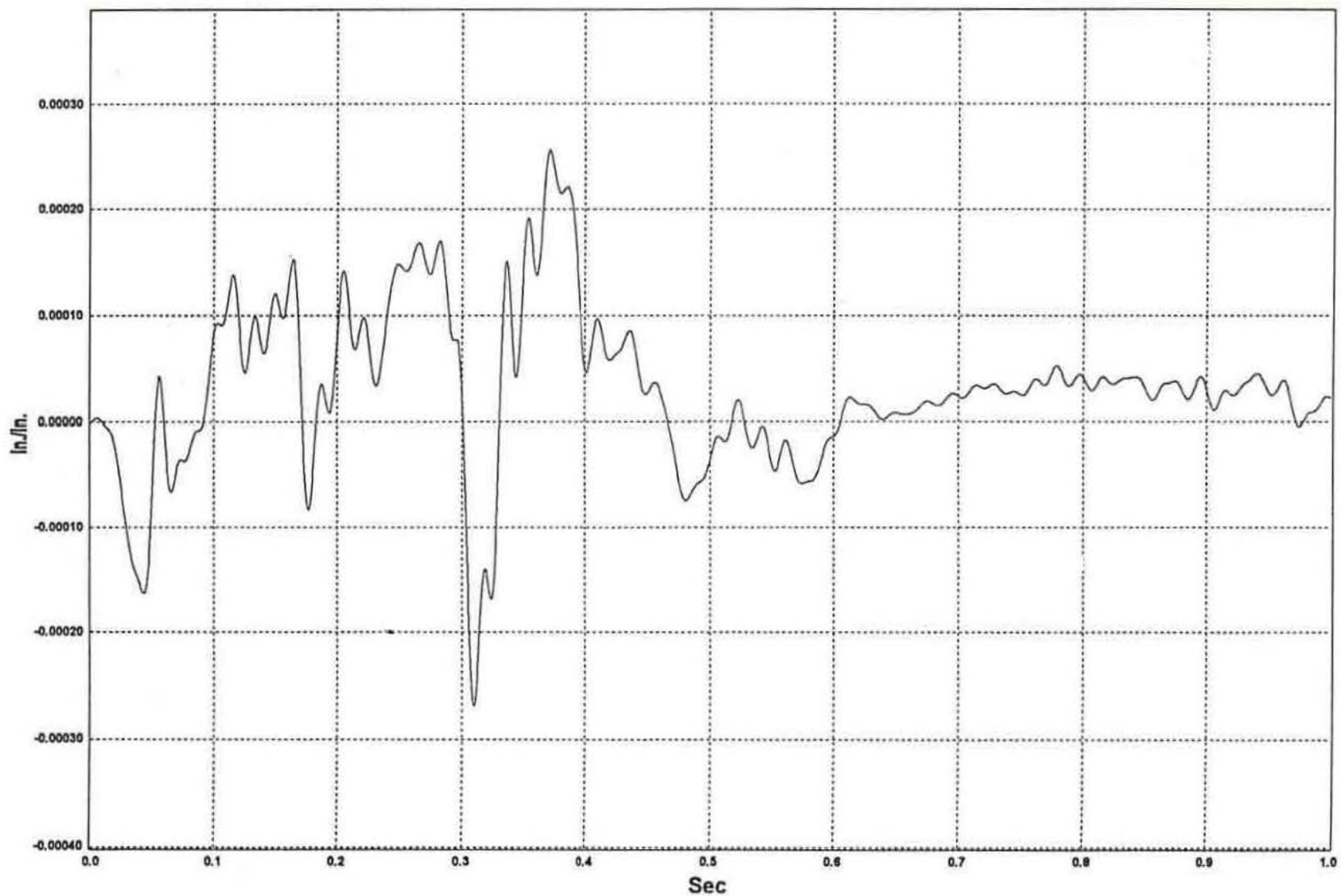
W6: Guardrail Strain - Strain Gauge No. 3 - Test MBN-3

Figure B-5. Strain Gauge No. 3 Data, Strain Data, Test MBN-3

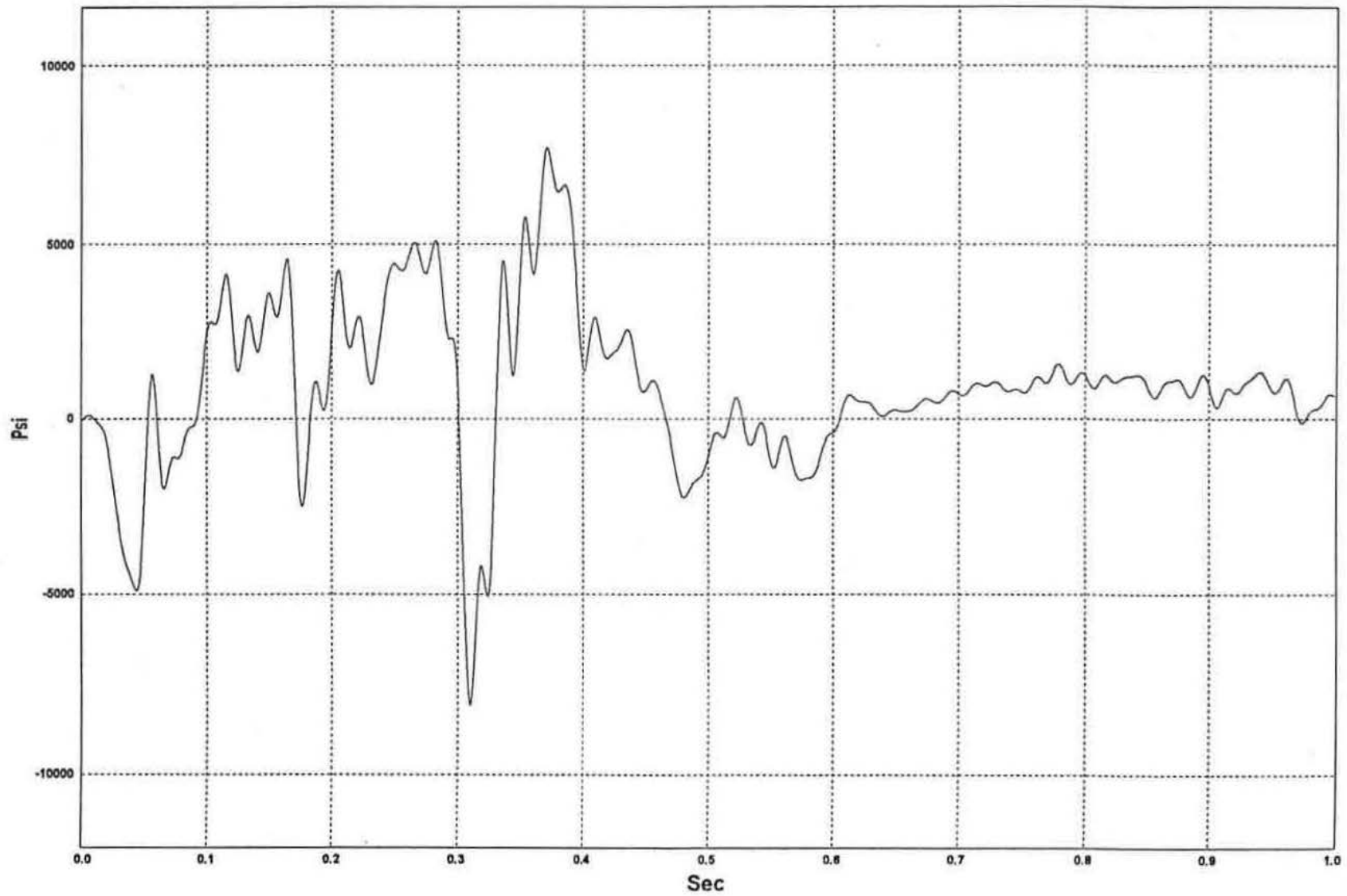
W7: Guardrail Stress - Strain Gauge No. 3 - Test MBN-3

Figure B-6. Strain Gauge No. 3 Data, Stress Data, Test MBN-3

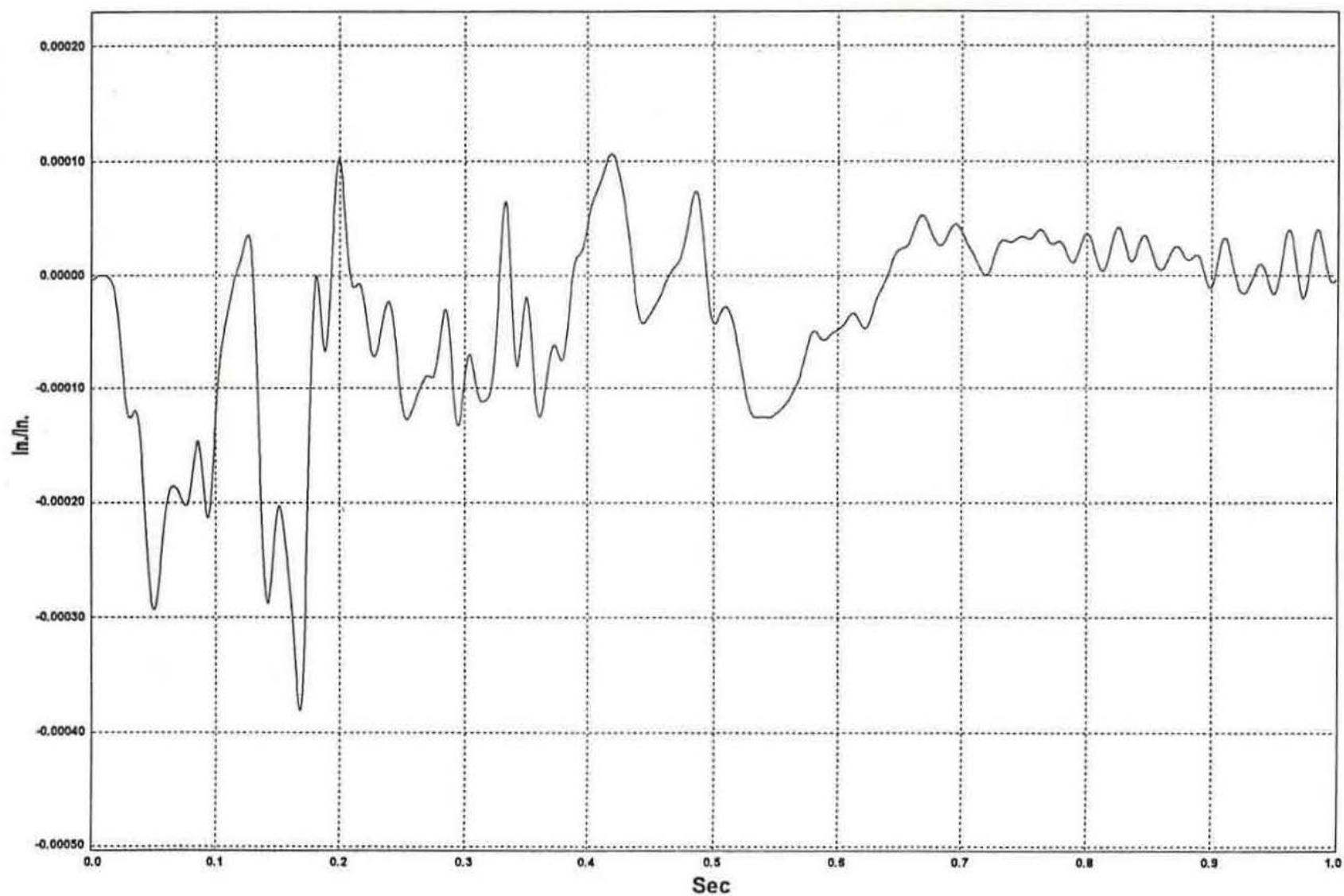
W6: Guardrail Strain - Strain Gauge No. 4 - Test MBN-3

Figure B-7. Strain Gauge No. 4 Data, Strain Data, Test MBN-3

W7: Guardrail Stress - Strain Gauge No. 4 - Test MBN-3

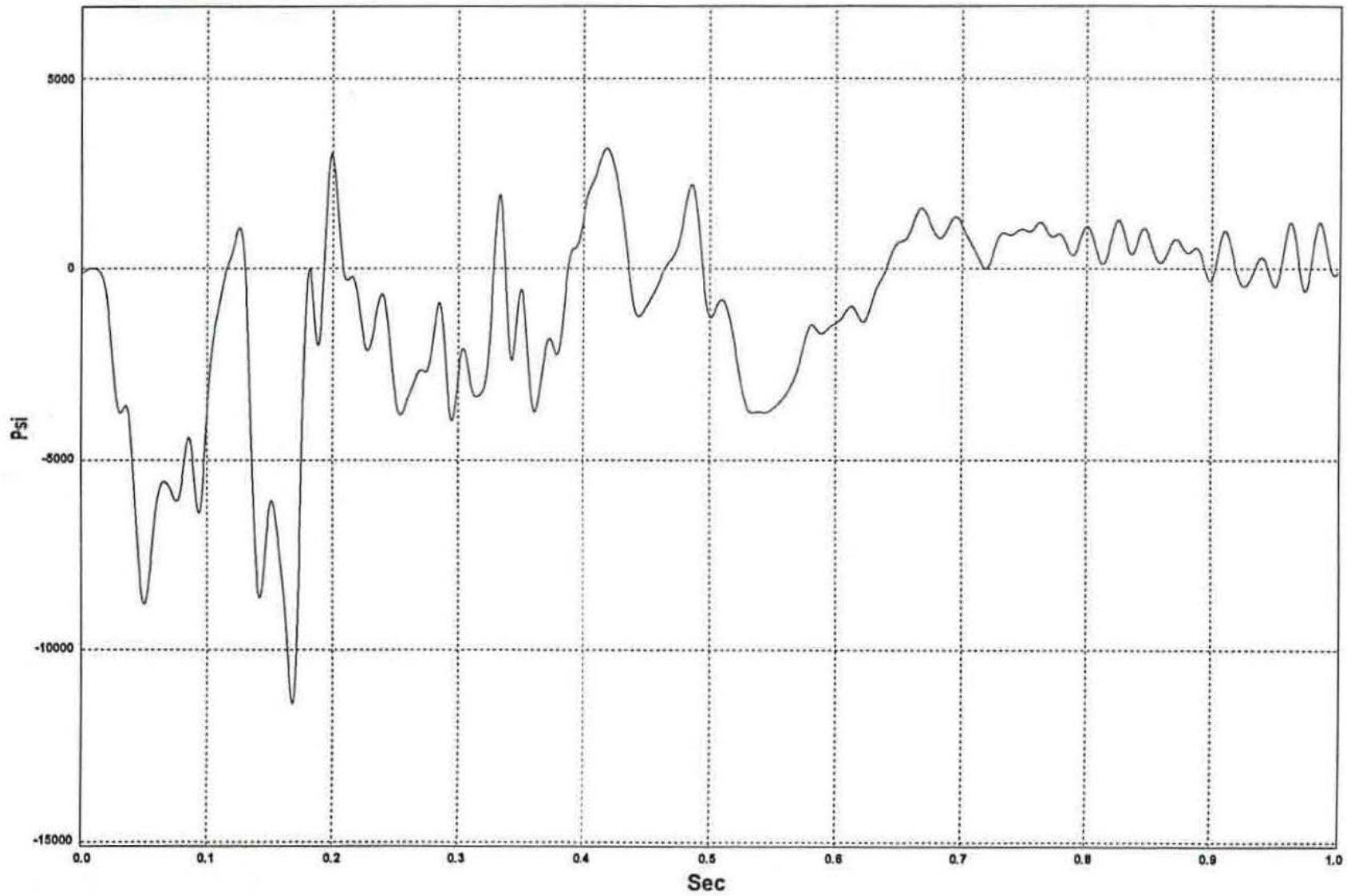


Figure B-8. Strain Gauge No. 4 Data, Stress Data, Test MBN-3

W6: Guardrail Strain - Strain Gauge No. 5 - Test MBN-3

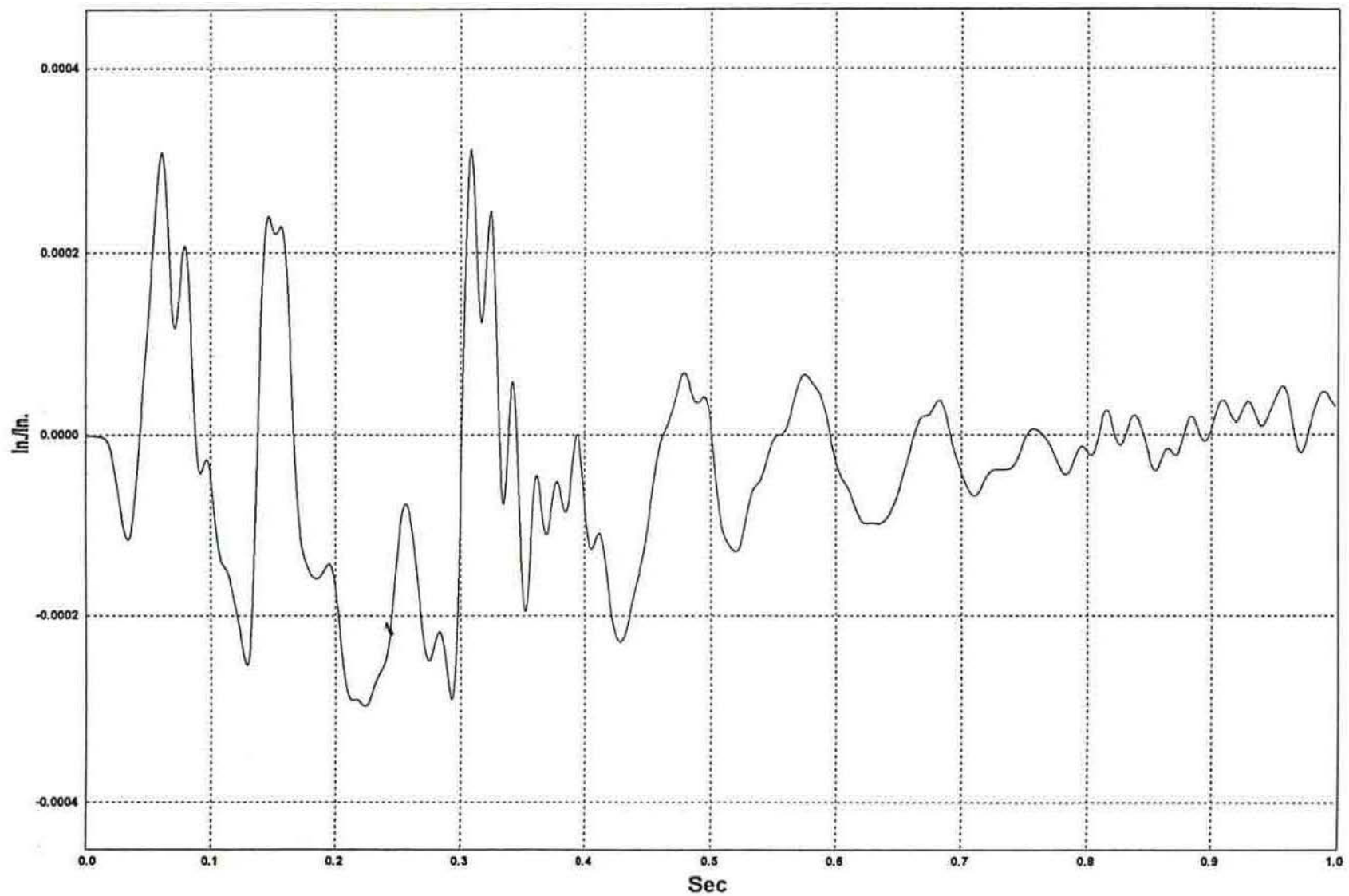


Figure B-9. Strain Gauge No. 5 Data, Strain Data, Test MBN-3

W7: Guardrail Stress - Strain Gauge No. 5 - Test MBN-3

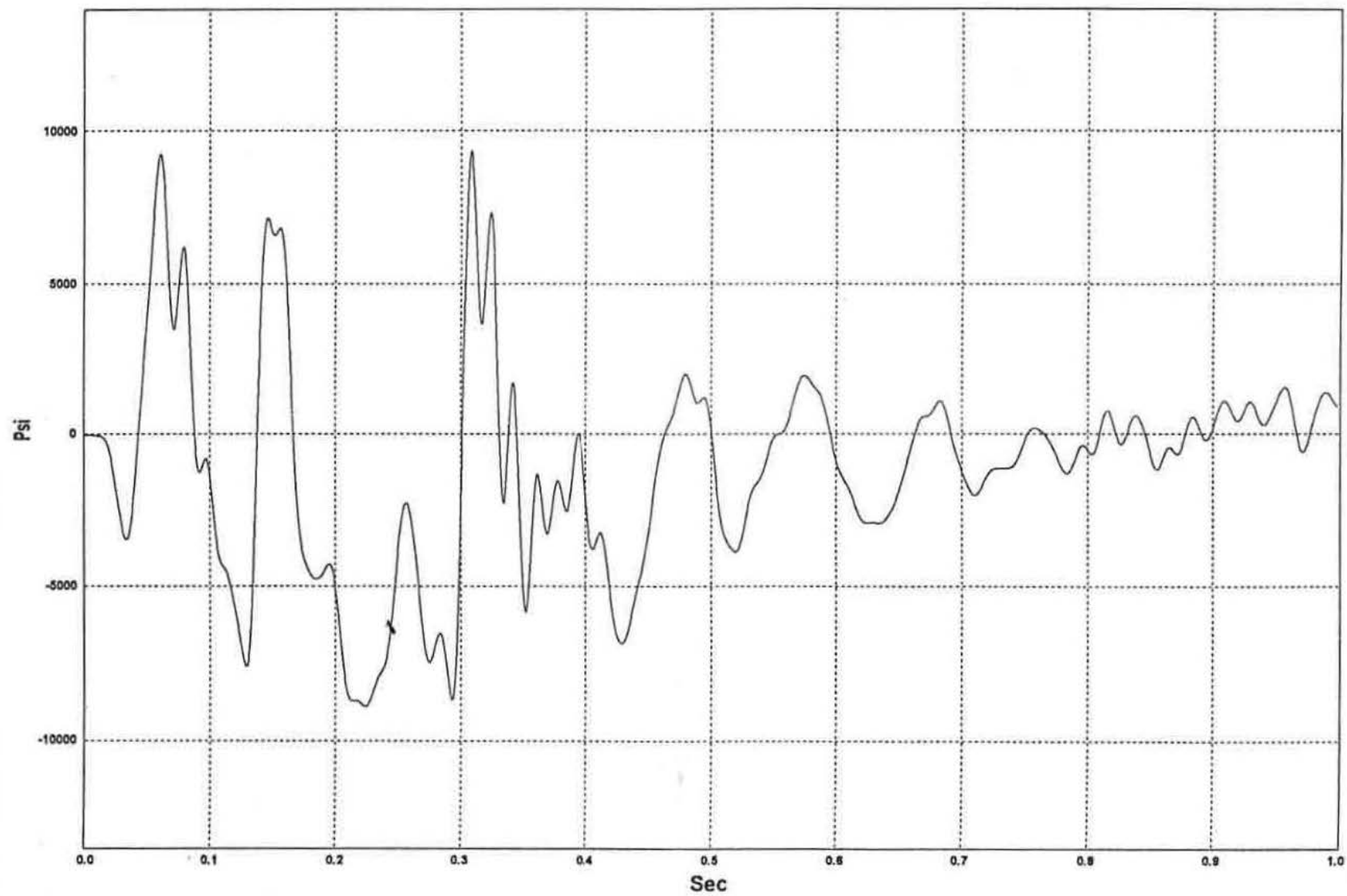


Figure B-10. Strain Gauge No. 5 Data, Stress Data, Test MBN-3

W6: Guardrail Strain - Strain Gauge No. 6 - Test MBN-3

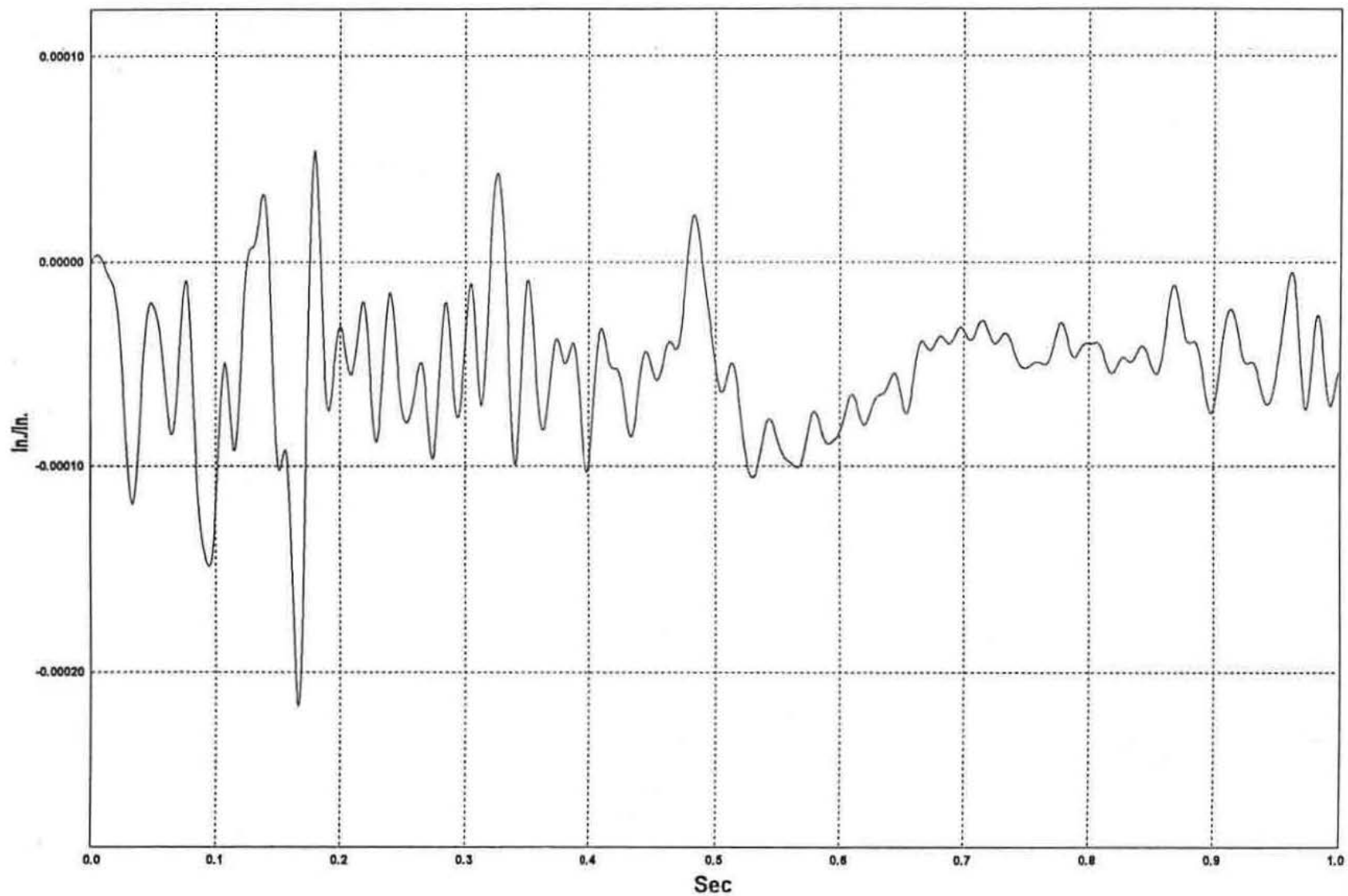


Figure B-11. Strain Gauge No. 6 Data, Strain Data, Test MBN-3

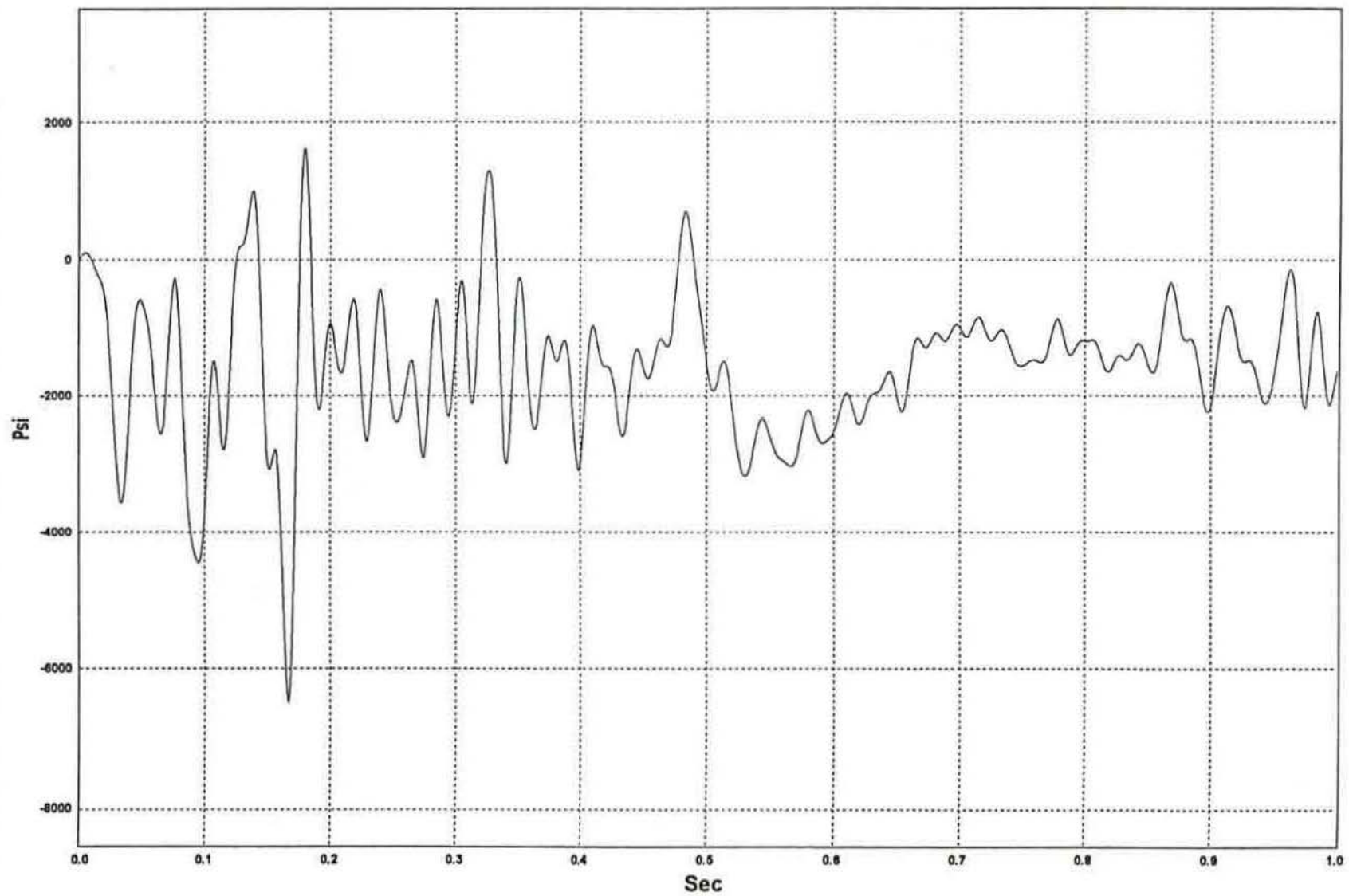
W7: Guardrail Stress - Strain Gauge No. 6 - Test MBN-3

Figure B-12. Strain Gauge No. 6 Data, Stress Data, Test MBN-3

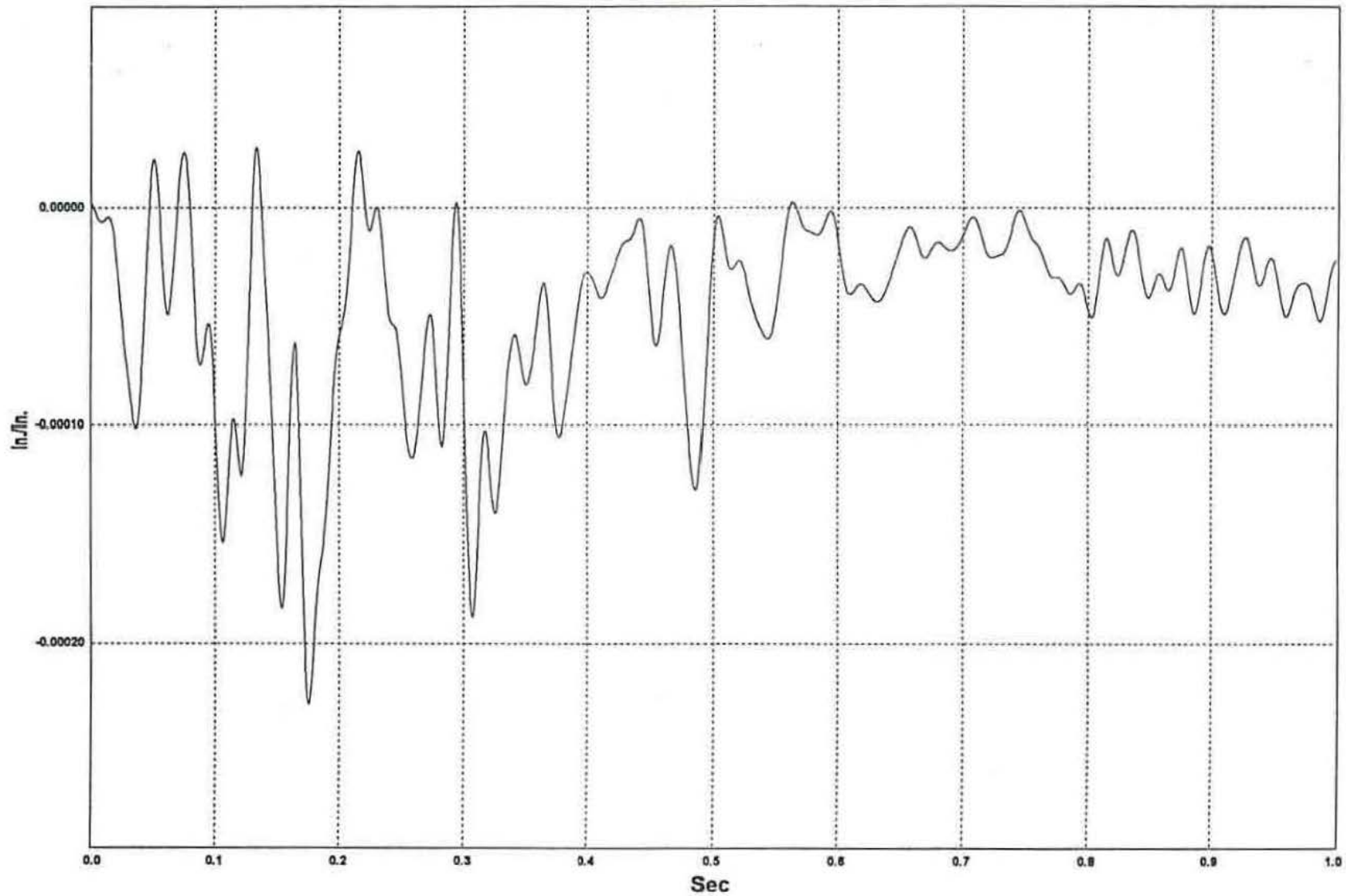
W6: Guardrail Strain - Strain Gauge No. 7 - Test MBN-3

Figure B-13. Strain Gauge No. 7 Data, Strain Data, Test MBN-3

W7: Guardrail Stress - Strain Gauge No. 7 - Test MBN-3

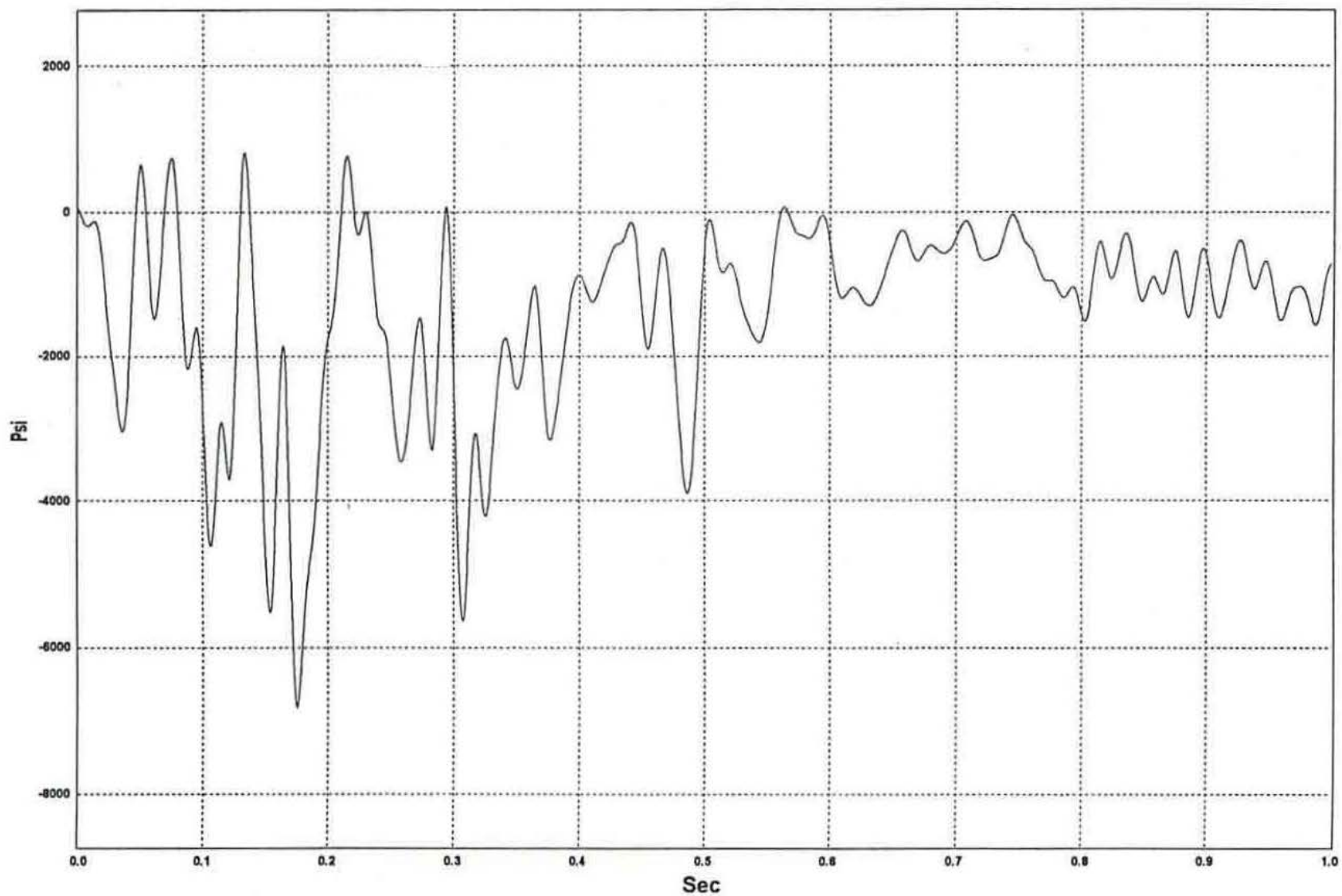


Figure B-14. Strain Gauge No. 7 Data, Stress Data, Test MBN-3

W6: Guardrail Strain - Strain Gauge No. 8 - Test MBN-3

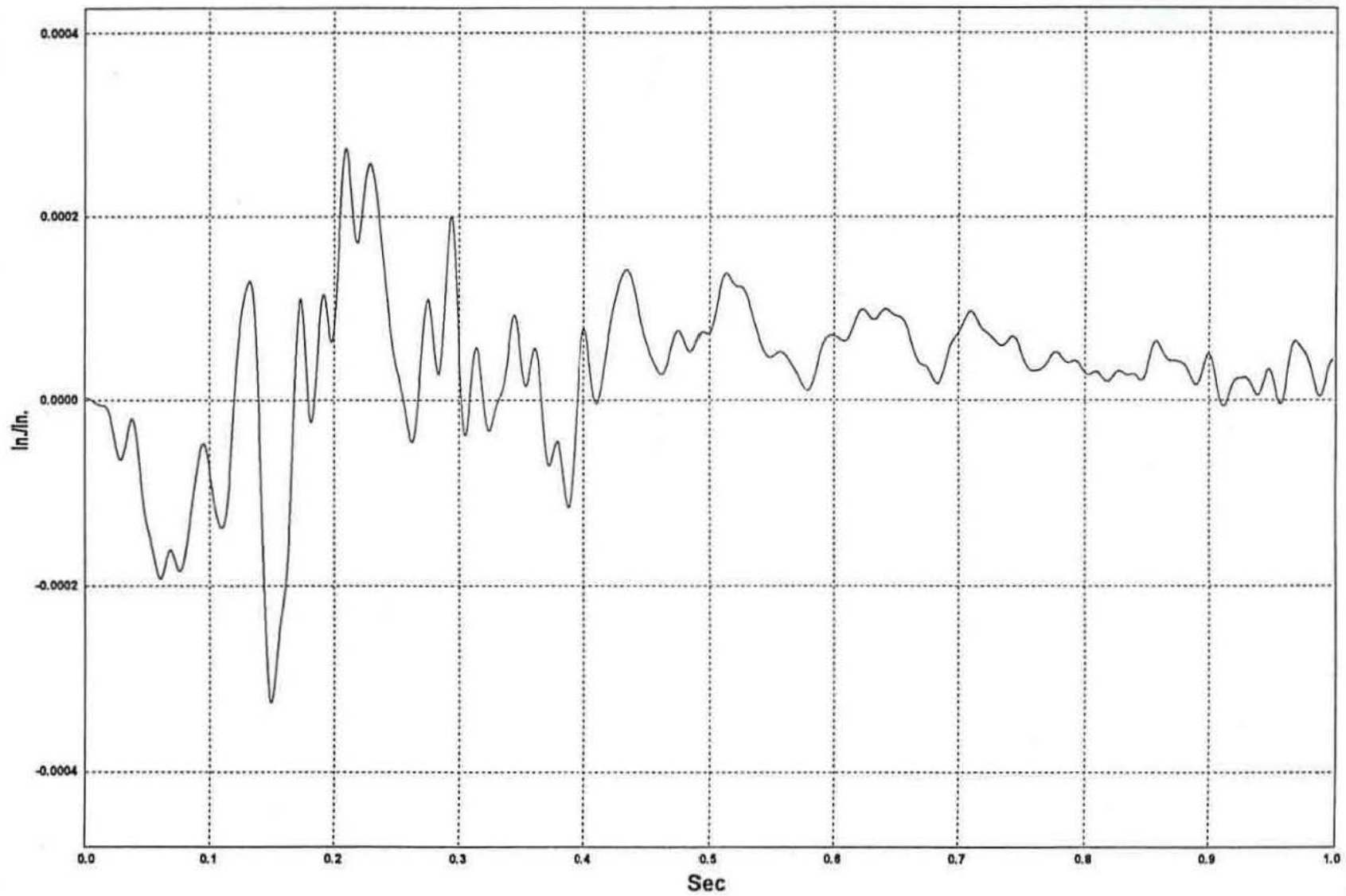


Figure B-15. Strain Gauge No. 8 Data, Strain Data, Test MBN-3

W7: Guardrail Stress - Strain Gauge No. 8 - Test MBN-3

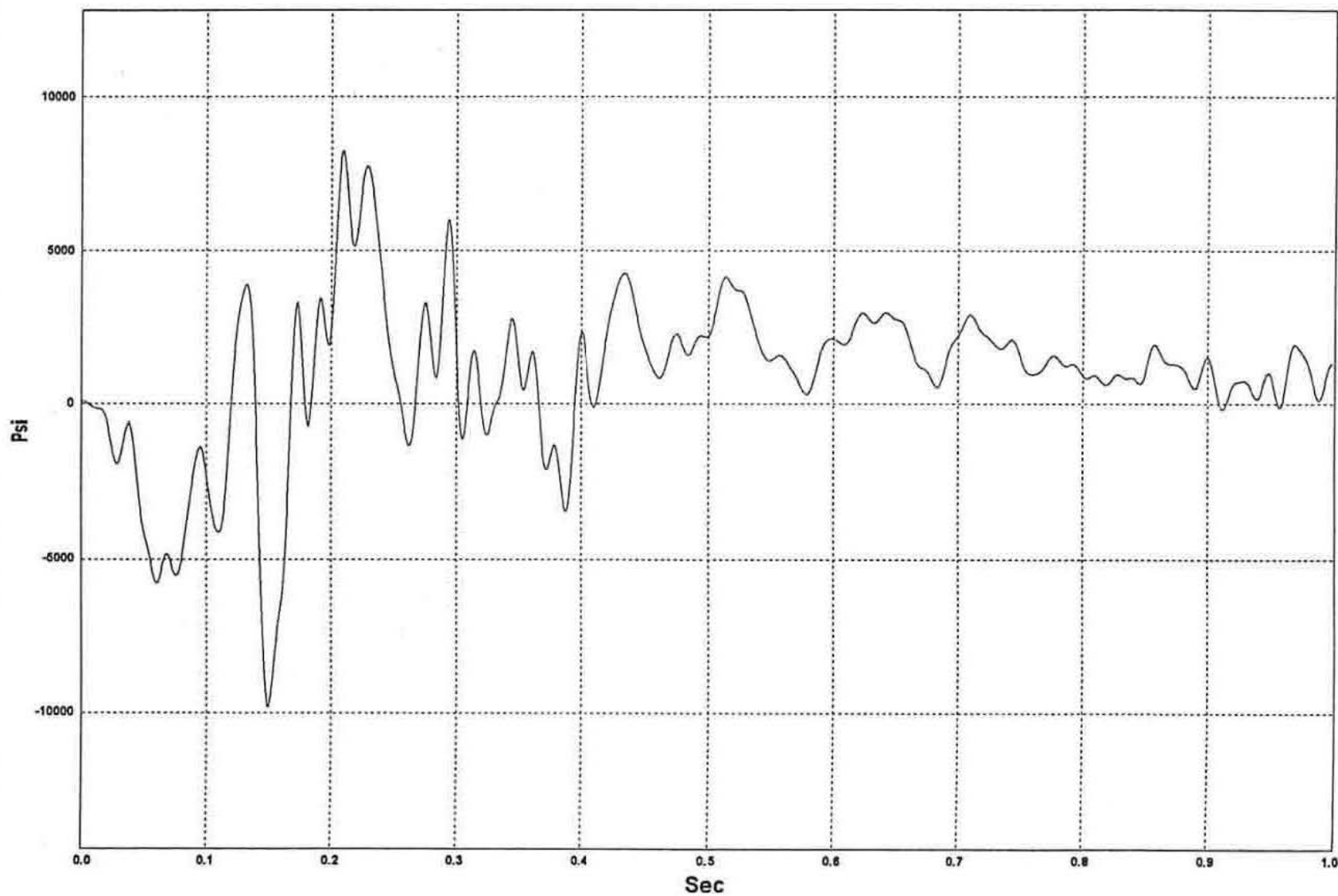


Figure B-16. Strain Gauge No. 8 Data, Stress Data, Test MBN-3